“Role of oxytocin in the contractility of the male reproductive tract: implications for the treatment of benign prostatic hyperplasia”

Inaugural Dissertation

Submitted for the degree of

Dr. med. vet. / Ph.D.

As part of the joint award Ph.D. program of the

Justus-Liebig-University Giessen and the Monash University Melbourne

submitted by

Beatrix Stadler

Degree in veterinary medicine, Giessen

Giessen 2021

From “The Institute of Veterinary Anatomy, Histology and Embryology”
at the Veterinary Faculty of the Justus-Liebig-University Giessen, Germany
Supervisor: Prof. Dr. Dr. Stefan Arnhold

and
“The Institute of Anatomy and Cell Biology”
at the Medicine Faculty of the Justus-Liebig-University Giessen, Germany
Supervisor: Prof. Dr. Ralf Middendorff

and
“Monash Institute of Pharmaceutical Sciences”
at the Monash University, Melbourne Australia
Supervisors: Dr. Betty Exintaris, Dr. Michael Raymond Whittaker and Prof. Dr. Kate Loveland

“Role of oxytocin in the contractility of the male reproductive tract: implications for the treatment of benign prostatic hyperplasia”

Inaugural Dissertation
Submitted to the Faculty 10-Veterinary Medicine
of the Justus-Liebig-University Giessen
for the degree of Dr. med. vet. / Ph.D.
as part of the joint award doctoral program
with Monash University

Submitted by **Beatrix Stadler**
Veterinarian, born in Lörrach
May 2021

With authorization

of the Faculty of Veterinary Medicine of the Justus-Liebig-University Giessen

Dean: Prof. Dr. Dr. h.c. M. Kramer

Examiners:

Prof. Dr. Dr. Stefan Arnhold

Prof. Dr. Ralf Middendorff

Prof. Dr. Axel Wehrend

Date of defense: 06.09.2021

Declaration

I declare that I have completed this dissertation single-handedly without the unauthorized help of a second party and only with the assistance acknowledged therein. I have appropriately acknowledged and cited all text passages that are derived verbatim from or are based on the content of published work of others, and all information relating to verbal communications. I consent to the use of an anti-plagiarism software to check my thesis. I have abided by the principles of good scientific conduct laid down in the charter of the Justus Liebig University Giessen „Satzung der Justus-Liebig-Universität Gießen zur Sicherung guter wissenschaftlicher Praxis“ in carrying out the investigations described in the dissertation.

Ich erkläre: Ich habe die vorgelegte Dissertation selbstständig und ohne unerlaubte fremde Hilfe und nur mit den Hilfen angefertigt, die ich in der Dissertation angegeben habe. Alle Textstellen, die wörtlich oder sinngemäß aus veröffentlichten Schriften entnommen sind, und alle Angaben, die auf mündlichen Auskünften beruhen, sind als solche kenntlich gemacht. Ich stimme einer evtl. Überprüfung meiner Dissertation durch eine Antiplagiat-Software zu. Bei den von mir durchgeführten und in der Dissertation erwähnten Untersuchungen habe ich die Grundsätze guter wissenschaftlicher Praxis, wie sie in der „Satzung der Justus-Liebig-Universität Gießen zur Sicherung guter wissenschaftlicher Praxis“ niedergelegt sind, eingehalten.

Acknowledgement

First and foremost, I would like to thank Ralf Middendorff for taking a chance on me and thereby giving me this fantastic opportunity. I learned so many valuable lessons for work and life. I could develop not only my all-around skillset but also my newly found passion for research. Thank you for allowing me to follow through with my research ideas and experiments and supporting me in all undertakings. I will never forget it!

And a big "thanks" to Stefan Arnhold for taking me on as an external doctoral student and being accommodating and supportive throughout the time.

I would also like to thank my Australian supervisors Betty Exintaris and Mikey Whittaker who supported me in every way possible and helped me to grow as a researcher and person while making me feel very welcomed half-way across the globe. I hope we will meet again!

A special thank you goes out to Cameron Nowell who used his Fiji genius to eradicate any concerns about image analysis and statistics and thereby helped making the content of this thesis while being such an enjoyable person to work with.

"Thank you" to our collaborators and all the people who made it possible to gain access to the different types of tissues at both universities.

I would like to thank all the colleagues and staff at both universities for their help and support. Especially I would like to thank my two desk buddies and forever EXIT partners. I sincerely hope we will keep our tradition alive as we have done so far. A shout out of course also goes to the "beer club" veterans. I am still counting on that reunion!

I would also like to thank the entire IRTG family for great events and fun meetings. A lot of love goes out to my Dromana buddies and Melbourne foody partners.

A special thanks goes out to two friends without whoms selfless effort and support the corrosion cast models would not have been possible.

And a huge "thanks" to Sabine Tasch who not only lent a hand, ear or shoulder at every turn, but became a close friend and vacation buddy, who I do not want to miss.

Finally, I would especially like to thank my mother for endless listening, believing, supporting and reading proof. It made my life a lot easier!

Table of Figures

Abbreviations

ADP	Adenosine diphosphate
ATP	Adenosine triphosphate
BSA	Bovine serum albumin
Ca^{2+}	Calcium
CaM	Calmodulin
DAB	3,3′-Diaminobenzidin
DAG	Diacylglycerol
DAPI	4′,6-Diamidin-2-phenylindole
DMEM/F12	Dulbecco's Modified Eagle Medium/Nutrient Mixture F-12
DMSO	Dimethyl sulfoxide
ER	Endoplasmic reticulum
fc	Final concentration
GPCR	G protein-coupled receptor
HEPES	4-(2-hydroxyethyl)-1-piperazineethanesulfonic acid
IP_3	Inositol trisphosphate
MEM	Minimal essential medium
MLCK	Myosin light-chain kinase
MLCP	Myosin light-chain phosphatase
NE	Norepinephrine
OT	Oxytocin
OTR	Oxytocin receptor
PB	Phosphate buffer
PBS	Phosphate-buffered saline
PFA	Paraformaldehyde

PIP_2	Phosphatidylinositol 4,5-bisphosphate
PKC	Protein kinase C
PLCβ	Phospholipase C β
PP	Phosphate buffer
PTA	5 % Phosphotungstic acid
RhoA	Ras homolog family member
S	Segment
SMA	Smooth muscle actin
TUR-P	Transurethral resection of the prostate

Abstract

This thesis investigated the contractile effect of oxytocin on the prostate and epididymis of rat and human ex vivo using live imaging. While only having a slight effect in most of the epididymis oxytocin evoked a uniquely forceful contractile response in the most distal part of the epididymis. This response was comparable to the one induced by noradrenaline. Oxytocin significantly increased contractions in the human prostate. These results substantiate the physiological involvement of oxytocin in male sexual function.

In addition, this thesis provides the first insight into the fine structure of the human prostatic duct system, using several investigative approaches.

Introduction

Multiple paragraphs in the "Oxytocin" section of this thesis were cited from the review entitled "Oxytocin in the Male Reproductive Tract; The Therapeutic Potential of Oxytocin-Agonists and-Antagonists".

(Stadler B, Whittaker MR, Exintaris B and Middendorff R (2020) Oxytocin in the Male Reproductive Tract; The Therapeutic Potential of Oxytocin-Agonists and-Antagonists. *Front. Endocrinol.* 11:565731. doi: 10.3389/fendo.2020.565731)

Initiation of smooth muscle contraction through different pathways

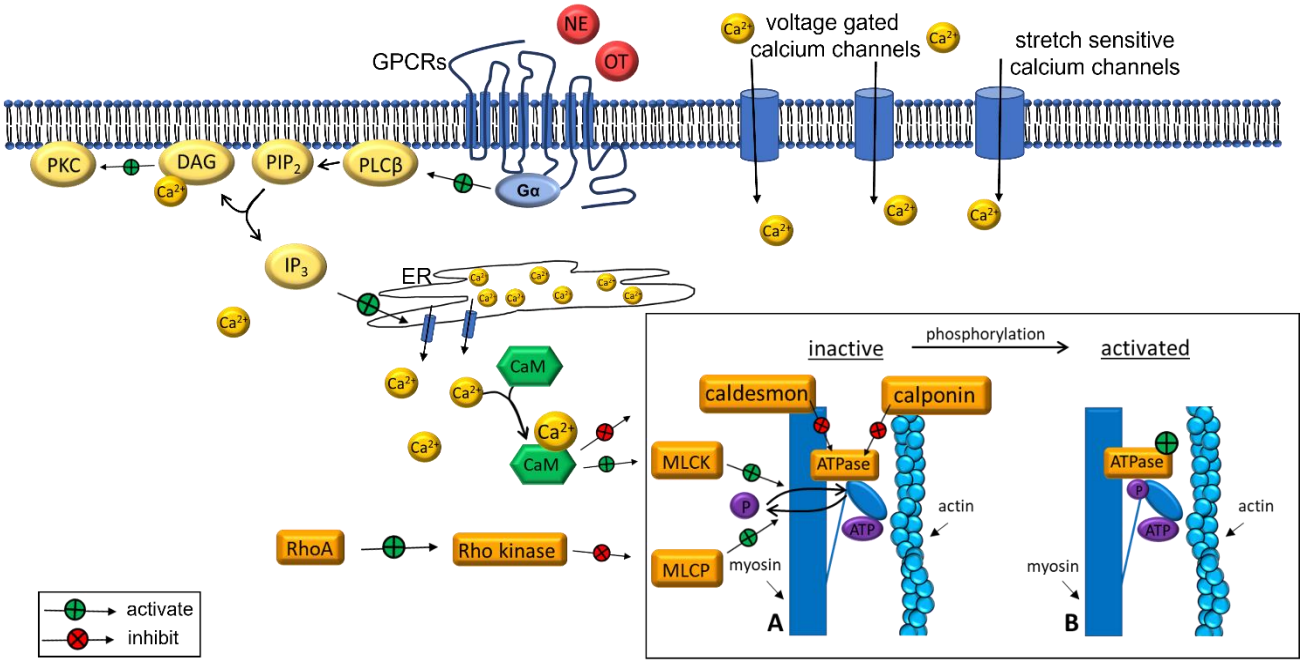

Figure 1: Calcium dependent initiation of smooth muscle contraction

GPCRs – G protein-coupled receptors; NE – norepinephrine; OT – oxytocin; Ca^{2+} - calcium ions; PLCβ – phospholipase C beta; PIP_2 - phosphatidylinositol 4,5-bisphosphate; DAG - diacylglycerol; PKC – protein kinase C; IP_3 - inositol trisphosphate; ER – endoplasmic reticulum; CaM – calmodulin; RhoA - Ras homolog family member A; MLCK – myosin light-chain kinase; MLCP – myosin light-chain phosphatase; P – phosphate; ATP - adenosine triphosphate;

The calcium-dependent contractions in smooth muscle cells are initiated by an increased intracellular concentration of calcium (Ca^{2+}). This is achieved in a number of ways (Fig. 8). On the one hand, there are voltage gated Ca^{2+} channels as well as stretch sensitive Ca^{2+} channels in the cell membrane that account for some of the inflow. Then there are receptors such as G protein-coupled receptors (GPCRs)

that once activated (by e.g. oxytocin (OT) or norepinephrine (NE)) stimulate phospholipase C (PLCβ) activity. PLCβ in turn cleaves phosphatidylinositol 4,5-bisphosphate (PIP_2) into the two second messengers inositol trisphosphate (IP_3) and diacylglycerol (DAG). IP_3 then binds to receptors on the endoplasmic reticulum (ER), resulting in the release of Ca^{2+} into the cytoplasm. DAG and Ca^{2+} activate protein kinase C (PKC). Ca^{2+} then binds to calmodulin (CaM) forming the Ca^{2+}/CaM complex which activates the myosin light-chain kinase (MLCK) and inhibits the inhibition of ATPase by both caldesmon and calponin (Fig. 8A). Now MLCK is able to phosphorylate the myosin light chain while ATPase is active enabling the molecular interaction of myosin with actin (Fig. 8B) (Webb 2003; Kraft and Brenner 2018).

Myosin light-chain phosphatase (MLCP) cleaves the phosphate from the myosin light chain, thus hindering myosin from binding to actin and resulting in a relaxation of the smooth muscle cell. Rho kinase (activated by RhoA (Ras homolog family member)) as well as PKC (activated by DAG + Ca^{2+}) inhibit the activity of MLCP and as such prolong the cycle of myosin and actin interaction as described below (Fig. 9) (Webb 2003; Christ and Andersson 2007).

Smooth muscle contraction

The visible contraction of every muscle in the body is a result of multiple microscopic shortenings by sliding the actin filaments along the myosin filaments under the consumption of energy.

The sliding of the actin (part of the thin filament) alongside the myosin (thick filament) is elicited by the repeated attachments and position changes of myosin heads to actin in the presence of adenosine triphosphate (ATP) as shown below (Fig. 9).

The energized myosin head has a low affinity to bind to the actin filament (Fig. 9A). However, when the myosin neck is phosphorylated and ATPase is activated (Fig. 9B), ATP's conformation is changed to adenosine diphosphate (ADP) + phosphate (P) and the myosin head tilts and binds with high affinity to the actin leading to the cross-bridging of the two filaments (Fig. 9C). When hydrolysis of ATP is completed the myosin releases ADP+P from its head. This causes an allosteric change in the myosin head resulting in a flexion of the head which in turn is pulling actin to slide alongside myosin (Fig. 9D) (known as the so-called power stroke). At this point the myosin head will be reenergized with ATP which leads to a detachment from the actin. If the myosin head stays phosphorylated (because MLCP activity is inhibited) the cycle starts over (Fig. 9B). This repeated attaching and flexion of the multiple myosin heads build up to one organized contraction (Cunningham 1997). If MLCP is active it will

cleave the phosphate from the myosin head which blocks the binding from myosin heads to actin (back to Fig. 9A) (Kraft and Brenner 2018).

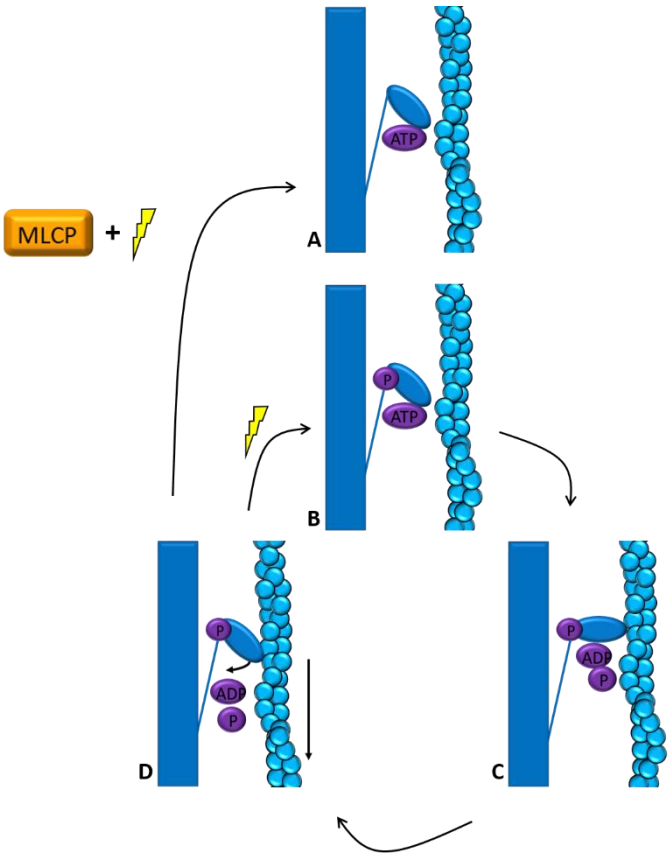

Figure 2: Interaction of actin and myosin resulting in contraction

ATP - adenosine triphosphate; P – phosphate; ADP - adenosine diphosphate; MLCP – myosin light-chain phosphatase

Leftover calcium will be recycled into the ER or transported out of the cell and the smooth muscle cell relaxes.

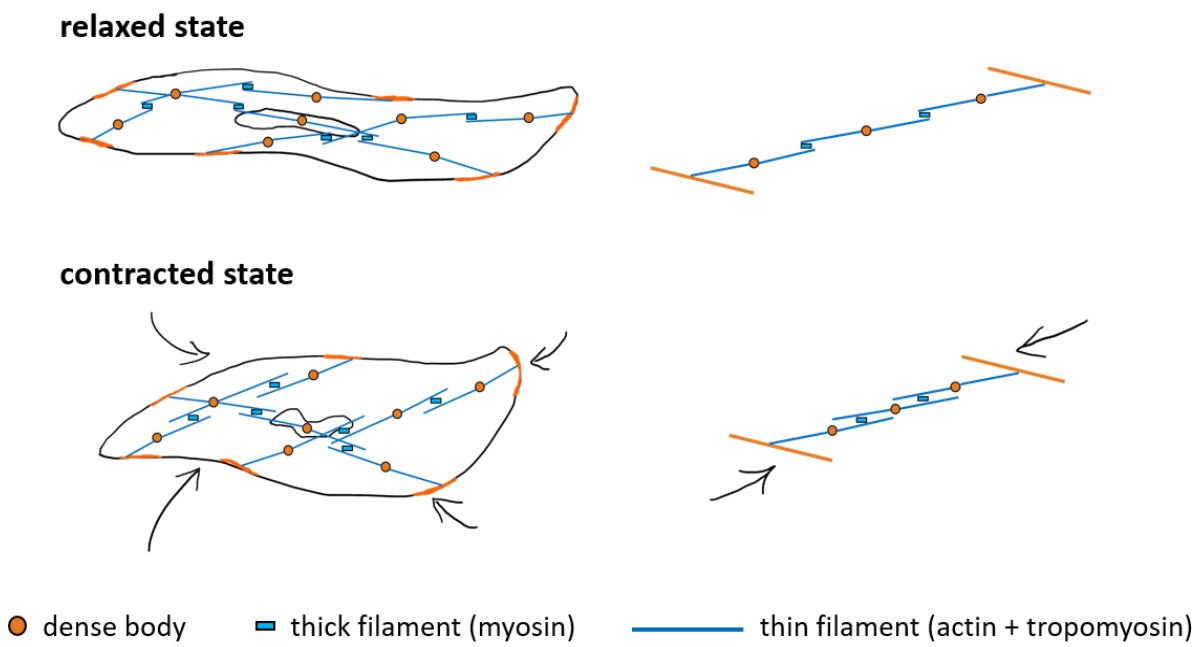

Figure 3: Schematic of smooth muscle contraction

For all smooth muscle cells, the organization of actin and myosin is not structured into microscopically visible striations (as in skeletal muscles) but in a crossing manner with so called dense bodies as anchors for the thin filaments, as shown below (Fig. 10).

The adrenergic pathway

Norepinephrine (NE), also called noradrenaline, has a molecular formula of $C_8H_{11}NO_3$ and is part of the catecholamine family. It can operate either as a hormone synthesized by the adrenal medulla or as a neurotransmitter. As a neurotransmitter it is (among others) synthesized by, stored in and released from the synapses of the central nervous system leading to the activation of sympathetic responses in numerous organs (Cunningham 1997; O'Donnell et al. 2012), one of them being the sympathetic activation of the tissues in the male reproductive tract.

NE elicits effects through binding to and activating adrenergic receptors. Adrenergic receptors can be divided into α- and β-adrenergic receptors which each can be subdivided into α1 and 2 and β1, 2 and 3. They all are G-protein-coupled receptors which function via the second messenger pathway but their location and thereby their effects differ (Strosberg 1993). α2 receptors for example are mainly located in the pre-synaptic membrane of the NE releasing synapses. When activated they promote the reuptake of NE from the synaptic gap into the presynaptic membrane, thereby leading to a decrease of available NE in the synaptic gap and thus moderating the sympathetic effects as well as restoring the NE reservoir of the synapse itself (Reid 1986). In comparison α1 receptors primarily mediate smooth muscle contractions, especially in the male reproductive tract (Caine et al. 1975; Michel 2007) and therefore will be the focus in this thesis. NE is one of the neurotransmitters acting on all adrenergic receptors (with differing affinities). Naturally occurring substances such as NE and their differentiating affinities to the adrenergic receptors resulted in a string of pharmaceuticals that can be selective to either α- or β-receptors (Baker 2010) or even to only one specific class such as α1 or subtype such as α1A (Lepor 2006). For example, targeting specifically the α1A-receptor has been the focus in the development of pharmaceuticals intended for the treatment of benign prostatic hyperplasia (Andersson 1995; Lepor 2006). There still might be some effects through the other adrenergic receptors but the high selectivity of these pharmaceuticals allows a targeted medication-effect relationship.

Gross anatomy of the male reproductive tract

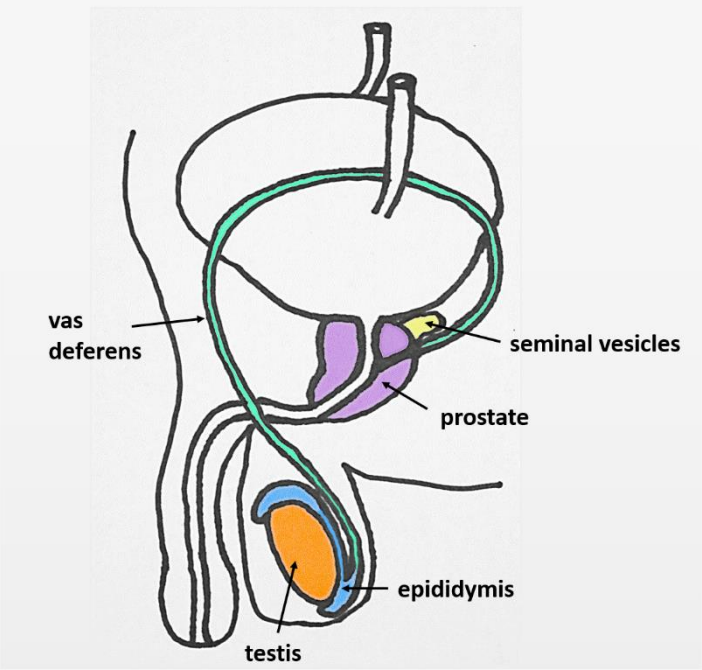

Figure 4: Gross anatomy of the human male reproductive tract (Stadler et al. 2020)

In most mammals (including the human) the male reproductive tract consists of the same organs (testis, epididymis, vas deferens, accessory sex glands, penis) (Fig. 1). The oval shaped male gonads, the two testes (orange), contain numerous seminiferous tubules that are lined with germinal epithelium. After puberty and under hormonal control these germ cells develop through spermatogenesis into infertile sperm cells (spermatozoa) over time. The small seminiferous tubules merge and once exiting the testis as efferent ducts eventually unite into one heavily coiled larger duct, the epididymal duct, the main structure of the epididymis. Immediately adjacent to the two testes lay the two epididymides (blue) that run along the side of the testes and can be divided into three parts: head, body and tail or caput, corpus and cauda epididymidis (Lippert 2017; Schulte 2017). During their transit through the epididymal duct the infertile sperm acquire motility and fertilizing ability and finally accumulate in the cauda epididymidis until the emission phase of the ejaculatory process. Distal to the cauda epididymidis the epididymal duct becomes the vas deferens (turqouise) and reascends into the pelvic cavity, running around the bladder and eventually opening into the urethra. The excretory ducts of all accessory sex glands (prostate (purple), ampulla of vas deferens, seminal vesicle (yellow), bulbourethral gland, coagulating gland, preputial gland) also open into the urethra (Schulte 2017). The ejaculatory process consists of two phases: emission and expulsion. During the emission phase sperm from the distal epididymis as well as fluids from the accessory sex glands drain into the proximal part of the urethra. In the second phase (the expulsion phase) the mixed components are expelled through the urethra and out of the body through the penis as ejaculate (Giuliano and Clément 2005; Alwaal et al. 2015).

Depending on the species there are differences with respect to anatomy, histology and the presence (or absence) of the different accessory sex glands while the main sexual function is preserved (Brinsko 1997).

General development of the male reproductive system

In utero the fetal gonads develop from the mesothelial layer of the peritoneum while the mesonephric duct (also known as Wolffian duct) develops from a portion of the pronephric duct. When the male gonads (precursor of the testes) start producing fetal testosterone around the 8th week of gestation the Wolffian duct begins to differentiate into the epididymis, the vas deferens and some of the accessory sex glands. In the human the seminal vesicles arise from the vas deferens and therefore also originate from the Wolffian duct while the prostate and the bulbourethral glands originate from the urogenital sinus and involve the surrounding mesenchyme (Moore et al. 2013; Carlson 2014).

The prostate

The prostate is an accessory sex gland of the male reproductive tract of most mammalians. It secretes a fluid contributing to the ejaculatory fluid which is directly drained into the urethra (pars prostatica). The prostate is located caudally to the bladder and is circumferentiating or riding on the urethra. The prostate differs in size, exact location and significance depending on the species. Like other organs of the male reproductive tract, the prostate is heavily innervated by the autonomic nervous system (McMahon et al. 2004; Lippert 2017).

The human prostate – development, anatomy, histology and function

In healthy younger men the human prostate is a walnut sized, slightly cone shaped solitary structure. Its base caudally attaches to the bladder, wraps around the urethra and is of firm consistence. It is located inside the male pelvic cavity anterior to the rectum and posterior to the symphysis (Lippert 2017). Humans possess three accessory sex glands (seminal vesicles, prostate and bulbourethral glands) of which the prostate contributes up to 30 % to the ejaculatory fluid. In the pars prostatica of the human prostate the tissues of the urethra and the prostate are fused together, thereby confining the prostate. The ductus deferens and the excretory ducts of the seminal vesicles join from each side, run through the prostate as ejaculatory ducts and drain into the pars prostatica of the urethra, specifically on the colliculus seminalis (Schulte 2017).

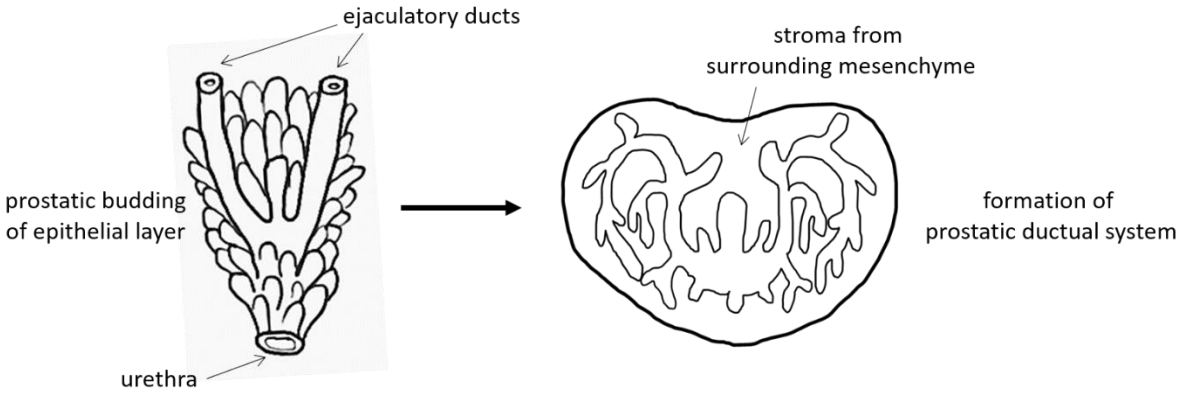

Figure 5: Embryological development of the human prostate

Embryologically the prostate consists of two parts: the epithelium and the stroma. The epithelial portion has developed through budding of the urethra from the urogenital sinus, whereas the stroma has formed

around the buddings from the surrounding mesenchyme as shown below (Fig. 2) by the different stages of the human prostate development (Moore et al. 2013).

The human fetal development of the prostate can be divided into multiple stages: pre-bud stage, initial budding, bud elongation and branching, ductal canalization, differentiation of luminal and basal epithelial cells and secretory cytodifferentiation. The process of budding seems to start in the human between the 9th and the 10th gestational week and ends with the secretory cytodifferentiation in the late second or third trimester (Cunha et al. 2018). In comparison, in rodents the prostatic development is not concluded at birth.

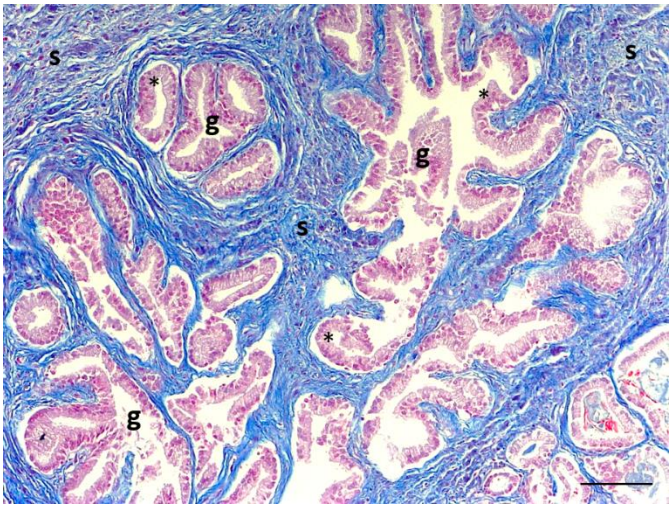

Figure 6: Histology of the human prostate

epithelium (*), tubulo-alveolar glands (g), surrounding stroma (s), scale bar: 100 µm

In the human prostate two prominent structures can be histologically distinguished: one being the epithelium layer that originally budded from the urethra and subsequently forms into the tubulo-alveolar glands (g) and the other representing the interstitial stroma (s) (Kummer and Welsch 2018) (Fig. 3). In humans the pseudostratified epithelium lining the glands consists of a luminal secretory layer of tall columnar cells and basal cells. The dense stroma throughout the prostate is composed of fibroblasts, collagen fibres and smooth muscle cells in varying percentages depending on the prostatic zone (Alves et al. 2018).

The histological heterogeneity of the human prostate allows a classification into McNeal's zones (McNeal 1988; Selman 2011): periurethral zone (red), transition zone (yellow), central zone (blue), peripheral zone (cyan) and anterior zone (grey) (Fig. 4). Most often, diseases of the prostate originate specifically in one region: benign prostatic hyperplasia (BPH) was found to mainly originate from the transition zone (yellow) and the central zone (blue), whereas carcinomas seem to occur predominantly in the peripheral zone (cyan) (Kumar 2007b). Unique to the human are the layers of collagenous fibres that enclose the prostatic tissue, the so called prostatic capsule (Lippert 2017).

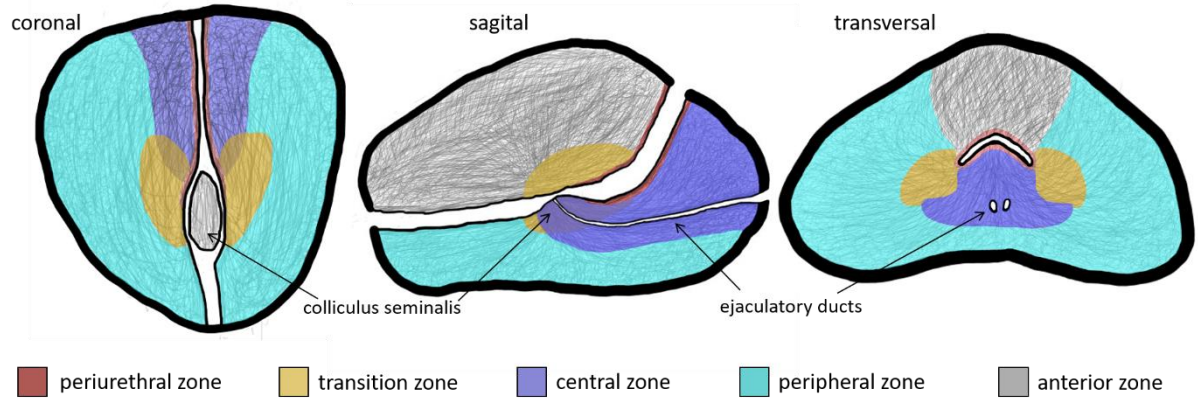

Figure 7: Histological classification of the human prostate into different zones after McNeal (McNeal 1988)

In rodents embryological budding and resulting formation of the ductal system has been thoroughly described (Lee et al. 1990b; Nemeth and Lee 1996) and the different lobes histologically characterized (Hayashi et al. 1991a; Ginja et al. 2019). In the human however, the microstructural arrangement of the prostatic ductal system as well as a histological characterization of possible differences between prostatic ducts and glands is missing. It has only been described that the human prostate consists of 30-50 tubulo-alveolar glands which drain through about 15 ducts into the urethra (Lippert 2000).

The rat prostate – development, anatomy, histology and function

Rodents also possess three accessory sex glands (prostate, seminal vesicles and coagulating glands) and their prostate is situated very similar to the human one. It is also located inside the pelvic cavity, ventral to the rectum and dorsal to the symphysis, attaching caudally to the bladder and wrapping partially around the urethra. However, the rodent's prostate is rather delicate in consistence and not as tightly attached to the urethra. It can be differentiated into distinct paired lobes: the ventral, lateral and dorsal lobes surrounding the urethra and the anterior lobes (or coagulating glands) of the prostate adjacent to the seminal vesicles (Fig. 5). Those lobes are separated from each other by fibrous and adipose tissue

and each present in a unique histological structure (Jesik et al. 1982; Ittmann 2017; Ginja et al. 2019). The morphology and distribution of glandular systems with the respective duct system within the different lobes have been investigated in rodents (Lee et al. 1990a; Hayashi et al. 1991b).

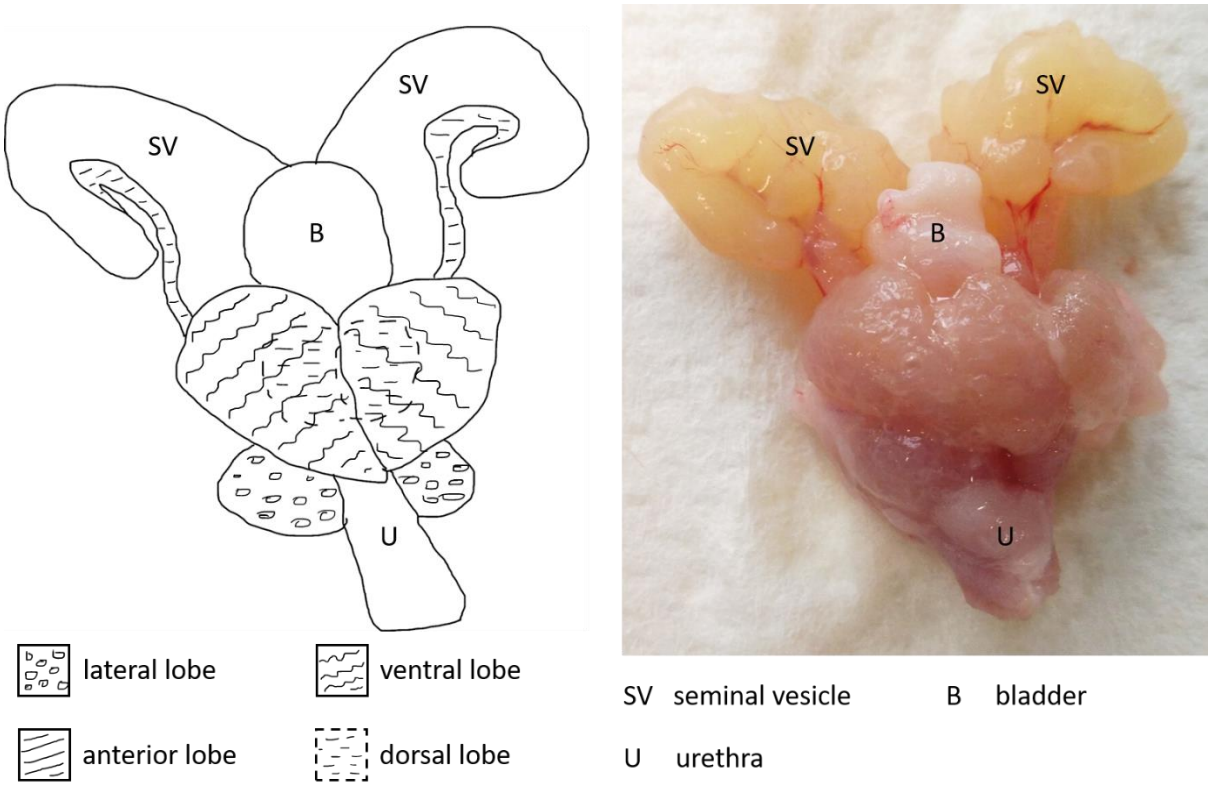

Figure 8: Anatomy of the rat prostate, bladder and seminal vesicles with differentiation of the prostatic lobes

Embryologically the prostate also originates from the urogenital sinus as in the human and forms through epithelial budding and the surrounding mesenchyme. However, in rodents fetal prostatic development stops at the initial budding stage (predetermining the respective lobes) until birth. Therefore, most of prostatic growth (branching, ductal canalization and differentiation of the luminal and basal epithelial cells) as well as formation of the distinct lobes occurs postnatally, which is a considerable difference in comparison to the human development (Hayashi et al. 1991a; Cunha et al. 2018).

The canine prostate in comparison

Dogs possess only one true accessory sex gland: the prostate. Its size differs significantly depending on race and weight while the location depends on the dog's age. The canine prostate is separated by a prominent median septum into the right and the left lobe which both are further separated into smaller lobules by capsular trabeculae (Sun et al. 2017b) but not surrounded by a prostatic capsule as in the human. The canine prostate is also circumferentiating the urethra close to the bladder but in contrast to human's the two tissues are not fused together, allowing the prostate to migrate depending on the dog's age. This can be segmented into different phases. The first phase begins with embryogenesis and lasts up to an age of two to three years and ends with full functionality of the prostate. To this point the prostate is of normal size and located inside the pelvic cavity just as seen in humans and rodents. Then the androgen dependent growth phase of the prostate begins which also leads to a more and more abdominal migration of the prostate, ending with a reduced testicular androgen synthesis, thereby leading to the senile involution of the prostate (Janthur 2016).

In dogs the histological homogeneity of their prostate makes a histological differentiation into zones impossible. In comparison to humans the prostatic stroma surrounding the epithelium is much thinner and consists of less smooth muscle cells (Sun et al. 2017b).

Benign prostatic hyperplasia

Benign prostatic hyperplasia – etiology and prevalence

The condition known as benign prostatic hyperplasia (BPH) is the clinical term for an age-related benign enlargement of the prostate whose spontaneous development only has been described in humans, chimpanzees (Madersbacher 1999), macaques and dogs (but not in rodents). Up to 75 % of 80-year-old men and up to 100 % of old uncastrated dogs present histological signs of BPH. In humans only 40-50 % of these cases are becoming clinically significant; for example, those developing lower urinary tract symptoms (LUTS) (Li et al. 2018a).

In humans, BPH is based on a hyperproliferative process involving epithelial and stromal cells in the periurethral zone and the transition zone of the prostate. In early stages of BPH the majority of nodules forming in the periurethral zone are purely stromal in character. In comparison, in the transition zone a majority of the early proliferations are glandular in character (Roehrborn 2008). The resulting nodular expansion of the transition zone into the peripheral zone eventually leaves the peripheral zone, restricted distally by the "prostatic capsule" around the other prostatic zones. This alone does not lead to clinical symptoms but the compression of the urethral lumen or the intrusion into the bladder neck through the inward expanding prostate increases the probability of developing LUTS (Lee and Kuo 2017).

In comparison, the dog's prostate being not constricted by a capsule proliferates outwards, thereby predominantly resulting in compression of the rectum causing difficulties defecating (Janthur 2016). Histologically, BPH of the canine prostate proliferates in two phases. The first phase of dog's BPH is a glandular hyperplasia in dogs up to 4 years of age. The secretory epithelium and the size of the alveolar glands increase as well as the degree of papillary infold. This is followed by the second phase, the cystic hyperplasia, also called the complex form of prostatic hyperplasia. It is characterized by a mixture of glandular hyperplasia together with atrophic secretory epithelium and an increased stroma (for example smooth muscle cells). There also might be small or large cysts present (Foster and Ladds 2007). This proliferation process is not bound to one specific zone as seen in humans but it can be observed throughout the entire canine prostate. More often though proliferation in the canine prostate is observed from the peripheral terminal glands, thereby leading to an outward proliferation in every direction (Sun et al. 2017a).

The two lines of BPH therapy

The physiology behind the proliferative process of BPH and the BPH-associated symptoms can be pooled into two main groups: one being the hormonal influence on spontaneous proliferation of the prostate's cells (mainly thought of as being mediated by testosterone) and the other being the built-up tension by the stroma in hyperplastic prostates. These two groups simultaneously represent the two main lines of BPH therapy by either counteracting androgen availability in the prostate or reducing the smooth muscle tone of the prostate and releasing urethral constriction.

To reduce the androgen level in the prostate it is important to know that the principal androgen in this tissue is dihydrotestosterone (DHT) which has been converted from testosterone by 5α-reductase. A delicate balance is necessary to maintain a regular-sized prostate (Roehrborn 2008; La Vignera et al. 2016) with a multitude of regulatory components involved. In case of BPH, prostatic DHT levels (as well as testosterone levels) are observed to be higher than in normal or cancerous tissue (Pejčić et al. 2017), therefore disturbing the balance of cell growth and cell death in the prostate. One treatment option for BPH aims to reduce DHT levels by decreasing 5α-reductase-activity with 5α-reductase inhibitors, such as oral medication with finasteride or (in veterinary medicine) removing the testosterone all together (surgically or medically). In veterinary medicine, castration is a treatment option in case of BPH or prostate cancer. The thereby missing testosterone can stagnate the proliferative process of the prostate and even lead to a decrease of the prostate's size (Janthur 2016).

First line of treatment in human medicine for mild to moderate cases of BPH is aimed to relax the prevalent smooth muscle cells in the stroma of the prostate, thus reducing prostatic tension. There are a lot of different receptor types with a variety of agonists and antagonists that need to be considered. The first line of medical treatment in BPH patients is targeting the α1-adrenergic pathway with therapeutics such as tamsulosin (Silva et al. 2014a; Lee et al. 2017). Often a combination treatment with medical options targeting both underlying pathologies of BPH can be tried (e.g. 5α-reductase inhibitors + α1 antagonists).

If micturition disorders in a BPH patient are severe or the patient does not respond to medical treatment, often the transurethral resection of the prostate (TUR-P) is used to reduce the prostatic tissue compressing the urethra and the bladder (Portis and Mador 1997). This is accomplished by introducing a resector into the urethra and stripping away parts of the transition and periurethral zone by using a sling-formed electrode or a laser. At the end of the procedure the excessive prostatic material that could be removed is flushed out and thereby some pressure on the bladder and urethra can be relieved.

The epididymis

The epididymis is the connecting organ between the testis and the vas deferens on each side of the body. It mainly consists of a highly convoluted single duct, the epididymal duct, that transports and stores the spermatozoa received from the testis until ejaculation. The epididymis can be classified into three portions, the head or caput, the body or corpus and the tail or cauda. The caput epididymidis is structurally connected to the proximal end of the testis with the corpus running down alongside it and the cauda curving around to become the vas deferens on the opposite distal end of the testis. The epididymis is also wrapped in the serous tunica vaginalis testes attaching the epididymis to the testis (Lippert 2017; Schulte 2017).

The development of the epididymis starts in the 8th week of pregnancy with its formation arising from the Wolffian duct (Carlson 2014). During prenatal development the ductuli efferentes of the testis connect to the proximal portion of the epididymal duct, which is growing in length while simultaneously shortening by folding. There are two phases of convoluting the epididymal duct to its final heavily coiled form. First, the entirety of the duct is folded and then in a second step the folds are coiled to minimize the epididymal length even further. The coiling of the caput and corpus is mostly finalized during prenatal development whereas the coiling of the cauda epididymis is only finalized in the first days after birth (Hinton et al. 2011). In the same way connective tissue septa creating multiple compartments of the epididymis start growing prenatally but only finalize after birth. The epididymis undergoes the final development during puberty when the epithelium differentiates into the pseudostratified epithelium containing principal, basal, apical, narrow and clear cells (Arrotéia et al. 2012). The smooth muscle cells surrounding the epididymal duct also seem to undergo a developmental change after birth resulting in an increasing thickness of smooth muscle layers from thin in the caput to thicker in the cauda in the adult rat epididymis (Holstein 1969) (Fig. 6).

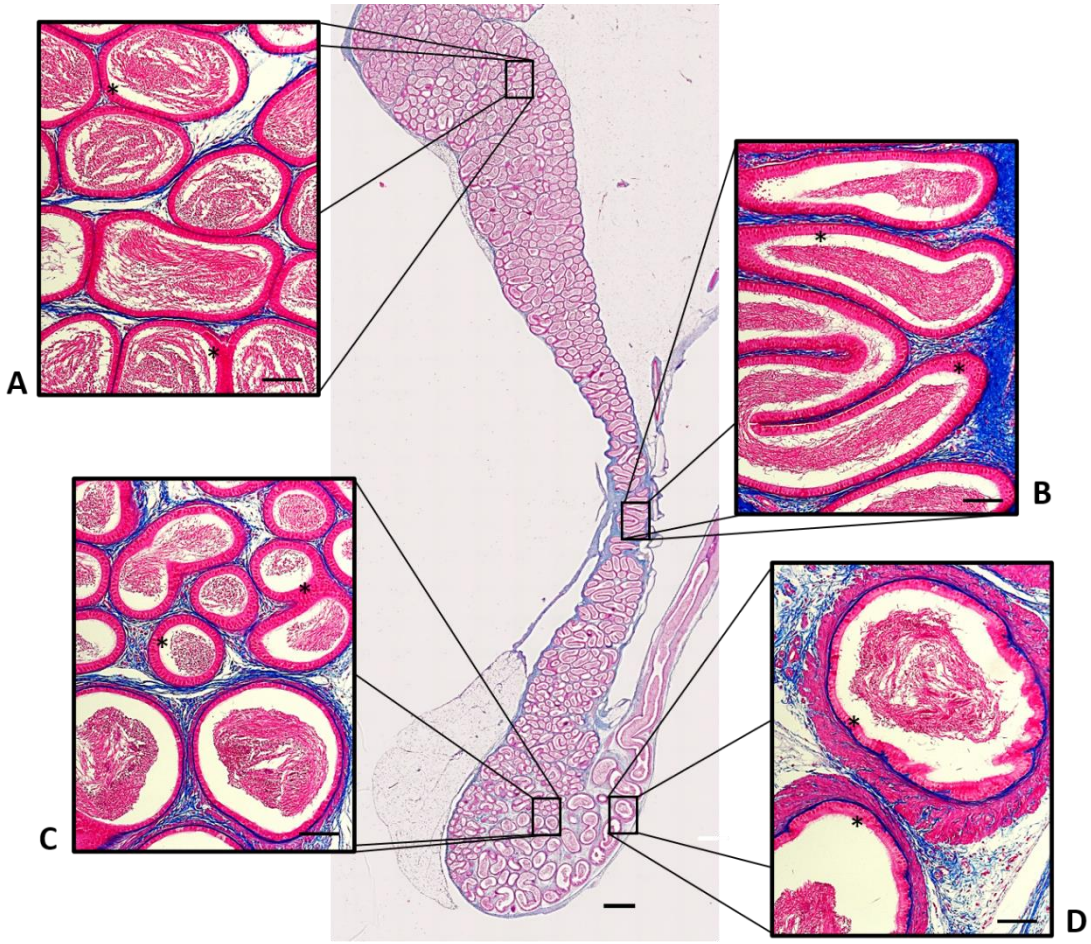

Figure 9: Histology of the adult rat epididymis

Overview of an AZAN-stained adult rat epididymis in the middle (scale bar: 1mm) with magnifications of the different regions (scale bar: 100 µm and epithelium (*)).

***A** magnification of caput epididymidis*
***B** magnification of corpus epididdymidis*
***C** magnification of proximal cauda epididymidis*
***D** magnification of the most distal part of the epididymis, close to the adjacent vas deferens*

Spontaneous contractions occur in the neonatal as well as in the adult epididymal duct and drive directional transport (Weiser et al. 2020). The spermatozoa arriving from the testis acquire motility and fertilizing ability while traveling through caput and corpus epididymis reaching the distal part of the cauda epididymidis where they are stored until ejaculation (Jones 1999). How exactly the spermatozoa acquire their mature status in not fully understood, but the microenvironment of the different segments (created by the connective tissue septa) supposedly is essential. Species-dependently the epididymal transit time varies from 5 to 15 days (Turner et al. 1990). The number of connective tissue septa and thus segments of the epididymis varies species-dependently as well.

Specifities of the human epididymis

The uncoiled human epididymal duct would be about 5 m long, while running alongside the testis it is convoluted to be only 5 cm in length (Lippert 2017). The number of connective tissue septa and therefore the number of segments (S) vary considerably in the human cauda epididymidis. For the purpose of this thesis the proposed classification of the human epididymis into 9 segments was used (Holstein 1969).

Specifities of the rat epididymis

The uncoiled rat epididymal duct reaches a length of 3,2 m (Turner et al. 1990) while in its anatomical position it is about 4 cm long. In the rat epididymis +/- 19 segments have been defined (Fig. 7) (Turner et al. 2003; Jelinsky et al. 2007).

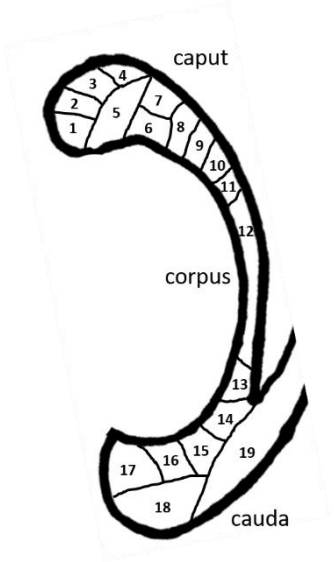

Figure 10: Segments of the rat epididymis

The ejaculatory process

Ejaculation consists of two main functional phases: the emission phase and the expulsion phase. During the emission phase contractions of the cauda epididymidis and vas deferens transport the spermatozoa into the proximal part of the urethra where they are mixed with the expulsed fluids from the accessory sex glands. In the second phase, the expulsion, this mixture is then transported outward by contractions of the urethra, exiting the body through the penis. All organs involved in the ejaculatory process are innervated through the autonomic nervous system. The ejaculatory reflex itself involves a multitude of receptors and pathways such as sensory receptors, afferent and efferent pathways as well as sensory and motor areas in the brain (McMahon et al. 2004).

Here, I would like to focus on the emission phase in which the sympathetic nervous system induces strong contractions in epididymis, vas deferens, prostate and other accessory sex glands depending on the species. These contractions seem to be mainly induced through activation of α-adrenergic receptors by the neurotransmitter norepinephrine (Michel 2007; Sanbe et al. 2007). Interestingly though, mice with all α-adrenoreceptor subtypes deleted were still able to reproduce resulting in a few successful pregnancies (Sanbe et al. 2007). For that and other reasons a multitude of effectors have been proposed to be involved in regulating the ejaculatory process such as dopamine, serotonin, acetylcholine, nitric oxide and oxytocin (McMahon et al. 2004; Alwaal et al. 2015).

Ejaculatory disorders - association to benign prostatic hyperplasia

Since, as mentioned above, there are several regulators involved in the ejaculatory process, there is a wide variety of possible etiologies of ejaculatory disorders. The main ejaculatory disorders are premature ejaculation, delayed ejaculation, retrograde ejaculation, anejaculation and anorgasmia (McMahon et al. 2004; Rowland et al. 2010). Premature and delayed ejaculation relate to the time passed until ejaculation is achieved and as such vary from man to man being partially consciously controlled. Anejaculation represents the true lack of ejaculate while retrograde ejaculation describes the occurrence of sperm in the bladder which is often thought of as being due to a lack of bladder neck contractility. Anorgasmia describes the lack of the cortical event of sensing muscle contractions and a sense of release after built-up tension (Rowland et al. 2010). Often ejaculatory disorders occur after nerve damage such as in spinal cord injuries (Ibrahim et al. 2016) or as a side effect of treatment with α-adrenoreceptor antagonists for high blood pressure or BPH (Narayan and Lepor 2001; Carbone and Hodges 2003). In both aspects the adrenergic system is inhibited. Therefore, there is a need for drugs targeting other pathways (such as oxytocin) in treating ejaculatory disorders.

Oxytocin

Oxytocin and its pathway

"Oxytocin (greek ὀξύς, oxys, and τοκετός , toketos, meaning "quick birth") has first been described in 1906 (by Sir Henry Dale) to have an uterotonic effect and was first synthesized in 1953 (by Vincent du Vigneaud (du Vigneaud et al. 1953)).

Oxytocin (OT) and oxytocin-like peptides are nonapeptides that occur in almost all vertebrate species. The oxytocin-family has a very similar structure to the arginine vasopressin (AVP)-family (differing only in the 3rd and 8th position), allowing either nonapeptide (coming from the OT-family or the AVP-family) to crosstalk with each receptor - especially in high concentrations (Song and Albers 2017). Therefore AVP-interactions must be considered when analyzing OT-effects (Barberis et al. 1998). It is important to note that both hormones and their receptors are encoded by different genes depending on the species, and thus exhibit species dependent structural and functional differences (Ivell et al. 1997). In both OT and AVP a disulfide bond between the two Cys residues at the 1st and 6th position results in a conformation of a 6 amino acid cyclic component with a 3 amino acid C-terminal part (Tom and Assinder 2010a; Tom and Assinder 2010b).

The oxytocin-receptor (OTR) and all three AVP-receptors (AVPR1A, AVPR1B and AVPR2) belong to the subfamily A6 of the rhodopsin-type (class I) G protein-coupled receptors and as such they consist of seven transmembrane helices, three intra- and three extracellular loops, an extracellular N-terminus and an intracellular C-terminus (Chini and Fanelli 2000; Gimpl and Fahrenholz 2001; Breton et al. 2001)." (Stadler et al. 2020).

"Coupling to different G-protein-subunits has been found to change OTR-signaling (q, i, s) (Gimpl and Fahrenholz 2001). Signaling pathways resulting from coupling via the $G\alpha_{q/11}$-subunit (present in smooth muscle cells) have been studied the most because of their presence in the myometrium and their established contribution to myometrial contractility. Other G-protein-subunits and their signaling pathways are gaining more attention because of their supposed proliferative (Busnelli et al. 2010) and anti-proliferative (Cassoni et al. 1994; Cassoni et al. 1996) effect using a multitude of signaling components (Chatterjee et al. 2016). Herein we focused on OTR signaling pathways suggested to be important in the male reproductive tract: smooth muscle contraction, and both proliferative and anti-proliferative processes (Lerman et al. 2018).

OTRs were found to change their downstream signaling pathway depending on their location inside or outside of caveolae. Activation of human OTR outside of caveolae resulted in inhibiting proliferation whereas inside of caveolae it resulted in promoting proliferation (Guzzi et al. 2002; Rimoldi et al. 2003).

It is important to note that activation of ERK 1/2 is present in both the proliferative and the anti-proliferative pathway and the resulting effect appeared to depend on the duration of activation. This activation seemed to be more persistent when the OTRs are located outside caveolar microdomains and inhibited cell growth by activating cell cycle inhibitor p21. In contrast ERK 1/2-activity was shorter when they were located inside caveolar microdomains resulting in cell growth (Rimoldi et al. 2003). In OT-treated cells the level of phosphorylated ERK 1/2 (compared to the total ERK 1/2) and MEK 1/2 (compared to the total MEK 1/2) in prostatic tissue was significantly higher than in the cultured cells used as a control (Xu et al. 2017b). The prevalence of OTRs inside caveolae has been found to be increased in BPH-tissue (Herbert et al. 2007). Both caveolin-1- and OTR-expression increase with age (Herbert et al. 2007) and their colocalization increases in BPH patients (Sendemir et al. 2008). In human cell culture experiments OT inhibited prostatic stromal cell proliferation but had no effect on prostatic epithelial cells when cultured alone. OT by itself had no effect on malignant cells, however, in combination with testosterone it stimulated androgen independent PC-3 cell growth (Whittington et al. 2007). Disruption of caveolae only removed the inhibitory effect of OT on the prostatic stromal cells but did not affect the stimulatory effect of OT on PC-3 cells cultured in the presence of androgens (Whittington et al. 2007). In prostate cancer tissue and malignant cell lines a stimulating cell proliferation was noticed resulting from movement of OTR out of caveolae onto lipid rafts accompanied by activation of alternative signal transduction pathways (Gould and Nicholson 2019).

There have been few investigations into the sensitization as well as desensitization of OTRs (Plested and Bernal 2001; Smith et al. 2006; Conti et al. 2009) and the activity of mRNA-transcription of the OTR (Kimura et al. 2003). The human OTR seems to be quickly (5-10min) internalized after activation (Gimpl and Fahrenholz 2001) – with both β-arrestin (Oakley et al. 2001) and clathrin (Smith et al. 2006) identified as being important in the internalization process. Newly discovered aspects of G-coupled receptors have been gaining increased attention such as the possibility of dimerization activation and biased activation (Wang et al. 2018; Smith et al. 2018). To date, there have been limited studies investigating the possibility of OTRs occurring as homo- or heterodimers (with the AVP-receptor) and oligomers (Terrillon et al. 2003; Devost and Zingg 2004) which opens up novel approaches for the development of targeted OT-agonists and -antagonists (Busnelli et al. 2016) and should receive more attention in the future. Similar attention should be given to exploring biased activation such as for example atosiban (more in chapter “Oxytocin-agonists and –antagonists”)(Reversi et al. 2005).

Oxytocinases such as cystinyl aminopeptidase (CAP) (also known as insulin-regulated aminopeptidase (IRAP) or human placental leucine aminopeptidase (PLAP)) are enzymes which cleave OT (making it inactive) and thereby attenuate the effect of OT over time (Tsujimoto et al. 1992). One study found that androgen levels seemed to regulate a putative member of the oxytocinase family of proteins in the epithelial cells of the rat prostate (Arenas and Pérez-Márquez 2002). One study showed that prostatic OT-levels as well as IRAP-specific-activity increased in the rat prostate after treatment with the α-1-

blocker doxazosin which is used in the treatment of BPH. This might point to the so far underappreciated role of oxytocinases in regulating OT-levels (Saníger et al. 2011).“ (Stadler et al. 2020).

Some of the oxytocin signaling pathways relevant for the male reproductive tract are depicted in F. 11.

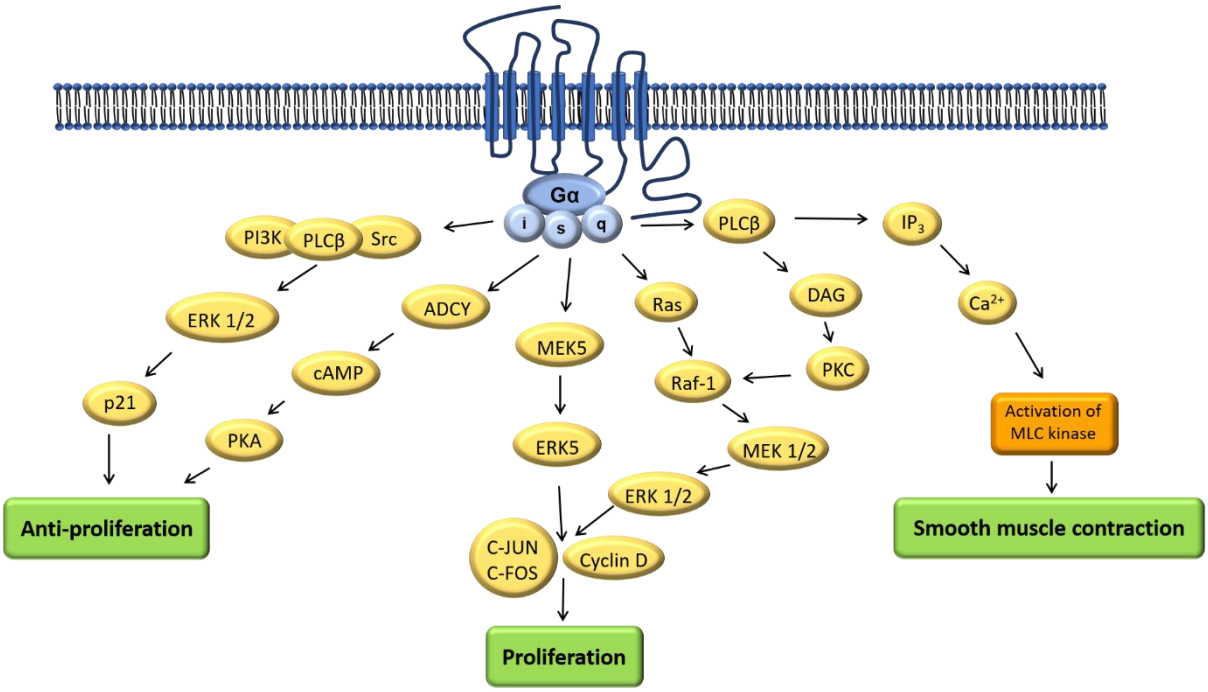

Figure 11: Signaling pathways of the oxytocin receptor modified from (Lerman et al. 2018) and extracted from (Stadler et al. 2020).

Oxytocin systemic and local

"OT as well as AVP are known to be synthesized in the hypothalamus as part of a larger pro-hormone (with carrier protein neurophysin I for OT and neurophysin II for AVP), stored in the posterior pituitary gland and released into the blood stream as a hormone. Neurophysin is responsible for proper packaging and storage of OT before systemic release (Gimpl and Fahrenholz 2001; Whittington et al. 2004).

Additional tissue specific local production of OT has been suggested to occur in multiple organs (Murphy et al. 1993) where local OT-levels surpass the plasma OT-levels (Thackare et al. 2006). Local production of OT in the human male reproductive tract has been identified via immunostaining for neurophysin I, radioimmunoassay or the detection of mRNA of the OT-gene in the testis (Nicholson et al. 1984) and prostate (Whittington et al. 2004). However, multiple studies in different animal species have shown controversial OT- as well as OTR-expression(Pickering et al. 1990) (Table 1). For example, a study in the marmoset monkey using immunohistochemistry staining (IHC) and detection of mRNA only found OT and OTR being synthesized in the testis but found no convincing evidence for local synthesis in the epididymis or prostate (Einspanier and Ivell 1997). Studies in rams (Knickerbocker et al. 1988) suggested that there is no local production of OT in the epididymis, but that the OT produced by the testis is resorbed in the epididymis (predominantly in the caput). Available evidence suggests this is a maturity related process, since circulating OT-levels in rams of different age groups did not alter, but testicular OT concentrations significantly increased with onset of spermatogenesis (with the main staining for neurophysin I found in Leydig cells, only weak staining in Sertoli cells) and OT was found to be present throughout the epididymis declining in concentration from caput to cauda in all but prepubertal animals. AVP-levels did not change in relation to maturation (Assinder et al. 2000). A ligation experiment of efferent ducts in rats (thereby cutting off an OT supply by the testis) suggested that OT in the caput epididymis might not be exclusively from the testis (Harris et al. 1996). Interestingly, androgens appear to inhibit OT-synthesis in the rat epididymis (Harris et al. 1996). In stallions no evidence for local production of OT in either testis or epididymis was found (Watson et al. 1999). In the marsupial bandicoot immunoreactive oxytocin and mesotocin were present in the ventral prostate but only oxytocin was found in the testis (Gemmell and Sernia 1989)." (Stadler et al. 2020).

Mesotocin is an oxytocin-like peptide present in non-mammalian vertebrates and most marsupials.

The relevance of possible crosstalk between oxytocin and arginine vasopressin

"A multitude of studies have investigated the selectivity of the neurohypophysial hormones and have shown crosstalk between the hormone OT and the AVP-receptors, as well as AVP and the OTR using a variety of techniques (e.g. IHC, immunofluorescence, western blot) in different species (Barberis et al. 1998; Akerlund et al. 1999; Song and Albers 2017). Importantly, these results taken together indicate that experiments conducted in for example rodents, might not translate to humans. Existing data suggest that AVP has a similar affinity to OT- and AVP-receptors whereas OT has a higher affinity to its own receptor than to AVP-receptors. AVPR1A might also play an important role in OT-mediated contractility as demonstrated in human myometrium (Wing et al. 2006) and the "ejaculatory tissue" (prostatic urethra, bladder neck and ejaculatory duct) of rats and rabbits (Gupta et al. 2008). The similarities of the two nonapeptides and their receptors, and their demonstrated potential to crosstalk underpins current interest in finding more selective OT- and AVP-agonists and -antagonists especially when administering the drug systemically (Hicks et al. 2014). Nevertheless, the classic roles of both peptides are still preserved; where OT is associated with contractile effects and social bonding whereas AVP is associated with water homeostasis and blood pressure regulation. OT acting through AVP-receptors in addition to its own receptor, might account for some of the observed OT side effects because of their possible relation to homeostasis (headache and dizziness). This cross-reactivity may also explain why, although AVP was described to show similar contractile potential as oxytocin in the male reproductive tract, it might also lead to more severe side effects because of its more prevalent effect on the kidney and vasculature. These observations provide further weight for the development of highly specific OTR-agonists and -antagonists. Still there is at least one AVP-antagonist that has shown some contractile potential (SR 49059) in the male reproductive tract (Gupta et al. 2008) (more in chapter "Oxytocin-agonists and –antagonists"." (Stadler et al. 2020).

Receptor distribution and consideration of colocalization

"Only one OTR-isoform is known to be expressed throughout different tissues. It has been demonstrated by western blotting (WB), real time polymerase chain reaction (RT-PCR) or IHC that the OTR in the human male reproductive tract is present in the testis (Frayne and Nicholson 1998; Filippi et al. 2002b), epididymis (Filippi et al. 2002b) and prostate (Frayne and Nicholson 1998; Filippi et al. 2002b; Sendemir et al. 2008). The OTR was further localized via IHC, immunofluorescence (IF) and WB to the interstitial Leydig cells and Sertoli cells of the testis (Frayne and Nicholson 1998) and the epithelial and stromal cells of the prostate (Whittington et al. 2004; Xu et al. 2017b; Gould and Nicholson 2019).

Although another study in the marmoset monkey using IHC and detection of mRNA only found OT and OTR to be synthesized in the testis but found no convincing evidence for being synthesized in the epididymis or prostate (Einspanier and Ivell 1997). In the tammar wallaby mesotocin receptors were found in the prostate, but not in the testes (Parry and Bathgate 1998). In rams OTRs were found in Leydig as well as Sertoli cells and throughout the epididymis (Whittington et al. 2001). Some hypotheses state that OTRs are present in the epithelium of the epididymal duct and that OT partially mediates its contractile effect in the epididymis by regulating the release of endothelin-1(ET-1) (Filippi et al. 2002b; Filippi et al. 2003; Filippi et al. 2005; Vignozzi et al. 2008) which in turn is estrogen-dependent (Filippi et al. 2002a; Filippi et al. 2005). Furthermore estrogen might influence epididymal contractility by upregulating the shared downstream signaling pathway (RhoA\ROCK) of the OTR and ET-1-receptor (Fibbi et al. 2009). The role of estrogens in the oxytocin system has been reviewed (Ivell and Walther 1999) and some hypothesize that estrogens modulate the expression of the neuropeptide gene for oxytocin (Richard and Zingg 1990; Koohi et al. 2005). One study found that OT and OTR are present in a subpopulation of GnRH neurons and OT might therefore influence neuronal activity centrally (which was independent of estrogen) (Caligioni et al. 2007). Androgen-binding protein and OT were colocalized in the reproductive tract of male rats (Herbert et al. 2005). Androgen receptor and OTR colocalization was upregulated in androgen-independent human prostate cancer cells (Gould and Nicholson 2019).“ (Stadler et al. 2020).

		OT	OTR
Testis	Human	— OT (cDNA library screening and NB) (Ivell et al. 1990) Ø OT (PCR) (Ivell et al. 1990) + OT and nI (RIA) (Nicholson et al. 1984)	+ (WB) (Frayne and Nicholson 1998) + in Leydig and Sertoli cells (IHC) (Frayne and Nicholson 1998) + (RT-PCR) (Filippi et al. 2002b)
	Marmoset	+ OT and nI in Leydig cells (IHC) (Einspanier and Ivell 1997) (+) OT and nI in Sertoli cells (IHC) (Einspanier and Ivell 1997) + mRNA (RT-PCR) (Einspanier and Ivell 1997)	+ (RT-PCR) (Einspanier and Ivell 1997) + in Leydig cells (IHC) (Einspanier and Ivell 1997)
	Macaque		+ (WB) (Frayne and Nicholson 1998) + in Leydig and Sertoli cells (IHC) (Frayne and Nicholson 1998)
	Mouse		+ (RT-PCR) (Anjum et al. 2018)
	Rat	+ OT and nI (RIA) (Nicholson et al. 1984) + OT, but — nI in Leydig cells (IHC) (Guldenaar and Pickering 1985) + OT in interstitial cells (RIA) (Nicholson et al. 1987) + OT in Leydig cells (IHC) (Yeung et al. 1988) + OT in Leydig cells (RIA) (Nicholson and Hardy 1992) (+) OT mRNA (PCR) (Foo et al. 1991)	+ (WB) (Whittington et al. 2004)
	Sheep	(+) probably in Sertoli cells mRNA (NB) (Ungefroren et al. 1994) + OT and nI in Leydig cells (IHC) (Ungefroren et al. 1994) + OT (RIA) (Assinder et al. 2000) + OT and nI (IHC) (Assinder et al. 2000) + nI (WB) (Assinder et al. 2000)	+ (WB) (Whittington et al. 2001) + in Leydig and Sertoli cells (IHC) (Whittington et al. 2001)
	Goat	+ mRNA (RT-PCR) (Inaba et al. 1999)	

		(+) OT and nI (IHC) (Inaba et al. 1999) + OT and nI in Sertoli cells (IHC) (Inaba et al. 1999)	
	Cow	(+) probably in Sertoli cells mRNA (NB) (Ungefroren et al. 1994) + OT and nI in Leydig cells (IHC) (Ungefroren et al. 1994)	
	Horse	+ OT, but — nI (IHC) (Watson et al. 1999)	
	Rabbit		+ (RT-PCR) (Filippi et al. 2002b)
	Marsupials	Bandicoot: + OT (not mesotocin) in Leydig cells (IHC) (Gemmell and Sernia 1989)	Wallaby: — (RT-PCR) (Parry and Bathgate 1998)
Epididymis	Human		+ (RT-PCR + WB + IHC) (Filippi et al. 2002b)
	Marmoset	— OT and nI (IHC) (Einspanier and Ivell 1997) (+) OT mRNA (RT-PCR) (Einspanier and Ivell 1997)	+ mRNA (RT-PCR) (Einspanier and Ivell 1997) (+) (IHC) (Einspanier and Ivell 1997)
	Macaque		+ (WB) (Frayne and Nicholson 1998)
	Rat	+ OT (declining from caput to cauda) (IHC + RIA) (Harris et al. 1996)	
	Sheep	+ OT (declining from initial segment or caput to cauda) (IHC) (Knickerbocker et al. 1988; Assinder et al. 2000) Ø nI (IHC) (Assinder et al. 2000) + nI (WB) (Assinder et al. 2000) — nI (IHC) (Knickerbocker et al. 1988)	+ (WB) (Whittington et al. 2001) + (IHC) (Whittington et al. 2001)
	Cow		+ (IHC) (Mewe et al. 2007) + (RT-PCR) (Mewe et al. 2007)
	Horse	+ OT (IHC) (Watson et al. 1999) — nI (IHC) (Watson et al. 1999)	
	Rabbit		+ (RT-PCR)(Filippi et al. 2002b)

	Marsupials		Wallaby: + (RT-PCR) (Parry and Bathgate 1998)
Vas deferens	Marmoset	— OT mRNA (RT-PCR) (Einspanier and Ivell 1997) — OT and nI (IHC) (Einspanier and Ivell 1997)	+ mRNA (RT-PCR) (Einspanier and Ivell 1997) (+) (IHC) (Einspanier and Ivell 1997)
	Rabbit		+ (RT-PCR)(Filippi et al. 2002b)
	Sheep		+ (IHC) (Whittington et al. 2001)
Prostate	Human	+ nI (IHC) (Whittington et al. 2004) In epithelial + stromal cells: + OT (intensity dependent on disease) (IHC) (Whittington et al. 2004; Xu et al. 2017b) BPH- and cancer tissue: + nI (WB) (Whittington et al. 2004)	+ (WB) (Frayne and Nicholson 1998) + (RT-PCR) (Filippi et al. 2002b) + (IHC) (Sendemir et al. 2008) In epithelial + stromal cells: + (WB) (Whittington et al. 2004; Gould and Nicholson 2019) + (IHC) (Whittington et al. 2004; Xu et al. 2017b) + (IF) (Xu et al. 2017b; Gould and Nicholson 2019) BPH- and cancer tissue: + (IHC) (Sendemir et al. 2008; Xu et al. 2017b) + (WB) (Whittington et al. 2004) + (IF) (Gould and Nicholson 2019)
	Marmoset	— OT and nI (IHC) (Einspanier and Ivell 1997) — OT mRNA (RT-PCR) (Einspanier and Ivell 1997)	+ mRNA (RT-PCR) (Einspanier and Ivell 1997) (+) in epithelial cells (IHC) (Einspanier and Ivell 1997) — in stromal cells (IHC) (Einspanier and Ivell 1997)
	Macaque		+ (WB) (Frayne and Nicholson 1998)
	Rat		+ (RT-PCR + WB) (Assinder et al. 2004)

			In epithelial and stromal cells: + (IHC + ARG)(Assinder et al. 2004)
	Rabbit		+ (RT-PCR) (Filippi et al. 2002b)
	Marsupials	Bandicoot: + OT (+ mesotocin) (IHC) (Gemmell and Sernia 1989)	Wallaby: + (RT-PCR) (Parry and Bathgate 1998)
Seminal vesicles	Marmoset	— OT and nI (IHC) (Einspanier and Ivell 1997)	— (IHC) (Einspanier and Ivell 1997)
	Rabbit		+ (RT-PCR) (Filippi et al. 2002b)

Table 1: Expression of OT and OTR in male reproductive tissues of different species

Modified from (Stadler et al. 2020)

(+ = positive; (+) = weak positive; — = negative; Ø = inconclusive; nI = neurophysin I; IHC = immunohistochemistry; IF = immunofluorescence; (RT-)PCR = (real time) polymerase chain reaction; RIA = radioimmunoassay; NB = northern blot (hybridization); WB = western blot; ARG = autoradiography)

	Effect on smooth muscle contractility	Effect on cell proliferation	Other effects
Testis	+ mouse (Nicholson et al. 1986) + rat at spermatogenesis stage VII-VIII (Harris and Nicholson 1998) Ø rat at spermatogenesis stage IV-V (Harris and Nicholson 1998) Ø rat, rabbit (Gupta et al. 2008)	<u>Spermatogenesis:</u> + rabbit spermatogonia (Melin 1971) Ø mouse (Assinder et al. 2002) + mouse (Anjum et al. 2018)	<u>After OT-addition:</u> Less degeneration of spermatocytes during meiosis in rats (Melin 1971) + spermatozoa output in sheep (Voglmayr 1975; Whittington et al. 2001) + OTR-expression (Anjum et al. 2018)
Epididymis	+ rat caput (Hib 1977; Studdard et al. 2002) Ø rat caput (Jaakkola and Talo 1981) + cow caput (Mewe et al. 2007) — cow corpus (Mewe et al. 2007) + rabbit cauda (Melin 1970) + sheep cauda (Knight 1974) Ø rat cauda (Jaakkola and Talo 1981) + mouse cauda (Hib 1974a; Hib 1974b) — cow proximal cauda (Mewe et al. 2007) + cow mid- and distal cauda (Mewe et al. 2007)		<u>tissue that had been blocked by an α-adrenergic-antagonist:</u> + ram cauda (while norepinephrine could not) (Knight 1974)

<table>
<tr><td></td><td>Ø rat, rabbit (not specified which part) (Gupta et al. 2008)</td><td></td><td></td></tr>
<tr><td>Vas deferens</td><td>+ sheep (Knight 1974)
Ø rat, rabbit (Gupta et al. 2008)
Ø cow (Mewe et al. 2007)
– rat (Beneit et al. 1980)</td><td></td><td></td></tr>
<tr><td>Prostate</td><td>+ human (BPH tissue) (Bodanszky et al. 1992),
+ rat, dog, guinea pig (Bodanszky et al. 1992; Sharaf et al. 1992)
Ø rat, rabbit (Gupta et al. 2008)</td><td>
<table>
<tr><td></td><td><u>Without gonadal steroids</u></td><td><u>With gonadal steroids</u></td></tr>
<tr><td><u>Human prostatic stromal cells (PrSC)</u></td><td>– (Whittington et al. 2007)
+ (Xu et al. 2017b)</td><td>– (Whittington et al. 2007)</td></tr>
<tr><td><u>Human prostatic epithelial cells (PrEC)</u></td><td>Ø (Whittington et al. 2007)
+ (Xu et al. 2017b)</td><td>Ø (Whittington et al. 2007)</td></tr>
<tr><td><u>PrSC (co-cultured with PrSC)</u></td><td>Ø (Whittington et al. 2007)</td><td>– (Whittington et al. 2007)</td></tr>
</table>
</td><td><u>5α-reductase-activity:</u>
+ PrEC but not in PrSC (Assinder 2008)

<u>Prostate size after OT injection:</u>
+ in castrated rats (Popović et al. 1990; Plećas et al. 1992)
+ in mice (Xu et al. 2017b)

<u>OTR-expression:</u>
+ in BPH-tissue (Frayne and Nicholson 1998; Sendemir et al. 2008; Xu et al. 2017b; Li et al. 2018b)
+ with age (Herbert et al. 2007; Sendemir et al. 2008)
+ in cancer tissue (Xu et al. 2017a)</td></tr>
</table>

		Androgen independent malignant cells (PC-3)	+ (Gould and Nicholson 2019) Ø (Whittington et al. 2007; Xu et al. 2017a)	+ (Whittington et al. 2007) Ø (Gould and Nicholson 2019)	— after OT-addition in PC-3 cells (Gould and Nicholson 2019) Ø after OT addition in PrEC (Gould and Nicholson 2019) OT concentration: + in BPH-tissue (Nicholson 1996; Whittington et al. 2004; Xu et al. 2017b) + in cancer tissue (Xu et al. 2017a) + in serum of BPH-patients (Xu et al. 2017b)
Seminal vesicles	Ø rat (Hib et al. 1983) + rat, dog, guinea pig (Sharaf et al. 1992) Ø rat, rabbit (Gupta et al. 2008)				

Table 2 : Overview of the effect of OT on the male reproductive tract

(+ = increasing; — = decreasing; Ø = no effect), modified from (Stadler et al. 2020)

Oxytocin related to emission and copulation

Research investigating oxytocin (OT) for its effects on ejaculate volume, sperm count and altered plasma OT-levels after stimulation of reproductive organs goes back as far as the 60s and 70s (for further details please see (Stadler et al. 2020)). The effect of OT on the contractility of the epididymis is summarized with respect to species and region of the epididymis investigated (Table 2).

The effect of oxytocin on the contractility of the epididymis

"Due to its role in propelling the sperm forward during the emission phase of the ejaculatory process, the epididymis was studied for its contractile responses to OT and AVP (Table 2). Special interest was paid to the contractile effect of the cauda epididymis which was found to either increase in frequency and amplitude in the mouse (Hib 1974a; Hib 1974b), rat (Hib 1977), rabbit (Melin 1970) and ram (Knight 1974) or to have no effect in the rat and rabbit (Gupta et al. 2008). One study in the rat found that OT had little to no effect, while AVP increased both frequency and tension in caput and cauda epididymis (Jaakkola and Talo 1981). Other studies found that both OT and AVP had an increasing effect on the contractility of the initial segment of the rat epididymis (Studdard et al. 2002) and AVP to be less effective than OT in ram cauda epididymis (Knight 1974). Interestingly, Knight also found that in ram cauda epididymis OT was able to contract tissue that had been blocked by an α-adrenergic-antagonist while norepinephrine could not (Knight 1974). A study in bulls demonstrated different reactions to norepinephrine and OT depending on the area of the epididymal duct investigated (Mewe et al. 2007). Both had similar positive effects in caput and cauda, whereas OT had a relaxing effect on corpus and proximal cauda epididymis. NE had a much bigger effect on the vas deferens of the bull than OT (Mewe et al. 2007). Other studies found OT to have either no effect in the vas deferens of rat and rabbits (Gupta et al. 2008), depress the contractile response in the rat (Beneit et al. 1980) or increase contractility in the ram (Knight 1974)." (Stadler et al. 2020).

"Despite all of OT's involvement in male and female reproductive functions OT-deficient mice had no defects concerning mating behavior, conception, pregnancies, litter size and labor (Nishimori et al. 1996), suggesting that either OT is only supporting reproductive functions or maybe that another OT-like agent is acting at the OTR in OT-deficient mice. However, OT was found to be essential for milk ejection (Cross 1955; Bisset et al. 1967). Without OT milk will still be secreted but will no longer be

ejected into the collecting ducts of the mammary glands which results in a lack of milk available for breastfeeding (Nishimori et al. 1996) and ultimately the death of the offspring.“ (Stadler et al. 2020).

Oxytocin in the prostate

In the prostate the effect of OT can be divided into contractile effects and proliferative effects (Table 2) (for proliferative effects please see (Stadler et al. 2020)). The oxytocin receptor (OTR) was detected in the stroma or the epithelium or both depending on the species and detection method used (Table 1).

The effect of oxytocin on the contractility of the prostate

“In organ bath studies OT has been shown to have an increasing effect on the spontaneous prostatic contractions as well as prostatic tone in guinea pig, rat, dog and human prostate (Bodanszky et al. 1992). The OT-induced contractions in the prostate were characterized as being slower and longer lasting than those induced by norepinephrine (Sharaf et al. 1992) in the guinea pig, rat and dog. While the first study found AVP to be less effective than OT, the second study found it to be more effective. More recently one study found no effect of either OT nor AVP on the tone or contractility of the prostates of rats and rabbits (Gupta et al. 2008).“ (Stadler et al. 2020).

Oxytocin-agonists and -antagonists

In search of desirable attributes such as receptor selectivity, potency, heat-stability (Beard et al. 2018; Chan et al. 1987) or bioavailability (Borthwick 2010) numerous oxytocin-agonists and antagonists were developed (for more details see (Stadler et al. 2020)). Designing new oxytocin-agonists and -antagonists started by small changes to the peptide structure (Hruby et al. 1990) (Fig. 12) but eventually much smaller non-peptide molecules were developed through drug discovery paradigms (Fig. 13).

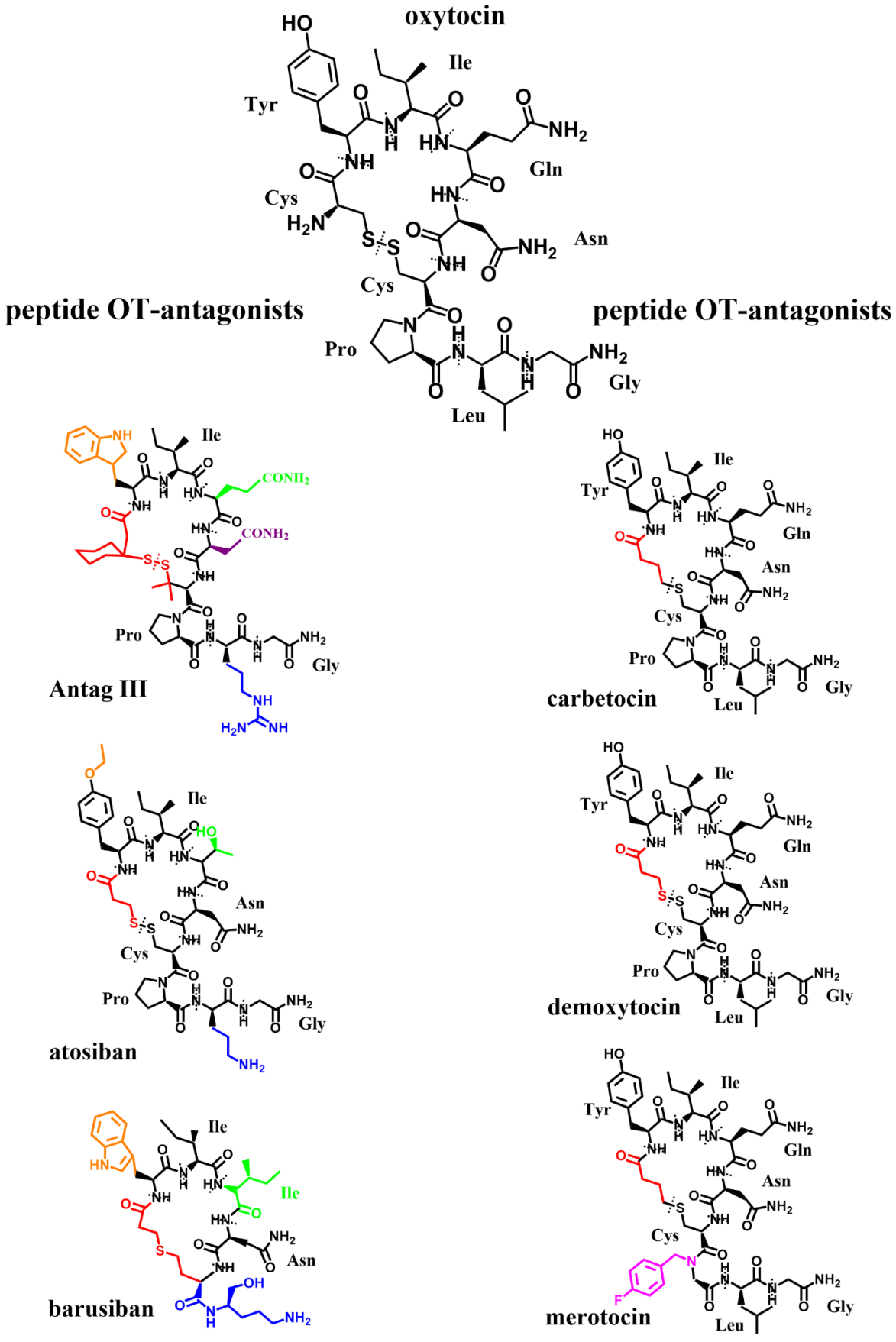

Figure 12: Chemical structures of peptide oxytocin-agonists and -antagonists (Stadler et al. 2020)

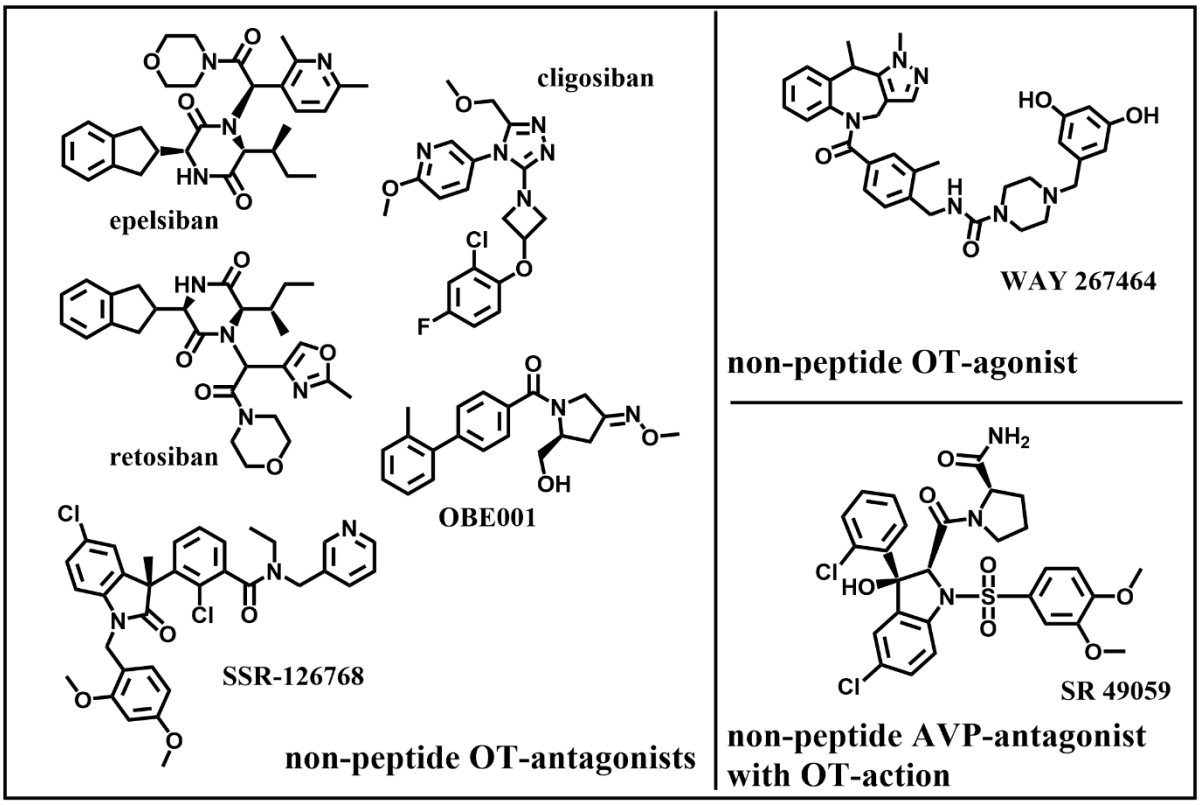

Figure 13: Chemical structures of non-peptide oxytocin-agonists and antagonists (Stadler et al. 2020)

"Promising agonists:

- The peptide carbetocin is used in several countries to restore uterine tone and prevent hemorrhage after cesarean section or to treat postpartum hemorrhage. Since recent studies show carbetocin not to be dependent on cold storage such as OT, carbetocin might prove essential in postpartum care in lower income countries while showing similar efficacy and safety as OT (Peters and Duvekot 2009; Widmer et al. 2018) or even more effectiveness (Attilakos et al. 2010; Hunter et al. 1992; Rath 2009) with less side effects in clinical trials (Barua et al. 2017). Carbetocin and its metabolites carbetocin metabolite I and II are shown to display the same binding affinity to the OTR as OT, however carbetocin's maximal contractile effect was 50% lower than OT's, carbetocin metabolite I and II had no contractile effect at all. Interestingly, all three compounds showed antagonistic properties at the OTR in vitro, making carbetocin a partial agonist/antagonist and also demonstrated some affinity to bind to the AVPR1A (Engstrøm et al. 1998).

- The peptide demoxytocin showed no superiority to PGE2-treated women in a clinical trial (whereas OT did) and induced more gastrointestinal side effects (Westergaard et al. 1983)

- WAY-267464 is a potent, selective, non-peptide OTR-agonist that showed a similar anxiolytic-like profile as OT (Ring et al. 2010).

Promising antagonists:

- The peptide atosiban is a competitive AVP/OTR-antagonist by inhibiting OT-induced IP3-release. Atosiban is the only OT-antagonist that is prescribed and is indicated as a therapeutic to delay preterm birth. Recent studies suggest that atosiban shows similar effectiveness in delaying preterm labor compared to β2-tocolytics although it appears that atosiban has less side effects (nausea, headache, dizziness, tachycardia, hyperglycaemia) than β2-tocolytics (Flenady et al. 2014; Tsatsaris et al. 2004). Studies could not find a significant difference to placebo-treated controls (Romero et al. 2000). Atosiban was found to have no effect on human sperm motility in vitro (Pierzynski et al. 2007). It has been suggested that atosiban's anti-proliferative effect in some cancer cell lines (including prostate cancer) might be due to a biased agonistic effect where atosiban blocks OT binding to $G\alpha_{q/11}$ coupling and thereby promotes OT-coupling to $G\alpha_i$ which leads to inhibition of cell growth (Reversi et al. 2005).

- The peptide barusiban is a selective OT-antagonist with a high selectivity for the OTR. Despite being reported to inhibit OT-related contractility as potent as atosiban (Pierzynski et al. 2004) or even more potent (Reinheimer et al. 2005; Nilsson et al. 2003), barusiban has failed to show effectiveness in human clinical trials so far (Thornton et al. 2009).

- Retosiban (GSK221149A) is a highly selective, orally active, non-peptide OTR-antagonist that inhibits OT-induced uterine contractions (McCafferty et al. 2007) and showed efficacy in human clinical trials (Thornton et al. 2015).

- OBE001 is an orally active, non-peptide OT-antagonist that is tested for management of preterm labor and showed no adverse effects on early embryonic development in the rat model (Pohl et al. 2016).

- The peptide TT-235 (Antag III) is a long-acting, competitive OT-antagonist that may inhibit the uterine response to OT by decreasing OTR-numbers and -affinity and therefore shows a prolonged activity in comparison to OT (Ahn et al. 2004).

- SSR-126768A is an orally active, selective, non-peptide OT-antagonist with a long duration of action as a tocolytic in the management of preterm labor (Serradeil-Le Gal et al. 2004).

- Relcovaptan (SR 49059) is an orally active, non-peptide AVP1A-receptor selective antagonist that also showed tocolytic properties in treatment of preterm labor (Steinwall et al. 2005) and was able to potently antagonize OT's effect in the rat and rabbit ejaculatory tissues (prostatic urethra, bladder neck and ejaculatory duct) (Gupta et al. 2008).

- Cligosiban is a potent, brain-penetrating, highly selective, non-peptide OT-antagonist that inhibited apomorphine-induced ejaculation in the rat (Wayman et al. 2018). In a human clinical trial however it failed to prove efficacy (Althof et al. 2019).

- Epelsiban (GSK557296) is a non-peptide OT-antagonist that dose-dependently inhibited ejaculations in rats both peripherally and centrally (Clément et al. 2013). In a human clinical trial however it failed to prove efficacy (Shinghal et al. 2013).

Both (cligosiban and epelsiban) might still prove valuable as a new treatment option in case of premature ejaculation." (Stadler et al. 2020).

Aim of this study

This study aims to investigate the effect of oxytocin on the contractility of the prostate and epididymis comparing rat and human tissue. For this purpose, live imaging will be used to monitor the change in movement of the different tissues in relation to oxytocin addition:

- In the prostate the effect of oxytocin will be observed and compared in human tissue obtained through either transurethral resection of the prostate for the treatment of benign prostatic hyperplasia or through prostatectomy resulting from prostate cancer. Simultaneously the effect of oxytocin will also be investigated in rat ventral prostate.
- The effect of oxytocin in the epididymis will be investigated in multiple defined segments of adult and neonatal rat epididymis comparing the effect of oxytocin in the different segments to each other following the hypothesis that oxytocin might play a role in the ejaculatory process and therefore help drive sperm expulsion from the cauda epididymidis. Simultaneously the effect of oxytocin will also be investigated in human epididymis.
- The segment with the biggest effect will be used to distinguish if the observed oxytocin effect is mainly mediated through its own receptor or through the structural similar arginine vasopressin receptor.
- Since the adrenergic pathway is thought of as being the main contractile mediator in the male reproductive tissue, the observed results with oxytocin will be put into contrast to experiments targeting the adrenergic pathway.
- Experiments with different antagonists will be performed to evaluate oxytocin-based medications for their usability in treating male reproductive disorders (benign prostatic hyperplasia and ejaculatory disorders).

This study will use immunostaining to visualize oxytocin receptor distribution in relation to smooth muscle cells in the prostate and epididymis of both human and rat.

In addition, piloting preliminary experiments using injection methods, micro-CT imaging and histology will be implemented to investigate the structural and histological fine structure of the human prostatic duct system evaluating if there are any indications for functional differences of the prostatic ducts.

Materials and Methods

Materials

Tissues

Tissue	Species	Origin	Ethics number
Prostate with adjacent tissue	Human	Body donors of the Institute of Anatomy and Cell Biology, Justus-Liebig-University (JLU), Giessen	AZ 129/14 Ethic committee of the faculty of medicine, JLU, Giessen
Prostate (n=6)	Human	Transurethral resection of the prostate for benign prostatic hyperplasia, Department of Urology, Pediatric Urology and Andrology of the JLU, Giessen	AZ 55/13 Ethic committee of the faculty of medicine, JLU, Giessen
Prostate (n=6)	Human	Prostatectomy for prostate cancer, Department of Urology, Pediatric Urology and Andrology of the JLU, Giessen	AZ 123/12 Ethic committee of the faculty of medicine, JLU, Giessen
Epididymis (n=3)	Human	Semicastration for testis cancer Department of Urology, Pediatric Urology and Andrology of the JLU, Giessen	AZ 152/16 Ethic committee of the faculty of medicine, JLU, Giessen
Prostate (n=3)	Rat 6-8 weeks old (Wistar)	Institute for Physiology, JLU, Giessen	JLU-Nr.: 469_M, 510_M Animal welfare office Giessen
Prostate (n=2)	Rat 6-8 weeks old (Wistar)	Institute for Physiology, JLU, Giessen	JLU-Nr.: 505_M, 506_M, 507_M
Epididymis (neonatal)	Rat 4 days old	Institute for Veterinary Physiology and Biochemistry, JLU, Giessen	JLU-Nr.: 580_M

(n=9)	(Wistar)		Animal welfare office Giessen
Epididymis (n=19)	Rat 6-8 weeks old (Wistar)	Institute for Veterinary Physiology and Biochemistry, JLU, Giessen	JLU-Nr.: 487_M Animal welfare office Giessen
Epididymis (n=15)	Rat 6-8 weeks old (Sprague Dawley)	Monash Institute of Pharmaceutical Sciences (MIPS), Melbourne	MIPS 2018-14149 Animal welfare office Melbourne

Devices

Leica TP1020 tissue processor	Leica Microsystems GmbH, Wetzlar, Germany
Microtome, RM2255	Leica Microsystems GmbH, Wetzlar, Germany
Medax 23001, Tissue Float Bath	Medax GmbH + Co. KG, Rendsburg, Germany
Medax 12801, Slide Warmer	Medax GmbH + Co. KG, Rendsburg, Germany
CO_2 Incubator ICO	Memmert GmbH + Co. KG, Schwabach, Germany
High-temperature Incubator	Heraeus, Hanau, Germany
Motic® dissection microscope	Motic Deutschland GmbH, Wetzlar, Germany
Olympus BX50WI microscope	Olympus Corporation, Tokyo, Japan
Leica DM5000 B microscope Germany	Leica Microsystems GmbH, Wetzlar,
Nikon® Eclipse Ti microscope	Nikon Instruments Inc., Melville, USA
Olympus BX51 fluorescence microscope	Olympus Corporation, Tokyo, Japan
Axioskop 2 plus fluorescence microscope	Carl Zeiss AG, Munich, Germany

Hamamatsu ORCA-Flash4.0 digital camera (C11440)	Hamamatsu Phototonics Deutschland GmbH, Geldern, Germany
Photometrics CoolSNAP MYO digital camera	Teledyne Photometrics, Tucson, USA
Olympus UC90 digital camera	Olympus Corporation, Tokyo, Japan
AxioCam MRc digital camera	Carl Zeiss AG, Munich, Germany
Moticam 3.0 digital camera	Motic Deutschland GmbH, Wetzlar, Germany
Culture Dish Micro-Observation Temperature Control System Bioptechs ΔTC3	Bioptechs Inc., Butler, USA
Delta T5® µ-Environmental Culture Dish Controller	Bioptechs Inc., Butler, USA
Micro-CT Sky Scan 1173	Bruker Corporation, Billerica USA

Software

LAS X	Leica Microsystems GmbH, Wetzlar, Germany
Nikon photometrics (Version 5.2)	Nikon Instruments Inc., Melville, USA
Olympus cellSens Dimension	Olympus Corporation, Tokyo, Japan
Carl Zeiss® AxioVision Rel. 4.8.	Carl Zeiss AG, Munich, Germany
Motic® Images Plus 2.0ML	Motic Deutschland GmbH, Wetzlar, Germany
ANALYZE® 9.0	Mayo Clinic, Rochester, USA
Data Viewer 1.5.6.0	Bruker Corporation, Kontich, Belgien
GraphPad Prism 8.4	GraphPad Software, San Diego, California, USA
ImageJ; Fiji	https://www.fiji.sc

Consumables

Coverslips	Engelbrecht Medizin- und Labortechnik GmbH, Edermünde, Germany
Tubes (15 ml, 50 ml)	Greiner Bio-One International GmbH, Frickenhausen, Germany
Reaction tubes (0,5 ml, 1,5 ml, 2,5 ml, 5 ml)	Sarstedt AG & Co. KG, Nümbrecht, Germany
Parafilm®	Bemis Company, Inc, Neenah, USA
Pipette tips (10 µl, 20 µl, 100 µl, 1000 µl)	STARLAB International GmbH, Hamburg, Germany
Serological pipettes (5 ml, 10 ml, 25 ml, 50 ml)	BD GmbH, Heidelberg, Germany
Microscope slides	R. Langenbrinck GmbH Labor- und Medizintechnik, Emmendingen, Germany
Urethral catheter	B. Braun Melsungen AG, Melsungen, Germany
Suture material (Ethicon VICRYL® 3-0)	Johnson &Johnson Medical N.V., New Brunswick, USA
Syringes (1 ml, 5 ml, 10 ml, 20 ml and 50 ml)	B. Braun Melsungen AG, Melsungen, Germany
Extension lines	B. Braun Melsungen AG, Melsungen, Germany
Three-way valve	B. Braun Melsungen AG, Melsungen, Germany

Reagents and substances

3,3′-Diaminobenzidin (DAB)	Carl Roth Gmbh & Co. Kg, Karlsruhe, Germany
4′,6-Diamidin-2-phenylindole (DAPI)	F. Hoffmann-La Roche AG, Basel, Switzerland
4-(2-hydroxyethyl)-1-piperazineethanesulfonic acid (HEPES)	Sigma-Aldrich now Merck KGaA, Darmstadt, Germany

Ammonium chloride	Fluka, now Honeywell International Inc., Charlotte, USA
Aniline	VWR International, Pennsylvania, USA
Aniline blue	Merck KGaA, Darmstadt, Germany
Azocarmine G	Chroma-Gesellschaft Schmid GmbH & Co, Stuttgart, Germany
Bovine serum albumin (BSA)	Sigma-Aldrich now Merck KGaA, Darmstadt, Germany
Dimethyl sulfoxide (DMSO)	Carl Roth GmbH & Co. Kg, Karlsruhe, Germany
Dulbecco's Modified Eagle Medium/Nutrient Mixture F-12 (DMEM/F12)	(Gibco)Thermo Fisher Scientific, Waltham, USA
DAKO EnVision® + System, Peroxidase kit (Peroxidase from horseradish)	Dako North America Inc, now Agilent Technologies, Inc., Santa Clara, USA
Ethanol	BERKEL AHK ALKOHOLHANDEL GMBH & CO. KG, Ludwigshafen, Germany
Eukitt®	Sigma-Aldrich now Merck KGaA, Darmstadt, Germany
Formaldehyde 37 %	Carl Roth GmbH & Co. Kg, Karlsruhe, Germany
Glacial acetic acid	Merck KGaA, Darmstadt, Germany
Glucose	Carl Roth Gmbh & Co. Kg, Karlsruhe, Germany
Glucose oxidase from Aspergillus niger	Sigma-Aldrich now Merck KGaA, Darmstadt, Germany
Glycerol	Merck KGaA, Darmstadt, Germany
Hydrochloric acid	Merck KGaA, Darmstadt, Germany
Hydrogen peroxide	Carl Roth GmbH & Co. Kg, Karlsruhe, Germany
Isopropanol	Th. Geyer GmbH & Co. KG, Renningen, Germany
Methanol	Merck KGaA, Darmstadt, Germany
MICROFIL® MV-Series	FLOW TECH INC., Carver, USA

Minimal essential medium (MEM)	(Gibco)Thermo Fisher Scientific, Waltham, USA
Natrium chloride	Sigma-Aldrich now Merck KGaA, Darmstadt, Germany
Nickel sulfate	Merck KGaA, Darmstadt, Germany
Normal goat serum	Sigma-Aldrich now Merck KGaA, Darmstadt, Germany
Normal horse serum	Sigma-Aldrich now Merck KGaA, Darmstadt, Germany
Orange G	Merck KGaA, Darmstadt, Germany
Paraplast X-tra®	Leica through Carl Roth Gmbh & Co. Kg, Karlsruhe, Germany
Paraformaldehyde (PFA)	Merck KGaA, Darmstadt, Germany
Picric acid	Fluka, now Honeywell International Inc., Charlotte, USA
Phosphotungstic acid hydrate	Carl Roth GmbH & Co. Kg, Karlsruhe, Germany
5 % Phosphotungstic acid (PTA)	Morphisto GmbH, Frankfurt, Germany
Potassium dihydrogen phosphate	Sigma-Aldrich now Merck KGaA, Darmstadt, Germany
Sodium azide	Sigma-Aldrich now Merck KGaA, Darmstadt, Germany
Sodium chloride	Carl Roth GmbH & Co. Kg, Karlsruhe, Germany
Sodium dihydrogen phosphate monohydrate	Merck KGaA, Darmstadt, Germany
Di-sodium hydrogen phosphate dihydrate	Carl Roth GmbH & Co. Kg, Karlsruhe, Germany
Sodium hydroxide	Carl Roth GmbH & Co. Kg, Karlsruhe, Germany
Technovit® 3040	Kulzer GmbH, Hanau, Germany
VECTASTAIN® Elite ABC-HRP Kit, Peroxidase (Goat IgG)	Vector Laboratories part of Maravai Life Sciences Inc., San Diego, USA
Xylol	Carl Roth GmbH & Co. Kg, Karlsruhe, Germany

Active agents

Norepinephrine or norepinephrine-bitartrate salt	Sigma-Aldrich now Merck KGaA, Darmstadt, Germany
Oxytocin acetate salt	Bachem, Bubendorf, Switzerland
Atosiban	Sigma-Aldrich now Merck KGaA, Darmstadt, Germany
Cligosiban	MedChemExpress, Monmouth Junction, USA
SR04959	Cayman Chemicals, Ann Arbor, USA
Tamsulosin hydrochloride	Sigma-Aldrich now Merck KGaA, Darmstadt, Germany

Antibodies

Anti-oxytocin receptor (goat polyclonal)	Abcam, Cambridge, United Kingdom Catalogue number: 87312
Anti-smooth muscle actin (SMA) (mouse monoclonal)	Sigma-Aldrich now Merck KGaA, Darmstadt, Germany Catalogue number: A5228
Cy3 anti-goat IgG	Merck KGaA, Darmstadt, Germany
Alexa Fluor 488 anti-mouse IgG	(Invitrogen) Thermo Fisher Scientific, Waltham, USA

Methods

Buffers and utility solutions

Phosphate-buffered saline (PBS)

2 l distilled water

+ 17,8 g Na_2HPO_4 $2H_2O$ (di-sodium hydrogen phosphate dihydrate)

+ 15,9 g NaCl (sodium chloride)

Set pH to 7,4 with HCl (hydrochloric acid).

PBS-BSA-NaN_3

100 ml PBS

+ 200 mg bovine serum albumin (BSA)

+ 100 mg NaN_3 (Sodium azide)

Phosphate buffer (PB)

2 l distilled water

+ 4,9 g KH_2PO_4 (potassium dihydrogen phosphate)

+ 29,2 g Na_2HPO_4 $2H_2O$ (di-sodium hydrogen phosphate dihydrate)

Set pH to 7,4 with HCl.

Phosphate buffer (PP)

Solution A: 1 l distilled water + 27,6 g NaH_2PO_4 H_2O (sodium dihydrogen phosphate monohydrate)	Solution B: 1 l distilled water + 35,6 g Na_2HPO_4 $2H_2O$ (di-sodium hydrogen phosphate dihydrate)

Mix 230 ml of solution A with 770 ml of solution B. Set pH to 7,4 with HCl.

Azocarmine utility solution

100 ml distilled water

+ 0,1 g azocarmine G

Heat until the solution boils, then filter and add 1 ml glacial acetic acid per 100 ml of the filtered solution.

Aniline blue – Orange G utility solution

100 ml distilled water

+ 0,5 g aniline blue

+ 2 g orange G

Add 8 ml glacial acetic acid to the mixture. Heat until boiling and filter the cooled solution.

Aniline-alcohol

100 ml 90 % ethanol

+ 0,1 ml aniline

4 % PFA utility solution

500 ml distilled water

+ 40 g paraformaldehyde (PFA)

Heat to 70°C. Clear the solution with drops of 2 M NaOH solution and let it cool. Add 500 ml 0,2 M PP and set pH to 7,2 – 7,4 with HCl. Filter the solution.

DAB utility solution

222 ml PBS

+ 5 g 3,3′-Diaminobenzidin (DAB)

Filter the solution. Sensitive to light.

DMEM utility solution

10 ml distilled water

+ 1,28 g Dulbecco's Modified Eagle Medium/Nutrient Mixture F-12 (DMEM/F12)

Preparation of rat collagen utility solution

Collagen fibres from rat tails were extracted by removing the skin and loosening the tendons. the extracted thin collagen fibres were then washed and incubated in 70 % ethanol (15 - 20 min).
Next the 70 % ethanol was drained and the collagen fibres left to air-dry overnight until crispy.
The dry collagen fibres were slowly dissolved in 250 ml 0,1 % glacial acetic acid while continuously stirring at 4°C (48 h). 0,1 % glacial acetic acid was added as required to keep the solution fluid enough to be stirred.
When the desired quantity and viscosity was achieved (yogurt like viscosity), remaining collagen fibres were removed and the solution cleared by centrifuging at 24.000g at 4°C (30 min).
If the viscosity was too dense after centrifugation, more 0,1 % glacial acetic acid was added.

1 g of this prepared rat collagen solution was combined with other components (DMEM utility solution, 1 M HEPES, 0,5 M NaOH) for tissue embedding for the live imaging experiments just before tissue was ready for the dishes. The proportions of the components vary depending on the batch of rat collagen produced and need to be tested out beforehand.
Roughly the proportions are as followed:
1 g rat collagen, + 150 µl DMEM utility solution, + 52 µl 0,5 NaOH, + 50 µl HEPES.

Preparation of the different tissues for live imaging

Human prostate

The human prostate samples (from transurethral resection of the prostate (TUR-P) as well as non-cancerous tissue from prostatectomy) were placed in tubes filled with minimal essential medium (MEM) and transported on ice from the operating theatre as quickly as possible to the laboratory. The samples were then placed in petri dishes and covered with MEM at all times (Fig. 14A). The edges of the tissue samples originating from TUR-P are burned due to the resection method used (blackened edges of the tissue samples visible in Fig. 14A). Therefore, the edges of these tissues were trimmed away prior to preparing to cut off the samples for live imaging. Human prostate is quite dense and homogenous in appearance. The only visible distinction of any sort that can be made is often a color change from paler flesh-tones to more red. By slicing thin strips out of the most central part of the tissue (Fig. 14B), the samples for live imaging were achieved (Fig. 14C).

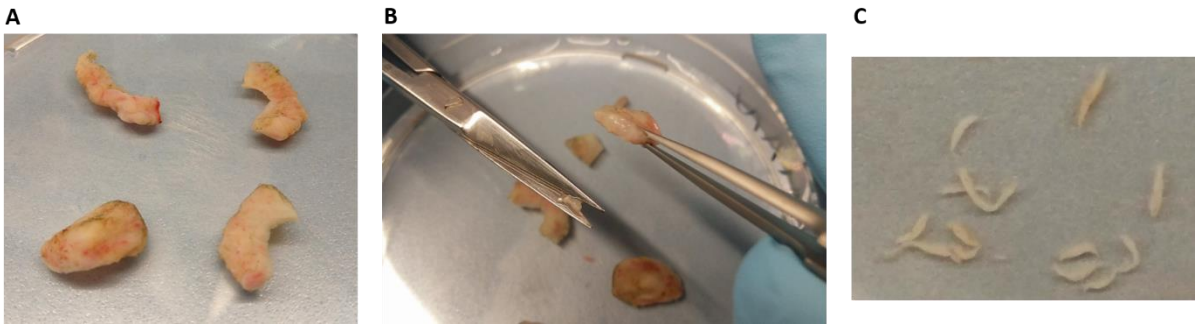

Figure 14: Preparation of human prostatic samples for live imaging

A *Samples received from TUR-P with burned edges and areas of either more red or more pale flesh-tones.*
B *Slicing the prostate samples for live imaging out of the middle of the TUR-P samples.*
C *Fine strips of human prostate tissue ready for live imaging.*

Rat prostate

Immediately after the rat was sacrificed, the bladder, seminal vesicles and prostate were extracted in total (Fig. 15A) and placed in a petri dish with MEM covering the entire tissue at all times. Next, one of the two very prominent ventral lobes (Fig. 15B) of the rat prostate was removed as close to the urethra as possible to conserve the branching structure of the duct system. Under a Motic® dissection microscope the ventral lobe was carefully dissected further with fine surgical tools to separate the layers (Fig. 15C) as much as possible while not tearing this very delicate tissue. Samples for live imaging were

achieved by dissecting as far as to a single layer of prostatic glands to allow for sharp contours when filming contractions (Fig. 15D).

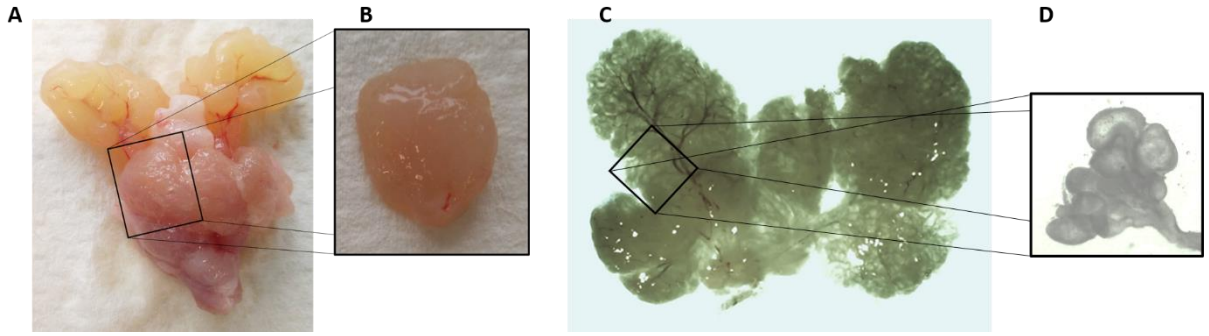

Figure 15: Preparation of rat prostatic samples for live imaging

***A** Bladder, seminal vesicles and prostate in total as extracted from the rat.*
***B** One of the two ventral lobes isolated from the rat prostate.*
***C** Fanned out ventral lobe of the rat prostate showing the different layers under the microscope.*
***D** Sample of prostatic glands of the rat's ventral prostate as used in the live imaging experiments under the microscope.*

Human epididymis

The human epididymal tissue samples were placed in tubes filled with MEM and transported on ice from the operating theatre as quickly as possible to the laboratory. Caput as well as cauda epididymidis samples (Fig. 16A) were then placed in petri dishes separately and covered with MEM at all times. Under a Motic® dissection microscope the tissue was then dissected further with fine surgical tools, removing fat and connective tissue (Fig. 16B). If possible, these samples for live imaging would only contain a single part of the epididymal duct with sharp contours for better contrast (Fig. 16C). The curvature of the epididymal duct was left intact as much as possible and only sections cut out without stretching the duct were used for live imaging.

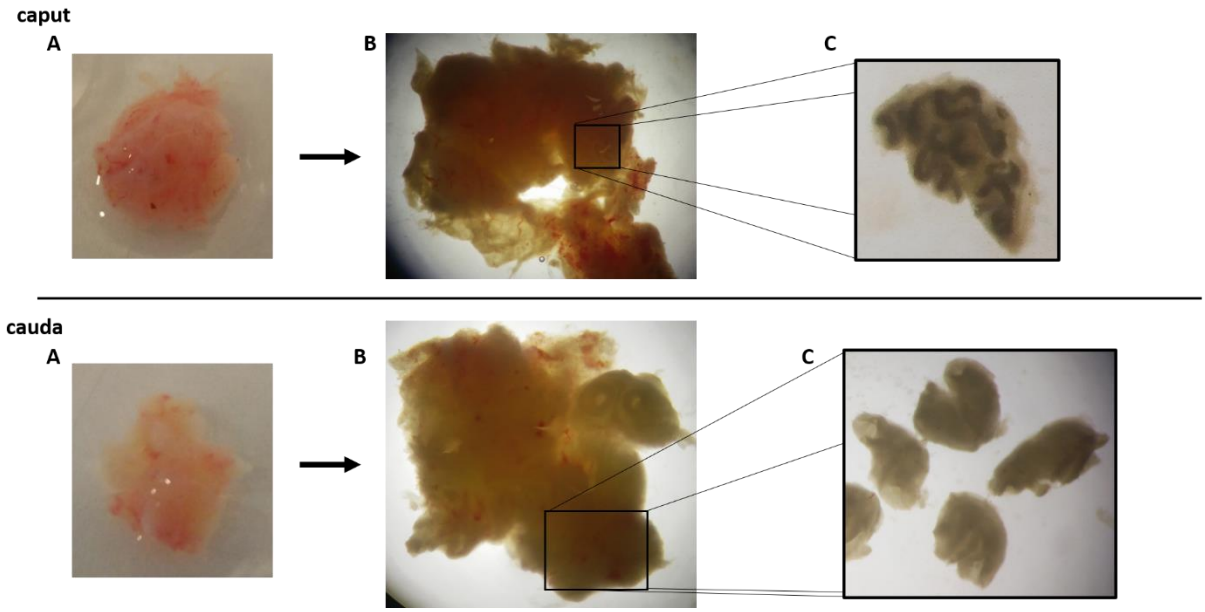

Figure 16: Preparation of human epididymal samples for live imaging

***A** Human epididymal tissue sample from the operation theatre in a petri dish.*
***B** Removing fat and connective tissue from the human epididymal tissue sample under the microscope.*
***C** Samples of human caput and respectively cauda epididymidis ready for live imaging.*

Rat epididymis

Immediately after the sacrifice of the rat, the testis and epididymis (Fig. 17A) of both sides were extracted from the animal. The fat surrounding the epididymis and the connecting tissue between the epididymis and the testis were removed as much as possible. The ductuli efferentes connecting the head of the epididymis to the testis were severed and the now solitary structure of the epididymis (Fig. 17B) placed in a petri dish and covered with MEM at all times. Under a Motic® dissection microscope the tunica surrounding the epididymal duct (Fig. 17C) was incised and carefully removed (Fig. 17D) with fine surgical tools. The adult rat epididymis samples for live imaging (Fig. 17D) were extracted from defined segments following the schematic from Turner dividing the adult rat epididymis into 19 segments. For the neonatal rat epididymis an approximation of these segments was used. The tunica of the neonatal epididymis was often left in situ since the tissue was much more delicate and removing the tunica led to tearing of the duct. For both age groups the curvature of the epididymal duct was left intact as much as possible and only sections cut out without stretching the duct were used for live imaging. If possible, these samples for live imaging would only contain a single part of the epididymal duct with sharp contours for better contrast.

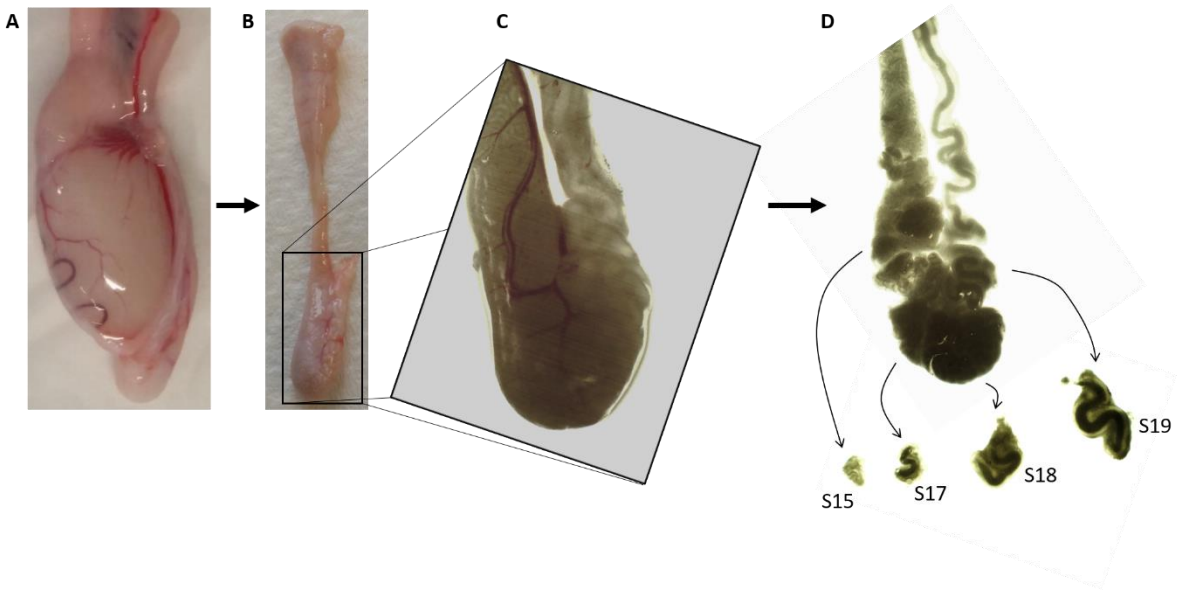

Figure 17: Preparation of rat epididymal samples for live imaging

A *Testis and epididymis of the adult rat in total.*
B *The adult rat epididymis with the connective tissue and fat removed.*
C *The adult rat cauda epididymidis (vas deferens leading away on the right) under the dissection microscope with tunica intact.*
D *The same cauda epididymis as in C with the tunica removed making the segments of the epididymis more apparent. The samples of single duct loops cut out of the respective segment ready for live imaging.*

Live imaging

300 µl of the prepared rat collagen utility solution was added to one dish each and distributed equally. Then the tissue samples were carefully placed into the dishes under visual control, making sure that the tissues lay flat in the dish and are covered by the rat collagen utility solution. The dishes were then placed into a CO_2 incubator at 37°C (30 min) to polymerize the rat collagen utility solution and thereby fixing the tissue in one place without restraining its movement or disturbing the delicate tissue by pinning it down. After the polymerization process the tissue was covered with MEM (1 ml at JLU, 1,5 ml at Monash). Samples were then ready for recording. Videos in each experiment were captured at 1 frame every 2 seconds.
The concentration of the agents that were added during the experiments into the dish as well as the volume of these additions were calculated as such to result in a dilution of (1:4) for each agent and addition. The stated final concentration (fc) in this thesis is the actual concentration achieved in the dish by mixing in the higher concentrated agent with the MEM that is already in the dish. Previous experiments of colleagues in the same working group showed no impairment of the tissue in these short-term experiments (lasting under 1 h) when not refreshing the MEM in the dish during the experiments. Therefore, no wash-out or continuous perfusion was performed to allow maximum exposure to the agents and record changes over time with as little fluid movement as possible. Dishes were kept at 33°C throughout the experiments using culture dish temperature control systems.

At the end of each experiment NE (fc of 10 µM) was given to check for tissue viability. In case where the reaction to NE was blocked because of pretreatment with tamsulosin, the strong reaction to the lastly added OT was also used as viability control.

Experiments with the rat or human prostate

The videos of the human or rat prostate were captured on a Leica DM5000 B microscope with an ORCA-Flash4.0 Hamamatsu digital camera (C11440) using LAS X software.
First, a 15-minute period was recorded to capture spontaneous contractility without treatment (no treatment). Then OT (fc of 500 nM) was added into the dish and another 15-minute period was recorded.

Experiments with the neonatal rat epididymis

The videos of the neonatal rat epididymis were captured on an Olympus BX50WI microscope with the Moticam 3.0 digital camera in combination with the Motic® Images Plus 2.0ML software.

First, a 10-minute period was recorded to capture spontaneous contractility without treatment (no treatment). Then OT (fc of 500 nM) was added into the dish and another 10-minute period was recorded.

Experiments with the adult rat or human epididymis

The videos of the adult rat epididymis at JLU and of the human epididymis were captured on a Leica DM5000 B microscope with an ORCA-Flash4.0 Hamamatsu digital camera (C11440) using LAS X software.
The videos of the adult rat epididymis at MIPS were captured on a Nikon Eclipse Ti microscope with a Photometrics CoolSNAP MYO digital camera using Nikon photometrics software (Version 5.2).

Experiments using different segments of the rat or human epididymis

First, a 10-minute period was recorded to capture spontaneous contractility without treatment (no treatment). Then OT (fc of 500 nM) was added into the dish and another 10-minute period was recorded.

Additionally, with the S19 (tissue important during the ejaculatory process) a second set-up was used to compare the effect of OT to the effect of NE. Therefore, again a 10-minute period was recorded to capture spontaneous contractility without treatment (no treatment). Then NE (fc of 10 µM) was added into the dish and another 10-minute period was recorded.

Experiments with S19 using three different concentrations of oxytocin

First, a 10-minute period was recorded to capture spontaneous contractility without treatment (no treatment). Then OT at the three different fc of 1 nM, 10 nM and 100 nM was added into the dish and another 10-minute period was recorded.

Experiments with oxytocin- and arginine vasopressin-antagonists

First, a 10-minute period was recorded to capture spontaneous contractility without treatment (no treatment). Then either one of the OTR antagonists (atosiban (fc of 5 µM) or cligosiban (fc of 40 µM)), the arginine vasopressin 1A antagonist (SR49059 (fc of 40 µM)) or the soluble agent dimethyl sulfoxide (DMSO) as a control was added into the dish and a 15-minute period was recorded. After which OT (fc of 500 nM) was added into the dish and another 10-minute period was recorded.

Experiments with pharmacological impairment of the adrenergic pathway

Firstly, a 10-minute period was recorded to capture spontaneous contractility without treatment (no treatment). Then the α1 adrenoreceptor antagonist tamsulosin (fc of 40 µM) was added into the dish and a 15-minute period was recorded. After which NE (fc of 10 µM) was added into the dish and another 10-minute period was recorded (to check for optimal blockage of the adrenergic pathway). Lastly, OT (fc of 500 nM) was added into the dish and another 10-minute period was recorded.

The final concentrations of all antagonists used in the rat experiments and presented in this thesis were derived from pre-experiments in which the concentration of each agent was subsequently adapted to a higher one until the desired complete blocking effect was sustained. In case of the arginine vasopressin-antagonist (SR49059) a complete blocking effect could not be achieved in the pre-experiments. Since there would also be a considerable amount of the SR49059 binding to the oxytocin receptor at high concentrations a complete blocking effect through the arginine vasopressin receptor alone was deemed unlikely. In our experiments with human tissue the same fc of the antagonists were used as in our previous rat experiments.

Injection experiments with fresh frozen (and thawed again) human prostate

The prostates were extracted one at a time from fresh frozen body donors that had been thawed again using surgical tools and anatomical expertise. The bladder and seminal vesicles as well as the surrounding adjacent tissue and a good portion of the urethra were extracted en bloc with the respective prostate to ensure easy injection later. Only two of the four prostates extracted were usable.

To prepare the prostate for injection, the tissue was placed into a large glass petri dish and the urethral catheter was inserted into the urethra and placed more than a centimeter before the prostatic part of the urethra. The urethral catheter was fixed in place by suture material and eventual air gaps closed using Parafilm®. The bladder was ligated as low as possible at the bladder neck using suture material and clamps. The urethral catheter was connected to a three-way-valve and syringe. The as such closed system was tested for air gaps by flushing multiple times with warmed sodium chloride solution and clamping off all visible exit points. The volume of sodium chloride solution injected was noted to prepare the right volume of the fluid plastic later in the experiments. Then the remaining sodium chloride was drained as much as possible. A vacuum was created using the three-way valve and the syringe before injecting the agent in a next step (Fig.18).

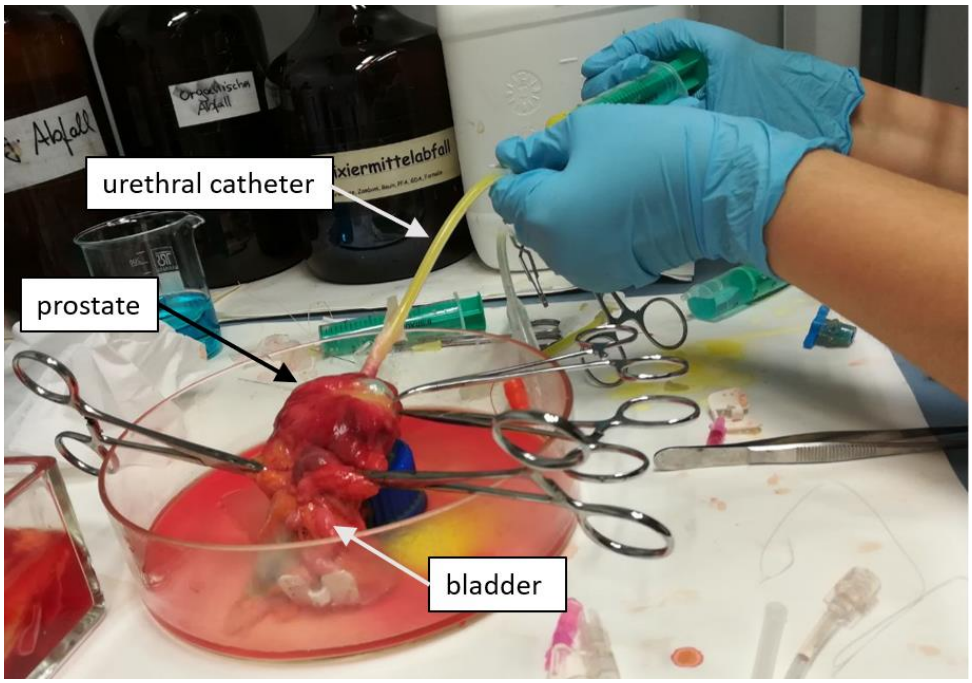

Figure 18: Injection of fluid plastic into human prostate

Microinjection of the human prostate using Technovit® 3040

Technovit® 3040 is usually used to create a play dough-like texture that hardens quickly for molds or as a connecting agent for external fixators in orthopedic surgeries. Technovit® 3040 consists of two components: a powder and a liquid, that need to be mixed in the desired proportions. Once mixed, an exothermic reaction is started and the cold-curing resin will harden with time. When the two components are mixed in a higher proportion of liquid to powder an injectable fluid is the result which also takes longer to harden then the play dough-like texture. In this experiment 20 g powder was mixed with 48 ml liquid. The solution was filled into a syringe and injected through the three-way valve. Probably due to the heat of the exothermic reaction and thus slight extension of the syringe, the stiff connecting point on the three-way valve was chipped off and the syringe then quickly reconnected directly to the urethral catheter. As seen in the image some fluid still leaked from the tissue during the injection process but mostly a pressure could be maintained, visibly extending the prostatic tissue over several minutes. The tissue was then left overnight until the rest of the fluid left in the syringe had hardened. The clamps and tubing were then removed and the injected prostate submerged in a cannister with 25 % NaOH solution. The cannister was placed into an incubator and left for two days at 40°C to dissolve the human tissue, leaving only the injected plastic. Securing the urethral catheter, the resulting corrosion cast model was carefully lifted out of the 25 % NaOH solution and submerged in distilled water multiple times to dilute the NaOH left on the structure. The corrosion cast model was then glued

to a petri dish in an upright position, standing up by the urethral catheter. The different sides and structures were captured in detail using the Moticam 3.0 digital camera in combination with the Motic® Images Plus 2.0ML software.

Microinjection of human prostate using MICROFIL® MV-Series

The MICROFIL® MV-Series is developed explicitly for the purpose of microinjection and detection through radiopacity afterwards. It consists of three components: the compound, the diluent and the hardener. For this experiment the syringe for injection was filled with a mixture of 32 ml compound, 40 ml diluent and 3,6 ml hardener and injected through the three-way valve. There were no visible gaps and the bladder neck and prostate extended visibly under the pressure build up. After 2-3 hours the clamps and tubing were removed and the injected prostate placed in a cannister with 4 % formaldehyde. The tissue was then handed to our collaborator in the biomedical research centre Giessen (in the working group of Prof. M. Kampschulte) for micro-CT imaging (Micro-CT Sky Scan 1173). The radiopaque injected fluid, being the only contrast rich structure, was easily detectable and the structures reconstructed using ANALYZE® 9.0 software.

Using prostates from human body donors for micro-CT imaging

The prostates were extracted from 4 % formaldehyde-fixed human body donors and submerged in 4 % formaldehyde until further preparation. Some of the tissue had been sagittalized beforehand. The surrounding tissue of the prostate was removed as much as possible (Fig.19), trying to only leave the prostate, a part of the urethra and the seminal vesicles to allow for better penetration of the 5 % phosphotungstic acid (PTA) later.

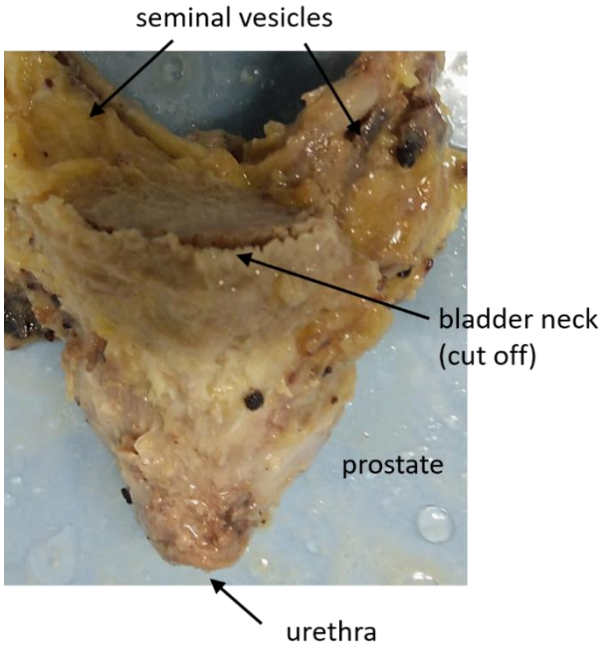

Figure 19: Human prostate from formaldehyde-fixed body donors as used for micro-CT imaging

The tissue was then handed to our collaborator in the biomedical research centre Giessen (in the working group of Prof. M. Kampschulte) for micro-CT imaging (Micro-CT Sky Scan 1173). There the samples would be scanned once without PTA and handed back to us. We then submerged the samples in 5 % PTA (1-4 weeks depending on density and size of the tissue) and applied vacuum periodically for better penetration. The PTA functions as a contrast agent, rendering the penetrated tissue radiopaque (Lesciotto et al. 2020). After full penetration of the tissue (and sometimes inbetween) the samples were scanned again. The microstructure of the prostate was now visible could be documented using Data Viewer 1.5.6.0 and selectively reconstructed in 3D.

(Immuno-) Histochemistry

Fixation and slicing

Human or rat tissue samples were fixed in Bouin's solution (30 ml picric acid (saturated aqueous solution, 10 ml glacial acetic acid and 2 ml 37 % formaldehyde) for 24 hours. Tissues were then kept in 70 % ethanol until embedding. Tissues were embedded in paraffin after an ascending alcohol series (70 %, 96 %, 100 %) and cleared with xylol either automatically (Leica TP1020 tissue processor) or manually. The paraffin-embedded samples were sliced (using a RM2255 microtome), stretched (in a

Tissue Float Bath) and mounted on slides to dry (on a slide warmer). After 24 hours in an incubator at 40°C, the slides were ready for long-term storage and staining.

Tissue from formaldehyde-fixed body donors and samples returning from micro-CT imaging (both submerged in 4 % formaldehyde until paraffin-embedding) were washed with distilled water and dehydrated with alcohol before embedding in paraffin and slicing + mounting as described above.

Heidenhain's AZAN trichrome staining

For a general overview of the tissue, AZAN staining after Heidenhain (staining cell nuclei red and collagen fibres blue) was performed as followed:

Slides were deparaffinized in xylol (3x5 min) and rehydrated in a descending alcohol series (100 %, 96 %, 70 %, 5 min each). After briefly washing with distilled water, the slides were submerged in the utility solution aniline-alcohol (5 min). Tissue was then dyed with the utility solution azocarmine (preheated to 56°C) (10-15 min) accounting for the red staining. After a quick wash with distilled water the tissue was then differentiated with the utility solution aniline-alcohol under visual control. After another quick wash with distilled water the tissue was mordanted with 5 % phosphotungstic acid (2 h) (fixing the dye to the tissue). After another quick wash with distilled water the slides were kept in the utility solution aniline-orange (1-2 h) accounting for the blue staining. After a last quick wash in distilled water the tissue was differentiated and dehydrated in isopropanol and 96 % ethanol under visual control, followed by clearing the slides in xylol (3x5 min). Finally, the slides were cover slipped using the quick hardening mounting medium Eukitt® and left to dry.

Immunohistochemistry

Chromogenic immunohistochemistry

First, paraffin-embedded tissue sections were deparaffinized with xylol (3x5 min) and rehydrated with a descending alcohol series (100 %, 96 %, 70 %, 5 min each) including an incubation period with 30 % hydrogen peroxide solution (diluted 1:25 in methanol) (30 min) to block endogenous peroxidase activity. Then the slides were washed with distilled water and submerged in PBS buffer.

Variation for detection of smooth muscle cells in the tissue:

The slides were incubated in a humidity chamber overnight at 4°C. The anti-smooth muscle actin (SMA) antibody was diluted (1:1000) in PBS-BSA-NaN_3 to stain smooth muscle cells in the tissue and applied to the slides. To confirm targeted staining of the antibodies, some slides or sections were incubated only with PBS-BSA-NaN_3 as a negative control.
After incubation overnight, the slides were washed in PBS (3x5 min) and then incubated with horseradish peroxidase (DAKO EnVision® + System peroxidase kit) (30 min) as the secondary antibody.

Variation for detection of oxytocin receptor distribution in the tissue:

The slides were incubated in a humidity chamber overnight at 4°C. The VECTASTAIN® Elite ABC-HRP Kit, Peroxidase (Goat IgG) was used. First, the slides were pretreated with a mixture of 30µl normal serum (rabbit) from the ABC Kit with 2 ml PBS (20 min). Afterwards, most of the fluid was removed from the slides by gently tapping the side of the slides on tissue paper. Then the anti-oxytocin receptor (OTR) antibody was diluted (1:250) in PBS-BSA-NaN_3 to stain for OTR distribution in the tissue and applied to the slides. To confirm targeted staining of the antibodies, some slides or sections were incubated only with PBS-BSA-NaN_3 as a negative control.
The next day, the slides were washed in PBS (3x5 min). Then 30µl normal serum (rabbit) from the ABC Kit were diluted in 2 ml PBS and then 10 µl Biotin (goat) from the ABC Kit were added to the mixture. This solution (as the secondary antibody) was then applied to the slides and incubated further (30 min). Next, the slides were washed in PBS (2x5 min). Then 40 µl of solution A from the ABC Kit were diluted in 2 ml PBS and then 40 µl of solution B from the ABC Kit were added to the mixture. This solution was then applied to the slides and incubated further) (30 min).

For both antibodies (anti-SMA or anti-OTR) the slides were then washed with first PBS (10 min) and then PB (10 min) before developing.
Meanwhile, the developing solution was prepared containing 180 ml PB, 4 ml DAB utility solution, 3,6 ml 10 % glucose solution, 400 µl of 3,4 M ammonium chloride solution and 3,6 ml of 0,05 M nickel sulfate solution. The mixture was then filtered and 600 µl of 0,12 % glucose oxidase solution was added when the slides were submerged in the filtered solution. The peroxidase activity was detected, and the staining developed under visual monitoring. The reaction was stopped after 5 minutes (anti-OTR) or 7 minutes (anti-SMA) by washing in PB and distilled water.
The slides were then dehydrated in an ascending alcohol series (70 %, 96 %, 100 %, 5 min each) and cleared with xylol (3x5 min). Finally, the slides were cover slipped using the quick hardening mounting medium Eukitt® and left to dry.

Immunofluorescence

Double staining with anti-SMA antibody and anti-OTR antibody was performed to visualize co-localization in the tissue.

First, paraffin-embedded tissue sections were deparaffinized with xylol (3x5 min) and rehydrated with a descending alcohol series (100 %, 96 %, 70 %, 5 min each). Slides were then washed in distilled water and submerged in PBS buffer.

In the next step the slides were incubated with a mixture of 40 µl normal horse serum and 960 µl PBS in a humidity chamber (1 h). Afterwards, most of the fluid was removed from the slides by gently tapping the side of the slides on tissue paper. The primary antibodies anti-SMA (1:1000) and anti-OTR (1:250) were diluted in PBS-BSA-NaN3, applied to the slides and incubated overnight at 4°C.

Slides were then washed with PBS (2x10 min). Then a mixture of fluorescence-labeled secondary antibodies and 4′,6-Diamidin-2-phenylindole (DAPI) diluted in PBS was applied. The secondary antibody Alexa 488 (1:500) was used to detect the primary antibody anti-SMA. The secondary antibody Cy3 (1:400) was used to detect the primary antibody anti-OTR. DAPI (1:250) was added to stain cell nuclei. The slides were incubated (1 h) in the dark as the secondary antibodies and DAPI are light sensitive.

After the incubation period the tissue was washed with PBS (2x10 min), fixed with 4 % PFA utility solution (10 min) and then washed again with PBS (2x10 min). For long term storage, the tissue was cover slipped using glycerol and stored in the fridge until capturing the images used in this thesis.

Image capture of slides

Axioplan 2 imaging microscope in combination with the Axiovision LE software was used to capture all AZAN-stained tissues and most fluorescent-labeled antibody experiments. The Olympus BX51 fluorescence microscope in combination with the Olympus cellSens Dimension software was used to automatically capture and stitch the overview images of the AZAN-stained as well as the fluorescent-labeled epididymis (neonatal and adult respectively) together.

Live imaging analysis

The Fiji distribution of ImageJ was used to process and analyze the images originating from live imaging (Schindelin et al. 2012).

In this thesis two different analytical methods for live imaging data were used depending on the type of contractions observed in the videos. In case of distinct contractions occurring throughout most of the rat epididymis, with the exception of the very last segment (S19) of the adult rat, contractions per minute were displayed and counted by reslicing the data following the previously established method by Mietens et al. (Mietens et al. 2014).

To accurately analyze multidirectional contractions in more than one location simultaneously (prostate) as well as to quantify the uniquely strong response of the very last segment of the adult rat (S19) and the human (S9) epididymis, another method was needed. Therefore, an evolution of the code based on the Wiggle Index (Denecke et al. 2015; Preston et al. 2015; Preston et al. 2016) was developed https://doi.org/10.26180/13653614. This adaptation (as the Wiggle Index before) compared how the sum of movements (extracted from standard deviation scores) of the entire field of view or defined region of interest evolved during the different time-points of the experiments. The extended coding now allowed us to additionally measure the fold change relative to baseline (and to each other addition) separately for each pixel while expressing the data as a population distribution allowing subtle differences in movement to be detected. This fold-change for each data point could then be exported into GraphPad Prism for statistical analysis. The sum of movement included in the statistical analysis was additionally visualized in heat map images, showing the location and the intensity of the movement in a color-coded manner (with red and grey as high intensity and blue as low). Thus, it was possible to show the change of movement throughout the different parts of the experiment in one image.

Statistical analysis

In the experiments in which contractions per minute were calculated, the data were analyzed with Wilcoxon matched-pairs signed-rank test. All data generated with the adaptation of the Wiggle Index (S19 and S9 of the epididymis and all data from prostate experiments) were analyzed as followed: First the frequency distribution was determined, followed by running a non-linear regression (curve fit) using exponential one phase association testing if one curve adequately fits all data sets. GraphPad Prism was used for all statistical analysis. Differences were considered significant if $*p<0.05$, $**p<0.01$, $***p<0.001$ and non-significant (ns) if $p\geq0.05$. There are two types of graphs used to display frequency distribution in this thesis. One is using the raw standard deviation data points of each part of a single experiment (f. ex. Fig. $25B_2$ or 33), creating a cumulative frequency distribution. The other is using the relative fold-change from one part of the experiment to another of the same experiment and then comparing this relative change to relative changes of other experiments with the same set-up, thus creating a cumulative relative frequency distribution (f. ex. Fig. 30D, or 32E). All cumulative frequency

distribution data (including the relative data) is displayed +/- standard error of means (SEM). The data included in the graphs of the “Results” has been evaluated as followed:

(i) For the cumulative frequency data figures the two data sets displayed in the graph were determined to be significantly different if by running a non-linear regression (curve fit) using exponential one phase association testing, one curve did not adequately fit both data sets.

(ii) In the relative cumulative frequency data figures: Each relative data set displayed in the graph (depicting one set of experiments) was first determined to be significantly different to baseline if by running a non-linear regression (curve fit) using exponential one phase association testing, one curve did not adequately fit both data sets. Second, using the relative fold changes of each of those experiments depicted in the graph, it was determined (also using curve fit) if the outcome of the experiments (e.g. the effect of oxytocin, or the blocking ability of an antagonist) was significantly different from one experimental set-up to another.

Results

Live imaging

The effect of oxytocin on the contractility of the prostate

The effect of oxytocin on the contractility of the human prostate

Human prostate tissue samples originating from either patients with BPH through TUR-P or from patients with prostate cancer through prostatectomy were investigated using live imaging. Because of the heterogeneity of contractions in the tissue, our newly developed analysis method was used to quantify the movements and their change after addition of OT. OT significantly increased pre-existing movement of the human prostatic tissue or induced it in samples originating either from TUR-P (n=4) ($p<0.0001$) (Fig. 20) or prostatectomy (n=6) ($p<0.0001$) (Fig. 21).

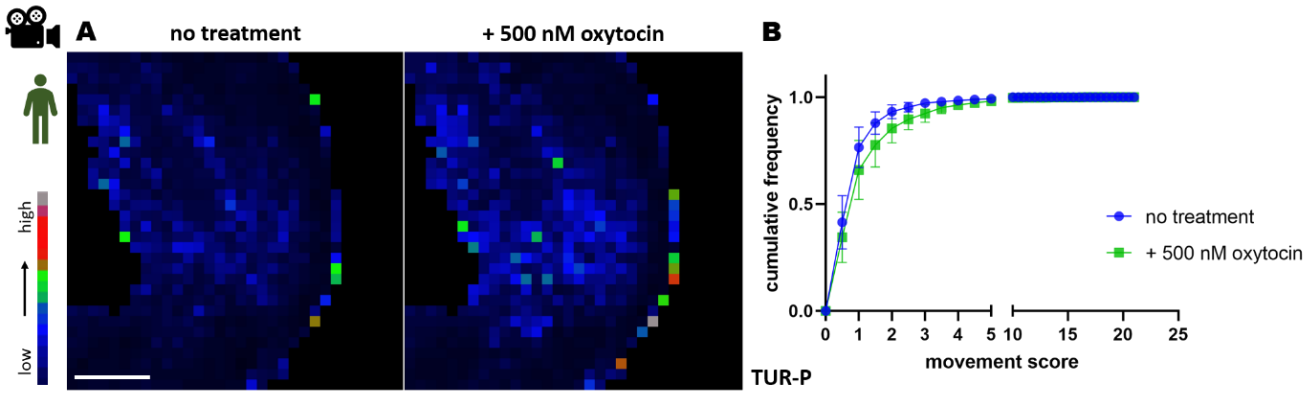

Figure 20: The effect of oxytocin on human prostate samples originating via TUR-P

The sum of movements analyzed is displayed using a color-coded heat map representation with blue representing low intensity and red and grey the high intensity movements (white scale bar: 300 µm).
***A** Heat map representation of the experiment.*
***B** Graph of the cumulative frequency distribution of the two parts of the experiments ("no treatment" vs after "+500 nM oxytocin") (+/- SEM) (n=4) ($p<0.0001$) (for more information see "Statistical analysis" (i)).*

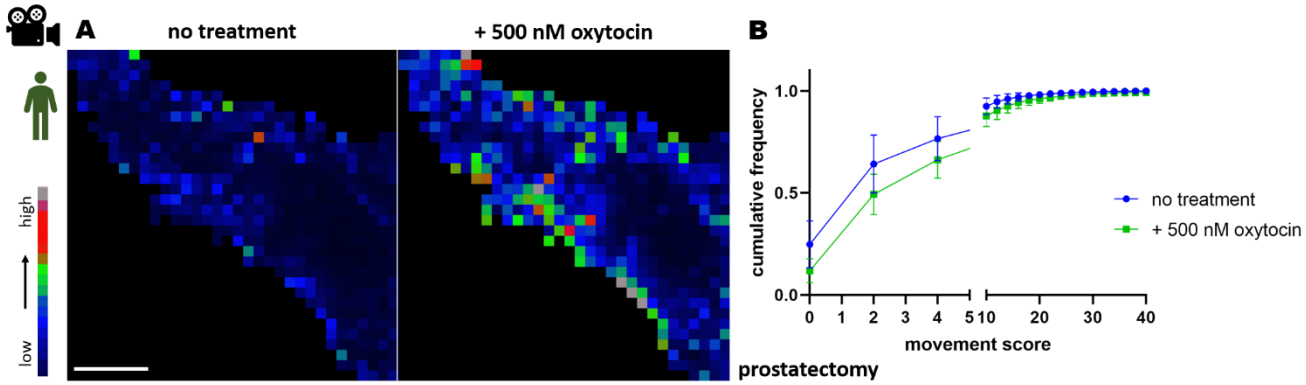

Figure 21: The effect of oxytocin on human prostate samples originating from prostatectomy

The sum of movements analyzed is displayed using a color-coded heat map representation with blue representing low intensity and red and grey the high intensity movements (white scale bar: 300 µm).
***A** Heat map representation of the experiment.*
***B** Graph of the cumulative frequency distribution of the two parts of the experiments ("no treatment" vs after "+500 nM oxytocin") (+/- SEM) (n=6) (p<0.0001) (for more information see "Statistical analysis" (i)).*

When compared, the relative change to OT was significantly higher in the prostatectomy samples (p<0.0001) (Fig. 22).

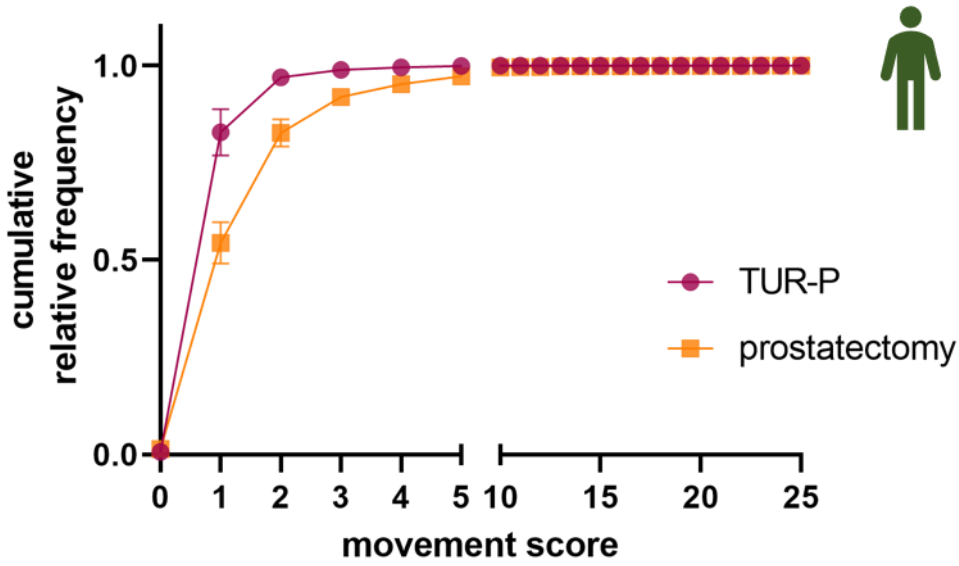

Figure 22: Comparison of the relative effect of oxytocin in human prostate samples originating from TUR-P vs prostatectomy

Graph of the cumulative relative frequency distribution of the change after oxytocin addition in TUR-P samples vs prostatectomy samples (+/- SEM) (p<0.0001) (for more information see "Statistical analysis" (ii)).

The effect of oxytocin on the contractility of the rat prostate (glands)

In the same setup as used with the human prostate samples, the rat prostatic glands from the ventral lobe of the prostate were investigated. Because of the heterogeneity of contractions in this tissue, our newly developed analysis method was used to quantify the movements and their change after addition of OT. OT had no significant effect on the rat prostatic glands (n=5) ($p \geq 0.05$) (Fig. 23).

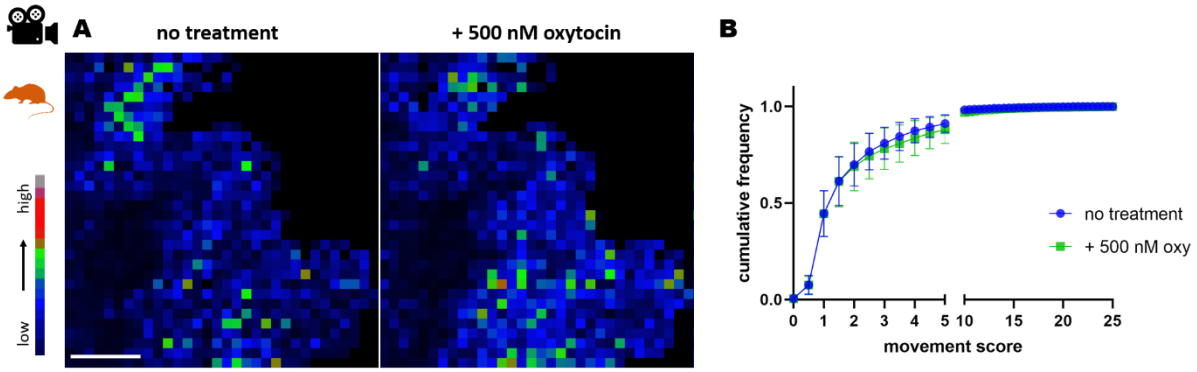

Figure 23: The effect of oxytocin on the rat prostatic glands

The sum of movements analyzed is displayed using a color-coded heat map representation with blue representing low intensity and red and grey the high intensity movements (white scale bar: 300 µm).
***A** Heat map representation of the experiment.*
***B** Graph of the cumulative frequency distribution of the two parts of the experiments ("no treatment" vs after "+500 nM oxytocin") (+/- SEM) (n=5) ($p \geq 0.05$) (for more information see "Statistical analysis" (i)).*

The effect of oxytocin on the contractility of the epididymis

The contractility of the rat epididymal duct originating from specific segments following the classification by Jelinsky and Turner (Jelinsky et al. 2007) was investigated using live imaging. Following the notion by Mietens et al. (Mietens et al. 2014) that in the epididymis reslicing the data is uniformly independent of the area used and as such reslicing the data is representative of the contractility of the epididymis, this method was used for all segments (S) of the epididymis with distinct single contractions (all except S19 of the adult rat and S9 of the human epididymis).

The published content (figures and figure legends) extracted from my research article entitled "Physiological and pharmacological impact of oxytocin on epididymal propulsion during the ejaculatory process in rodents and men" (Stadler et al. 2021) are indicated at the end of each respective figure legend.

The difference of effect of oxytocin on the contractility of specific segments of the adult rat epididymis

The segments S5 (caput), S12 (corpus) and S15 (cauda) of the adult epididymal duct of the rat showed spontaneous distinct contractions during the "no treatment" period. After addition of OT, these contractions significantly increased in S5 ($n=6$) ($p<0.05$) (Fig. 24A) as well as S15 ($n=6$) ($p<0.05$) (Fig. 24B) but not in S12 ($n=6$) ($p\geq0.05$) (Fig. 24C).

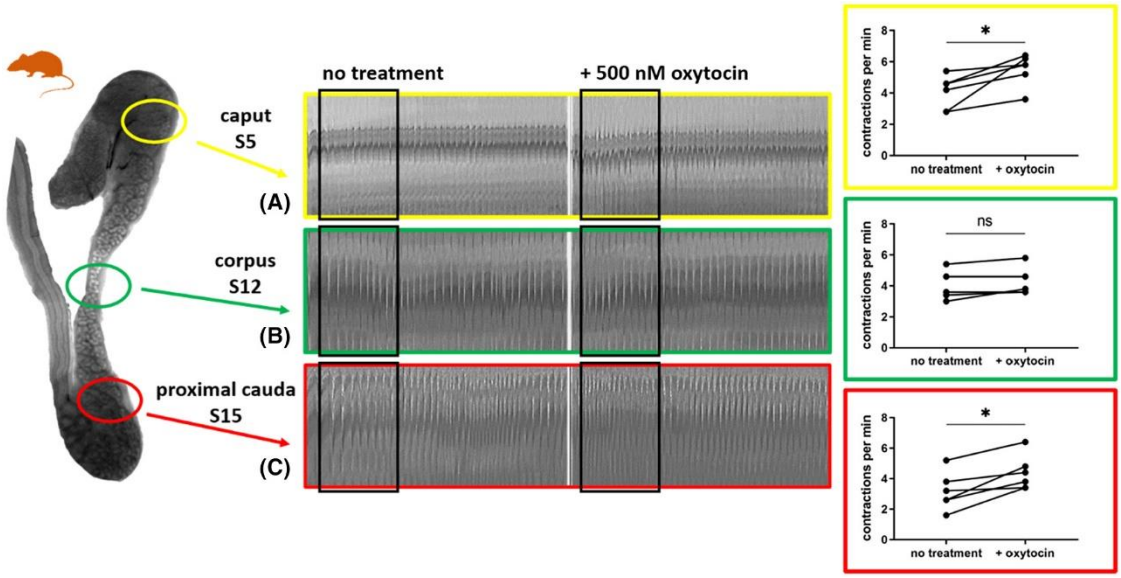

Figure 24: The effect of oxytocin on defined segments of the epididymal duct of the rat

*Contractions are displayed by reslicing the data and countable as vertical "stripes." Contractions were counted for 3 minutes each (black frames) and summarized as contractions per minute. Oxytocin only slightly increased contractions per minute in caput, corpus, and proximal cauda of the rat epididymis (each n = 6). This effect was significant (P < .05) in segments of the caput (S5) (**A**) as well as proximal cauda (S15) (**C**) of the rat epididymis, but not significant (P ≥ .05) in the corpus epididymidis (S12) (**B**).*

Extracted from (Stadler et al. 2021)

Only the two last segments S18 and S19 of the adult rat epididymal duct showed no spontaneous contractions during the "no treatment" period.

In S18 OT induced a series of single strong contractions that were statistically significant (n=6) ($p<0.05$) (Fig. 25A).

In S19 OT induced a series of multidirectional and forceful contractions that displaced and compressed the duct, thereby expulsing the content of the duct segment which is visible in the recorded videos.

These contractions started immediately after OT addition and lasted for 3-5 minutes, after which the duct mostly returned to its original resting state. Although this impressive response of S19 was detectable by reslicing the data as with other parts of the epididymal duct, it was not quantifiable this way (Fig. $25B_1$). Therefore, for all experiments using S19 we used our newly developed image analysis method. The response of S19 to OT was statistically significant (n=7) ($p<0.0001$). The change of movement during the "no treatment" period compared to after the addition of OT is displayed in the heat map as well as in the graph (Fig. $25B_2$).

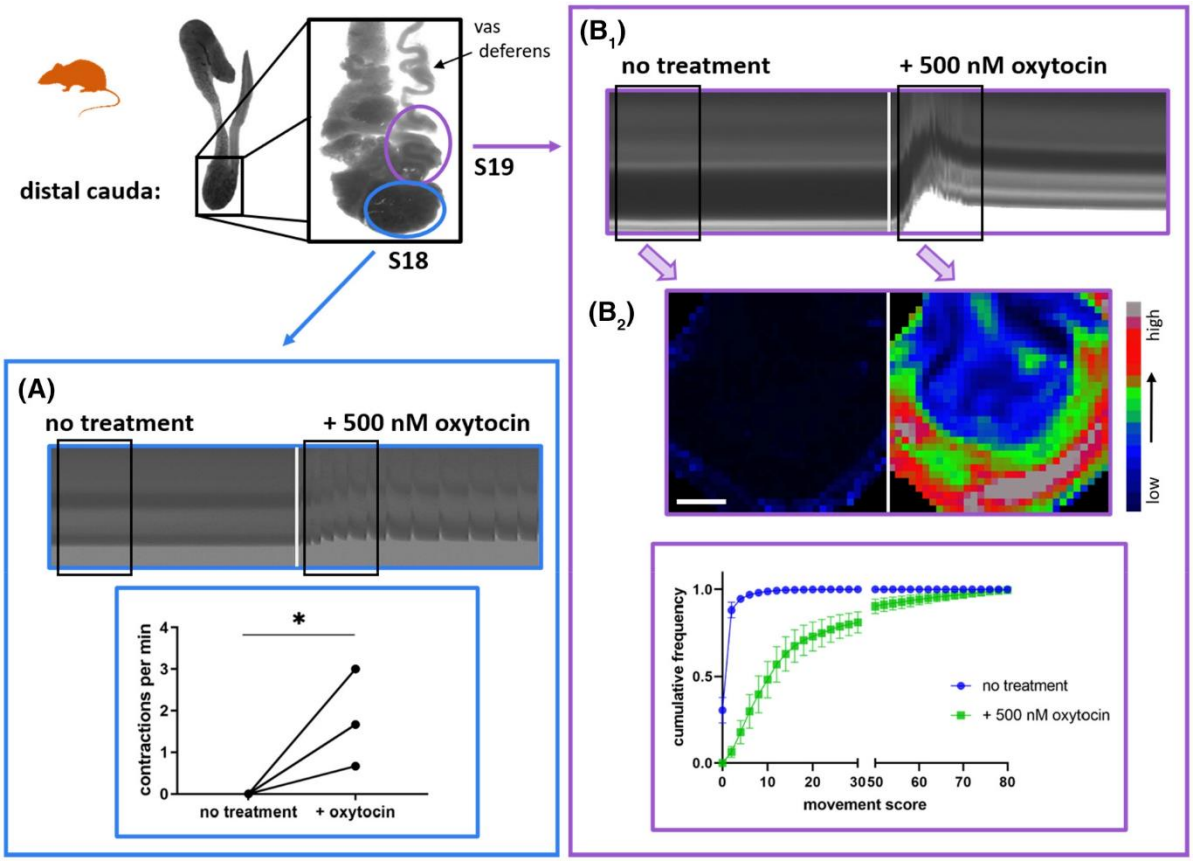

Figure 25: The effect of oxytocin on S18 and S19 of the epididymal duct of the rat

***A**, In S18 contractions are displayed by reslicing the data and countable as vertical "stripes." Contractions were counted for 3 minutes each (black frames) and summarized as contractions per minute. Oxytocin had a significant effect in S18 of the rat epididymis (n = 6) (P < .05) by inducing distinct single contractions.*
***B**, In S19 oxytocin induced a strong series of contractions quickly following each other thereby creating a complex movement with displacement of the duct (including expulsion of content). Reslicing this data (**B₁**) displayed the difference in quality of the reaction compared to the other segments investigated (Figure **1A-C** and Figure **2A**) and is indicative of a very forceful reaction. However, it was not possible to quantify the reaction this way, therefore a new analyzing method (**B₂**) was introduced to display and quantify the intensity of the movement. In the heat map representation of the results of this new analyzing method, the intensity of the sum of movements over the 3 minutes analyzed is displayed in a color-coded manner with blue representing low intensity and red and gray the high intensity movements (white scale bar: 300 µm). The data collected through this new method showed that the reaction to oxytocin in S19 (n = 7) was significant (P < .0001) (± SEM) (for more information see "Statistical analysis" (i)).*

Extracted from (Stadler et al. 2021)

In the setup with NE as a first addition, S19 also showed no contractions during the "no treatment" period. NE induced a very similar series of multidirectional contractions that also displaced and compressed the duct leading to expulsion of its content. These contractions also started immediately after the addition of NE, however they did not stop altogether after the 3-5 minutes as seen previously after OT addition but single contractions persisted until the end of the recoding. The response of S19 to NE was statistically significant (n=6) (p<0.0001). When compared, the responses after the first 30

seconds after addition of either OT (Fig. 26A) or NE (Fig. 26B) were not significantly different from each other (Fig. 26C) and therefore the two responses deemed equal. The change of movement during the "no treatment period" compared to after the respective addition of either OT or NE is displayed in the heat map. The relative change of movements from the "no treatment" period to after the addition of the respective agent (OT (Fig. 26A) or NE (Fig. 26B)) was compared and displayed in the graph (Fig. 26C).

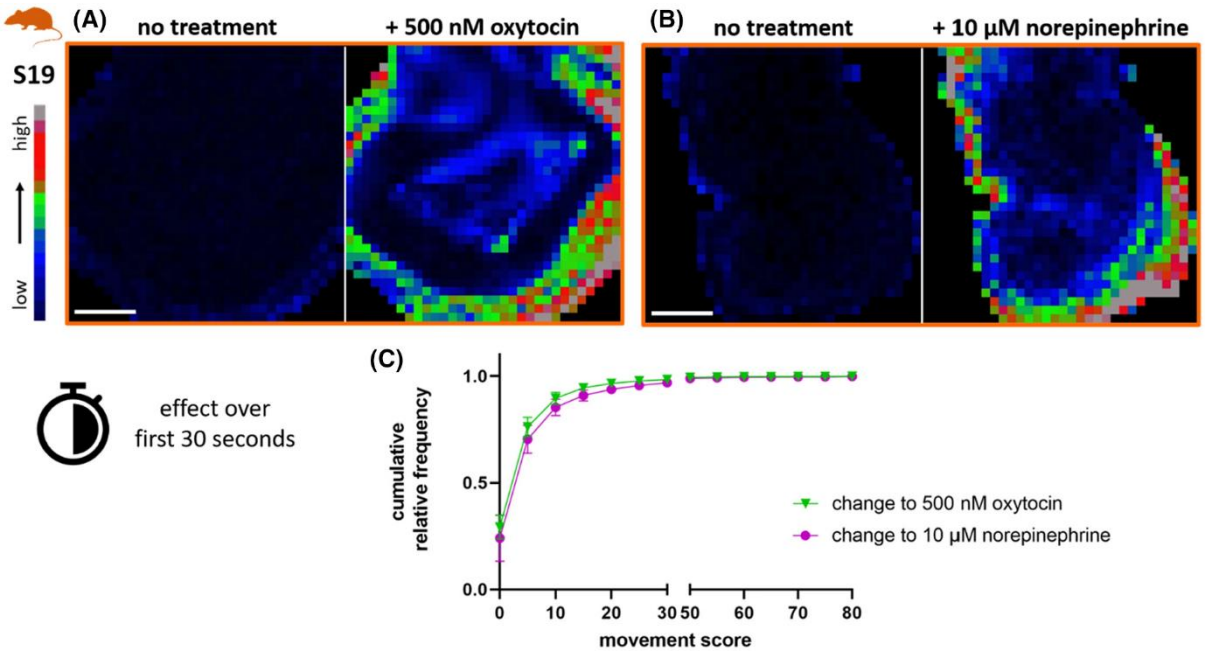

Figure 26: The effect of 500 nM oxytocin in comparison to 10 µM norepinephrine on S19 during the first 30 seconds after administration of the agents

The sum of movements analyzed is displayed using a color-coded heat map representation with blue representing low intensity and red and gray the high intensity movements (white scale bar: 300 µm).
***A**, The effect of 500 nM oxytocin on S19 (n = 7) during the first 30 seconds after application.*
***B**, The effect of 10 µM NE on S19 (n = 6) during the first 30 seconds after application.*
***C**, Graph of the changes of "no treatment" to either oxytocin or NE during the first 30 seconds after application, respectively (± SEM). The difference between the two changes was not significant (P ≥ .05) (for more information see "Statistical analysis" (ii)).*

Extracted from (Stadler et al. 2021)

The difference of effect of oxytocin on the contractility of specific segments of the neonatal rat epididymis

All segments investigated from the neonatal rat epididymal duct showed spontaneous distinct contractions during the "no treatment" period, with the last segment being markedly quieter than the rest. OT significantly increased contractions in caput (n=6) ($p<0.05$) (Fig. 27A), but neither in the corpus (n=6) ($p\geq0.05$) (Fig. 27B) nor in the proximal cauda (n=6) ($p\geq0.05$) (Fig.27C) of the neonatal epididymis. In S19 OT did induce single strong contractions that were statistically significant (n=9) ($p<0.01$) (Fig. 27D), however this response to OT was entirely different to the one seen in the adult as visible in the movie or by reslicing the data. The response of the neonatal S19 to NE was stronger than the one induced by OT, however both agents did not elicit that forceful complex series of contractions as seen in the adult.

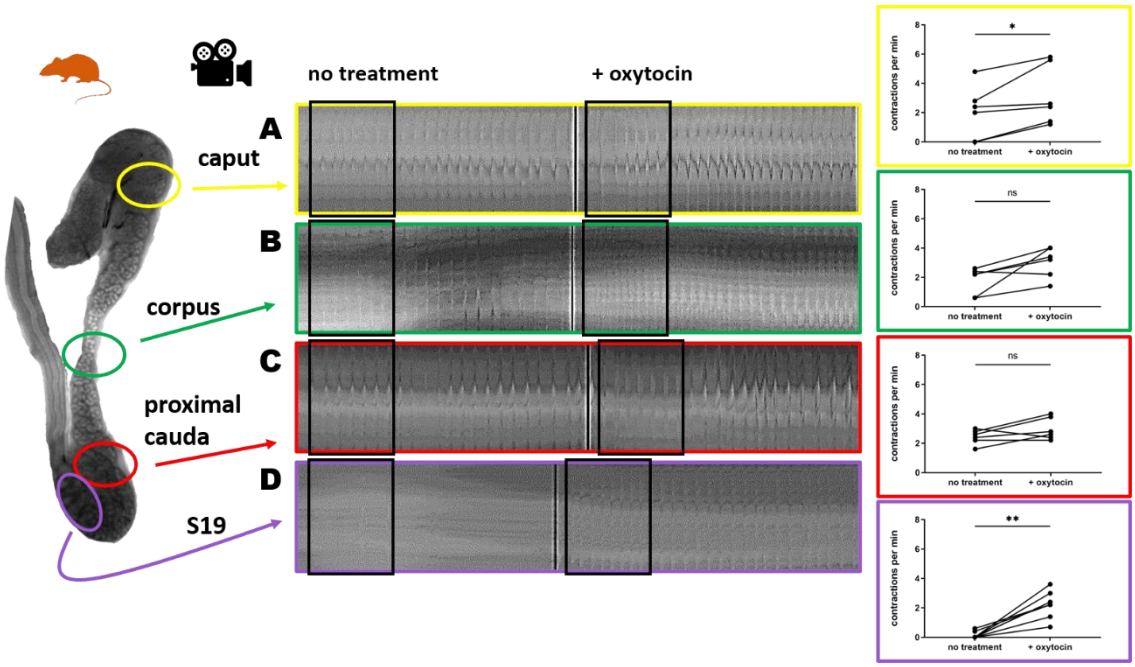

Figure 27: The effect of oxytocin on defined segments of the epididymal duct of the neonatal rat

Contractions are displayed by reslicing the data and countable as vertical "stripes". Contractions were counted for 3 minutes each (black frames) and summarized as contractions per minute.
*Oxytocin only slightly increased contractions per minute in caput, corpus and proximal cauda of the rat epididymis (each n=6). This effect was significant ($p<0.05$) in the caput (**A**) of the neonatal rat epididymis, but not significant ($p\geq0.05$) in the corpus and proximal cauda epididymidis (**B** + **C**). S19 of the neonatal epididymis was also rather quiet, but instead of the big response to a stimulus (oxytocin or NE) as previously seen in the adult, oxytocin only induced single strong contractions which was significant (n=9) ($p<0.01$) (**D**).*

The effect of oxytocin on the contractility of the human epididymis

To investigate how transferable to the human the data generated in the rat would be, a limited number of experiments could be performed with parts of the human epididymal duct.

Similar to the rat, the caput epididymis of the human epididymis (n=2) showed spontaneous contractions which were only slightly increased by OT (Fig. 28A). Likewise, in agreement with the rat data the last two segments of the human (S8 and S9) showed little to no spontaneous contractions during the "no treatment" period. OT then induced or accelerated single contractions in S8 (n=1) (Fig. 28B) while inducing multiple strong contractions that displaced the duct in S9 (n=2) (Fig. 29). Because of the limited tissue access, the reaction to NE was only evaluated in the OT experiment in which NE was given as a last addition to check tissue viability as in all experiments. The response of S9 to NE in these experiments was forceful and stronger than the one before to OT. The number of experiments able to be conducted was insufficient for a statistical analysis to be performed due to the rarity of the tissue (during 8 months we obtained 2 human epididymal samples).

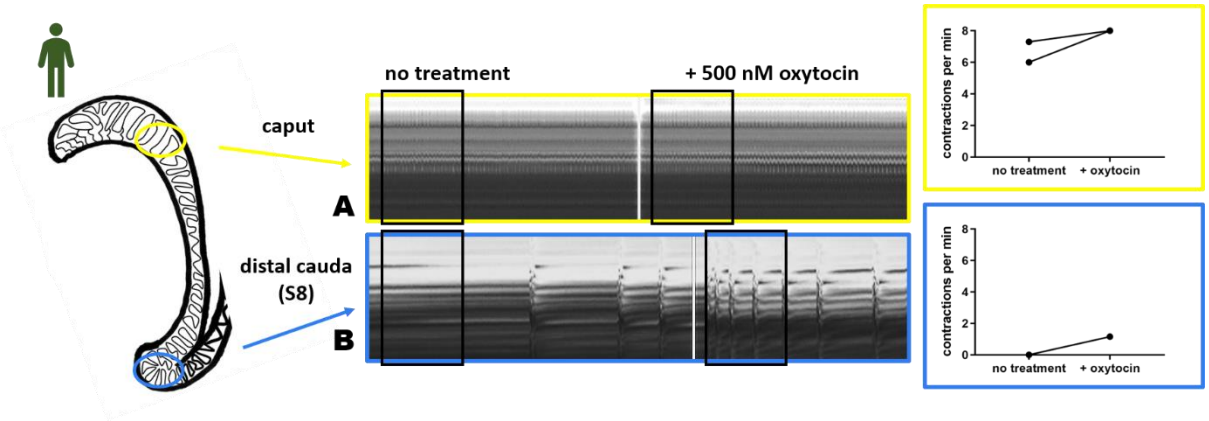

Figure 28: The effect of oxytocin on parts of the human epididymal duct

A *Oxytocin slightly increased the pre-existing regular spontaneous contractions in caput epididymidis.*
B *Oxytocin induced single strong contractions in S8 of the human epididymis.*

Modified from (Stadler et al. 2021)

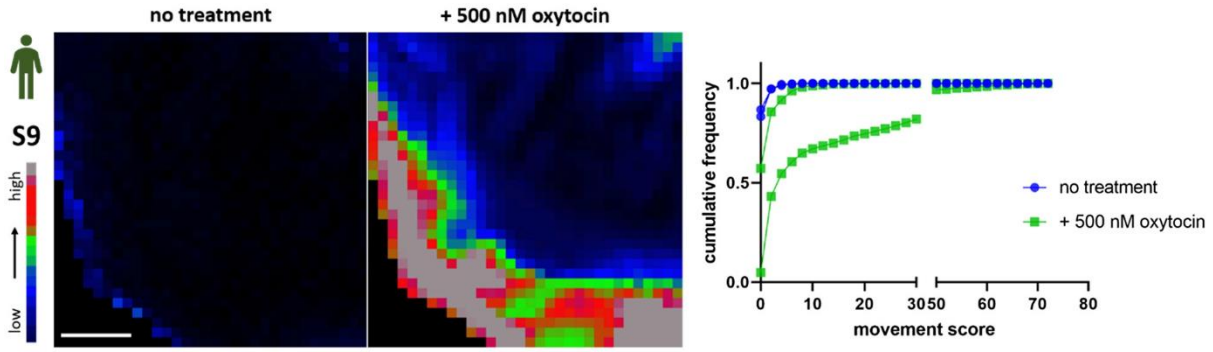

Figure 29: The effect of oxytocin on distal cauda of the epididymal duct in men

The sum of movements analyzed (during the 3 minutes) is displayed using a color-coded heat map representation with blue representing low intensity and red and gray the high intensity movements (white scale bar: 300 µm). Oxytocin induced strong contractions in the most distal part (S9) of the human epididymal duct (n = 2).

Extracted from (Stadler et al. 2021)

The effect of different concentrations of oxytocin on the contractility of S19 of the adult rat epididymis

The response of S19 to OT changed depending on the concentration (Fig. 30). Three additional concentrations to 500 nM of oxytocin were tested. 1 nM oxytocin induced small indentations of the wall in S19 that were still statistically significant (n=6) ($p<0.05$) (Fig. 30A). 10 nM oxytocin induced single strong contractions in S19 that were statistically significant (n=6) ($p<0.0001$) (Fig. 30B). However, they were not forceful enough to expulse content or displace the duct. 100 nM oxytocin induced the previously observed series of multidirectional and forceful contractions which were statistically significant (n=6) ($p<0.0001$) and displaced and compressed the duct including expulsion of content (Fig. 30C). The relative change of movements from the "no treatment" period to after the addition of the respective concentration of OT was compared and displayed in the graph (Fig 30D). In relation to each other the relative change after addition of 100 nM oxytocin was significantly greater than the relative change after addition of 10 nM oxytocin ($p<0.0001$), and the one after 10 nM oxytocin greater than the one after 1 nM oxytocin ($p<0.0001$).

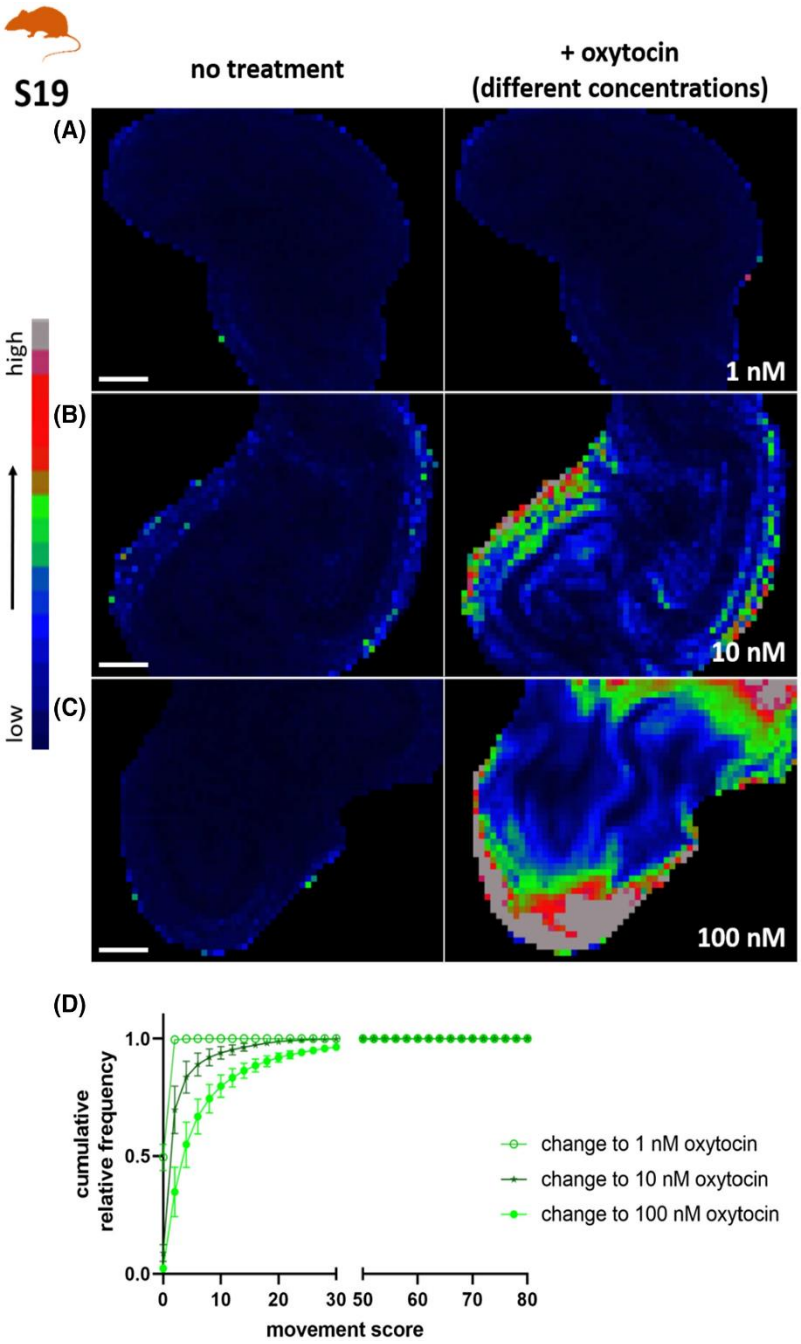

Figure 30: Concentration-dependent oxytocin effects on S19 of the epididymal duct of the rat

The sum of movements analyzed (during the 3 minutes) is displayed using a color-coded heat map representation with blue representing low intensity and red and gray the high intensity movements (white scale bar: 300 µm).
***A**, 1 nM oxytocin induced very small contractions in S19 (n = 6), which were still significant (P < .05).*
***B**, 10 nM oxytocin induced single strong contractions in S19 (n = 6) (P < .0001).*
***C**, 100 nM oxytocin induced a strong series of contractions quickly following each other thereby creating a complex movement with displacement of the duct (including expulsion of content) (n = 6) (P < .0001).*
***D**, Graph of the three changes of "no treatment" to one of the three doses of oxytocin (1, 10, or 100 nM), respectively (± SEM) (for more information see "Statistical analysis" (ii)). In relation to each other, the 100 nM oxytocin dose elicited a significantly greater effect than 10 nM oxytocin (P < .0001), and 10 nM oxytocin greater than 1 nM oxytocin (P < .0001).*

Extracted from (Stadler et al. 2021).

Blocking oxytocin in S19 of the adult rat epididymis

To investigate whether the response to OT is mediated through the OTR or the arginine vasopressin receptor, three antagonists (atosiban, cligosiban and SR49059) were tested for their ability to block the previously observed response of S19 to OT. Since two of the agents (cligosiban and SR49059) (and later on tamsulosin as well) were not soluble in water, experiments with pretreatment of the soluble agent DMSO (fc of 1,6 % and 4 %) (each n=3) were performed, pooled and used as a control (Fig. 32A). In these control experiments, the same significant response to OT (n=6) ($p<0.0001$) was detected as seen before without DMSO pretreatment. Additionally, when compared the relative change to the addition of OT, once after the "no treatment" period and once after the DMSO control treatment period, were found to be not significantly different (Fig. 31). Therefore, any blocking effect seen in the following antagonist experiments can be attributed to the respective antagonist itself and not to DMSO.

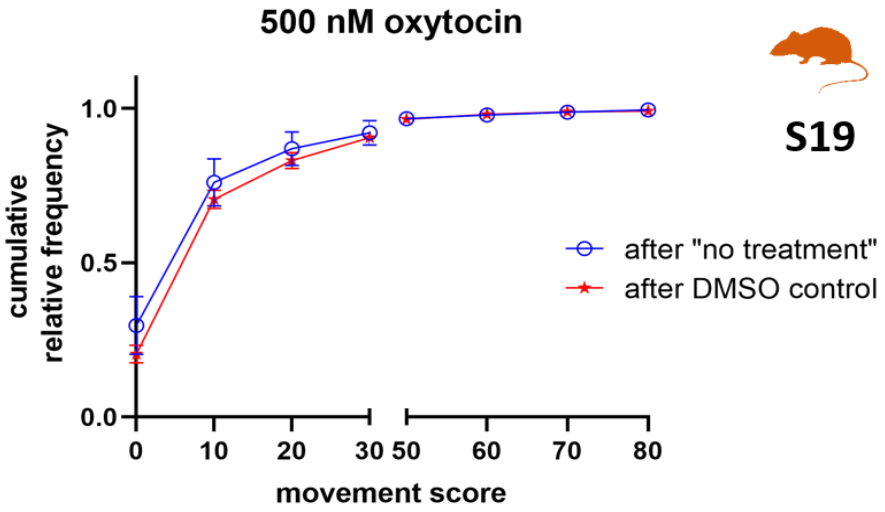

Figure 31: Comparison of the effect of oxytocin after "no treatment" to after "DMSO control"

The graph of the cumulative relative frequency distribution (+/- SEM) of oxytocin addition after "no treatment" (blue) (n=7) in comparison to after DMSO control (red) (n=6) in S19 of the rat epididymis was not significantly different (p≥0.05) (for more information see "Statistical analysis" (ii)).

The blocking effect of the three antagonists was analyzed for 8 minutes and only deemed as complete when no contraction could be observed after OT addition. S19 that had been pretreated with atosiban showed no significant response to the addition of OT over the entire 8 minutes (n=6) (Fig. 32C) analyzed. Likewise, S19 that had been pretreated with cligosiban also showed no significant response to the addition of OT over the entire 8 minutes (n=6) (Fig. 32D) analyzed. However, S19 pretreated with SR49059 started to contract after roughly 2 minutes after the addition of OT. These single contractions were not the forceful response to OT as seen in the control experiments, however the

response was statistically significant (n=6) ($p<0.001$) (Fig. 32B). The relative change of movements from the pretreatment period with the respective agent after the addition of OT was compared and displayed in the graph (Fig. 32E).

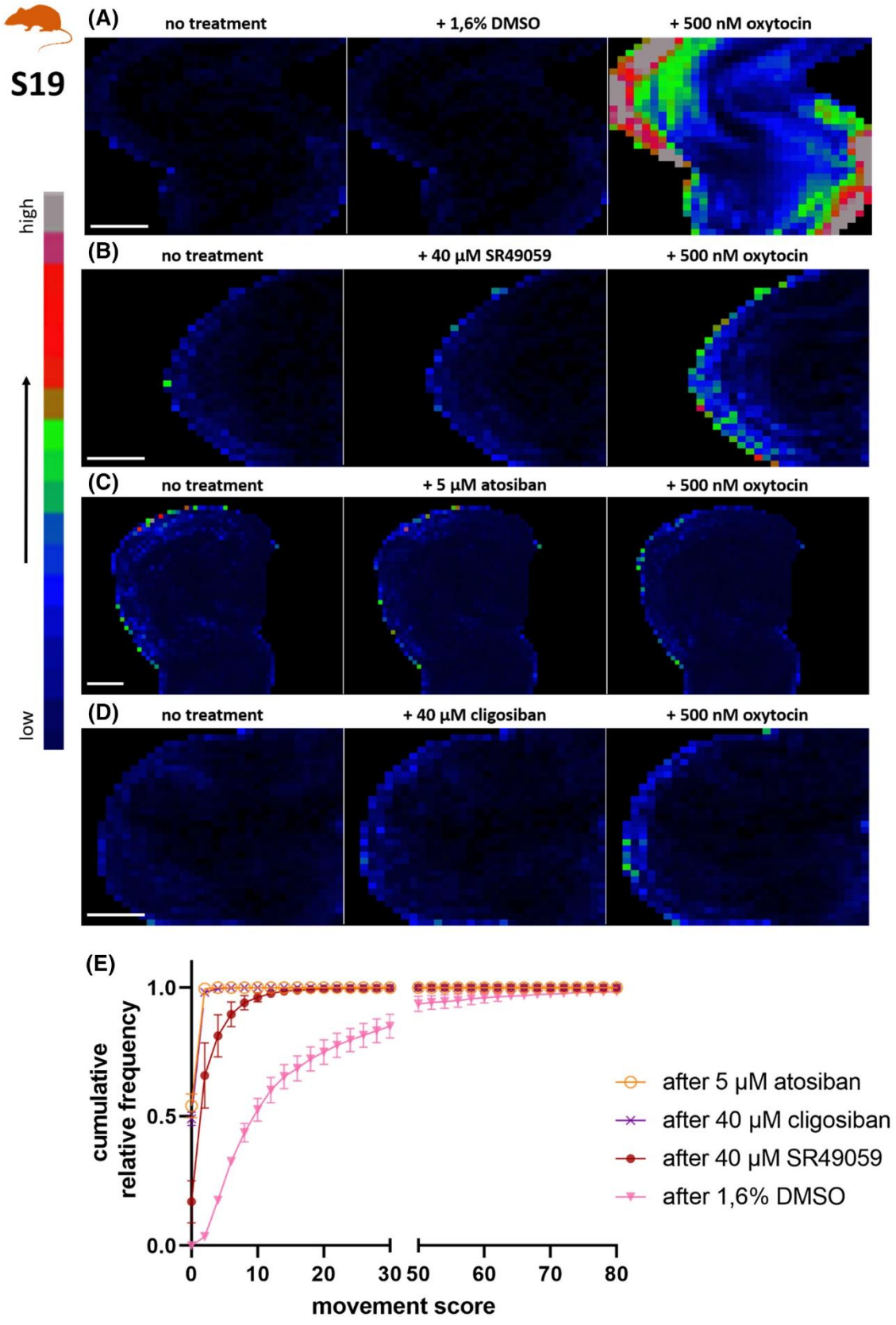

Figure 32: Oxytocin effects after pretreatment with atosiban, cligosiban or SR49059 in S19 of the rat epididymal duct

The sum of movements analyzed (during the 8 minutes) is displayed using a color-coded heat map representation with blue representing low intensity and red and gray the high intensity movements (white scale bar: 300 µm).
***A**, Pretreatment with 1,6% DMSO did not prevent the oxytocin effect and is used as a control in this set of experiments (n = 3) (P < .0001).*
***B**, Pretreatment with 40 µM SR49059 did not completely prevent the oxytocin effect (see above, **A**) resulting in a significant difference between SR49059 and SR49059 + oxytocin (n = 6) (P < .001).*
***C**, Pretreatment with 5 µM atosiban prevented the oxytocin effect (see above, **A**) resulting in no significant difference between atosiban and atosiban +oxytocin (n = 6) (P ≥ .05).*
***D**, Pretreatment with 40 µM cligosiban prevented the oxytocin effect (see above, **A**) resulting in no significant difference between cligosiban and cligosiban +oxytocin (n = 6) (P ≥ .05).*
***E**, Graph of the oxytocin effects after pretreatment with either of the three agents (atosiban, cligosiban, and SR49059) and the soluble agent DMSO used as a control in comparison to each other (± SEM). The oxytocin effect after pretreatment with SR49059 was significantly decreased compared to DMSO control (P < .0001), but only atosiban and cligosiban completely blocked a reaction to oxytocin (for more information see "Statistical analysis" (ii)).*

Extracted from (Stadler et al. 2021)

Addition of oxytocin to adrenergically blocked S19 of the adult rat and S9 of the human epididymis

Adrenergically blocked S19 was pharmacologically produced by incubating S19 with the α1 adrenoreceptor antagonist tamsulosin. The blocking effect was verified when S19 was unresponsive following addition of NE. Finally, OT was added to investigate whether the OT pathway was still viable in this tissue.

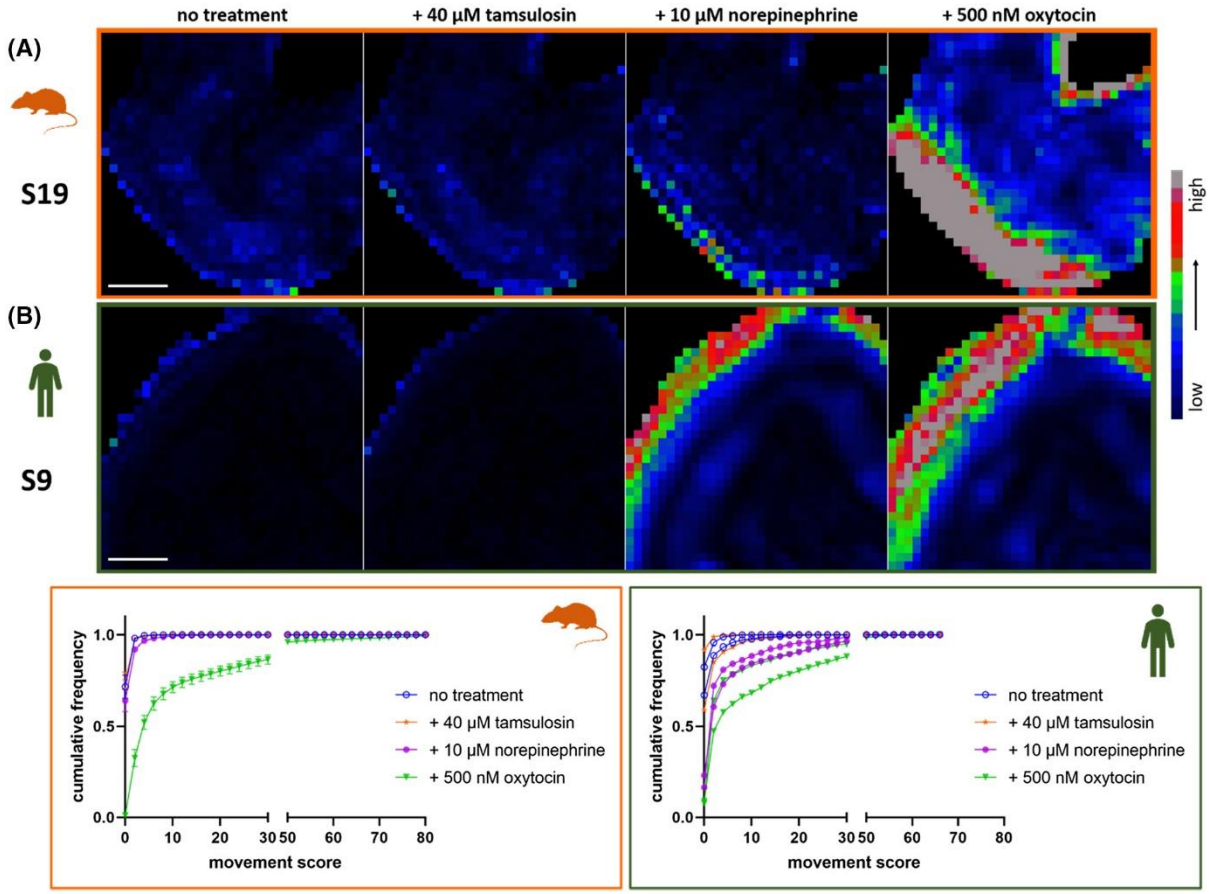

Figure 33: Oxytocin effect after pretreatment with adrenergic-blocker tamsulosin

The sum of movements analyzed (during 3 minutes) is displayed using a color-coded heat map representation with blue representing low intensity and red and gray the high intensity movements (white scale bar: 300 µm).
***A**, In the rat S19 (n = 7) pretreatment with 40 µM tamsulosin prevented a significant reaction to an afterward addition of NE (P ≥ .05). Additional treatment with oxytocin induced a strong series of contractions quickly following each other thereby creating a complex movement with displacement of the duct (including expulsion of content) (P < .0001) (± SEM).*
***B**, In the human S9 (n = 2) pretreatment with 40 µM tamsulosin did not prevent a reaction to an afterward addition of NE, but lessened NE's effect. Oxytocin then induced forceful contractions that were stronger than the ones induced by NE in the tamsulosin pretreated tissue (for more information see "Statistical analysis" (i)).*

Extracted from (Stadler et al. 2021)

S19 of the rat epididymis pretreated with the α1 adrenoreceptor antagonist tamsulosin showed no significant response to NE (n=7) ($p \geq 0.05$). This adrenergically blocked tissue then showed the same significant response as previously described after the addition of OT (n=7) ($p < 0.0001$) (Fig. 33A). When compared, the relative change to the addition of OT, once after the "no treatment" period and once after the tamsulosin (+ NE) period, was found to be not significantly different. Therefore, the response of S19 to OT was unimpaired by blocking the adrenergic pathway (Fig. 34).

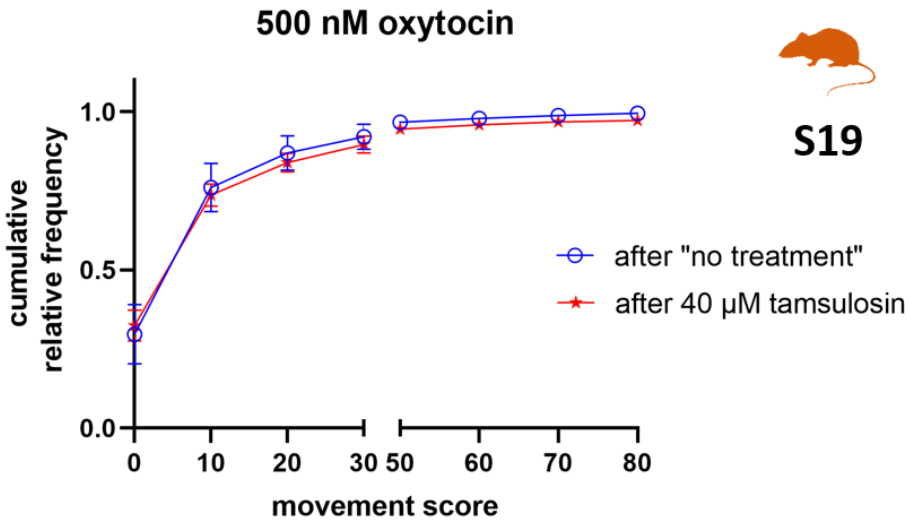

Figure 34: Comparison of the effect of oxytocin after "no treatment" to after "40 µM tamsulosin"

The graph of the cumulative relative frequency distribution (+/- SEM) of oxytocin addition after "no treatment" (blue) (n=7) in comparison to after tamsulosin (red) (n=6) in S19 of the rat epididymis was not significantly different ($p \geq 0.05$) (for more information see "Statistical analysis" (ii)).

S9 of the human epididymis that had been pretreated with the α1 adrenoreceptor antagonist tamsulosin still showed single strong contractions after the addition of NE. However, they were less forceful than the response observed in the experiments without tamsulosin pretreatment. OT still induced a response that was stronger than the one to NE and similar to the forceful response seen previously (Fig. 33B).

The change of movement during the "no treatment period" compared to after each subsequent addition is displayed in the heat maps as well as on the two graphs respectively (Fig. 33).

Distribution of the oxytocin receptor

Human prostate

The human prostatic ducts were defined here through preliminary findings from the micro-CT imaging experiments described later.

Using immunohistochemistry, it was found that the OTR was expressed in the human prostate (n=3).

In the chromogenic immunohistochemistry images, the OTR was found to be expressed throughout the human prostate (around glands as well as ducts) and in a similar manner to the expression of SMA-positive cells. There might also be a slight staining of OTR in the epithelium (*) of the human prostate (Fig. 35).

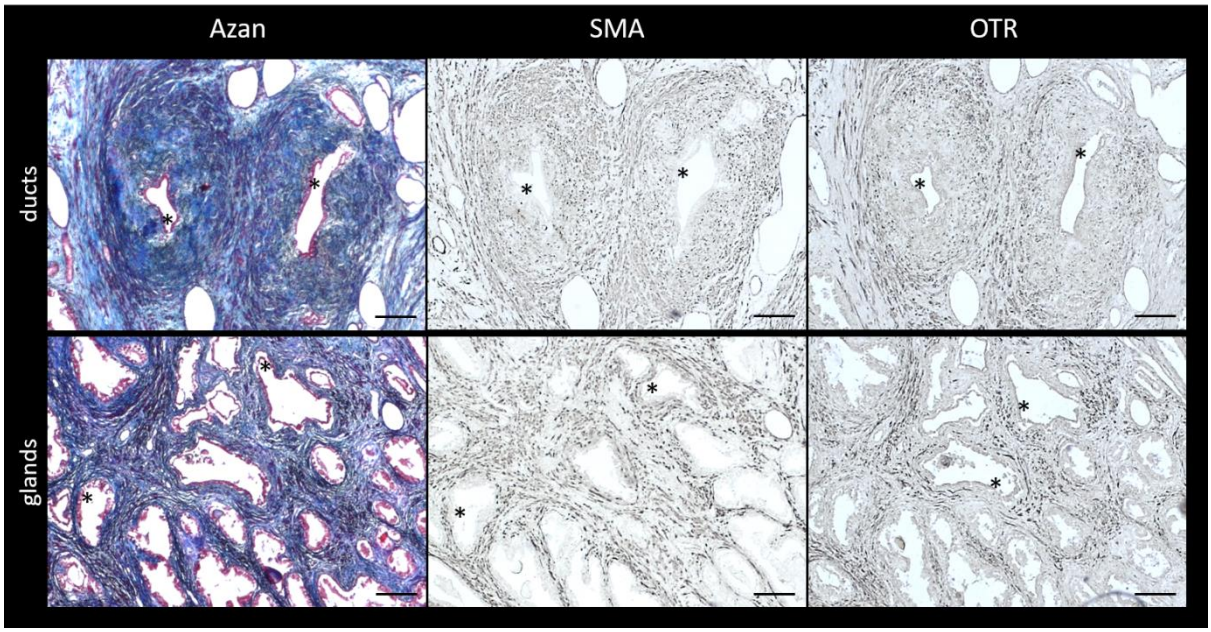

Figure 35: Detection of the distribution of SMA- or OTR-positive cells in the human prostate using chromogenic immunohistochemistry

Ducts and glands from human prostatic tissue samples were identified and displayed using AZAN staining. The distribution of SMA- or OTR-positive cells was detected using chromogenic immunohistochemistry (black scale bar: 100 µm, epithelium (*)). The distribution of SMA and OTR staining seems very similar, suggesting an expression of OTR in the smooth muscle cells of the human prostate. A slight staining of OTR in the epithelium (*) could be possible.
(Negative controls without primary antibodies showed no staining.)

In the human prostate (glands (Fig. 36) as well as ducts (Fig. 37)), double staining for SMA and OTR using immunofluorescence (n=3) showed that all OTR were localized in SMA-positive cells. There was no detectable staining of OTR in the epithelium (*). There were no cells expressing only SMA or OTR surrounding the human prostatic glands (g) (Fig. 36). It seems that there might be some SMA-positive cells surrounding the ducts (d) of the human prostate (closer to the lumen) that do not express the OTR (Fig. 37).

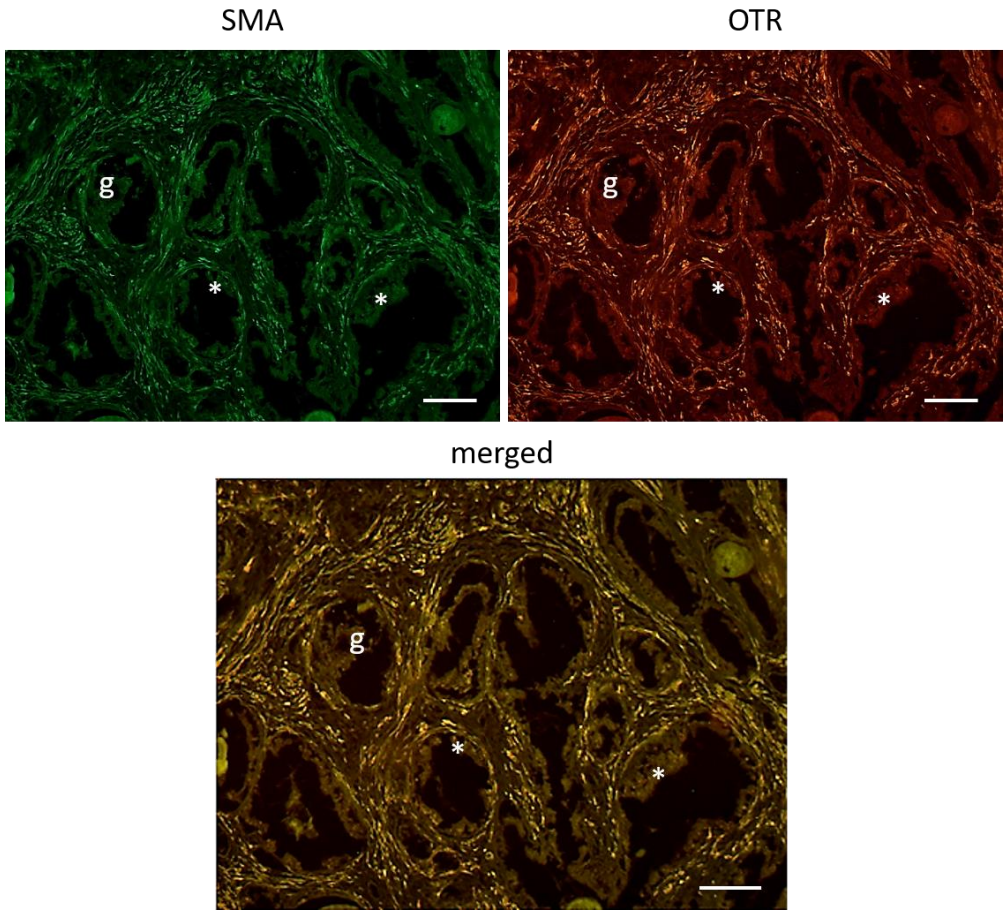

Figure 36: Detection of the distribution of SMA- and/or OTR-positive cells surrounding glands of the human prostate using immunofluorescence

The distribution of SMA- and/or OTR-positive cells around the prostatic glands (g) of the human prostate using immunofluorescence showed that all OTR seem to be expressed in smooth muscle cells (white scale bar: 100 µm). Here no staining of OTR was found in the epithelium (*). There seem to be no cells expressing only the OTR or SMA. (Negative controls without primary antibodies showed no autofluorescence or non-specific fluorescence.)

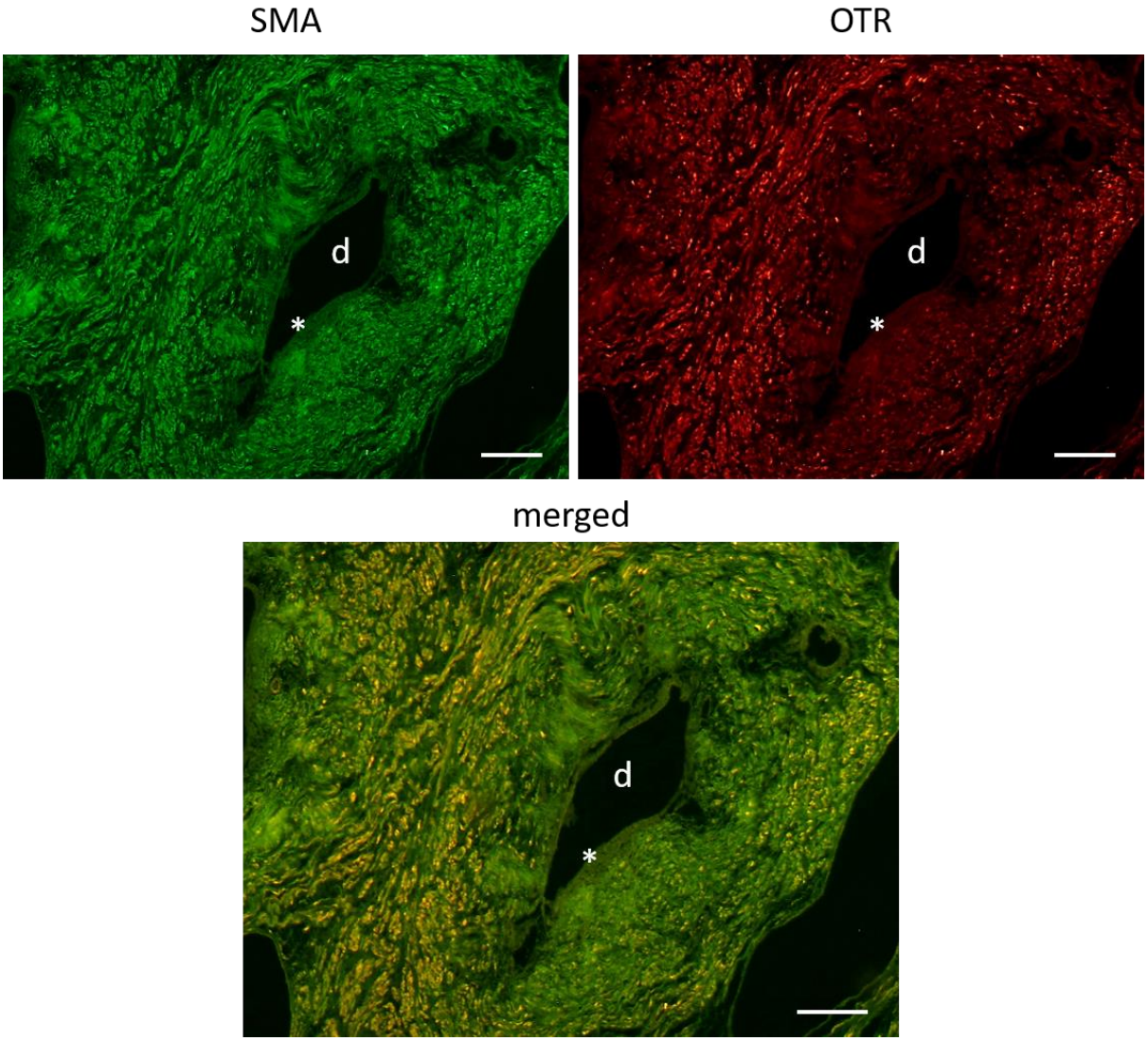

Figure 37: Detection of the distribution of SMA- and/or OTR-positive cells surrounding a human prostatic duct using immunofluorescence

The distribution of SMA- and/or OTR-positive cells around the prostatic ducts (d) of the human prostate using immunofluorescence showed that all OTR seem to be expressed in smooth muscle cells (white scale bar: 100 µm). Here no staining of OTR was found in the epithelium (*). There seem to be some smooth muscle cells closer to the lumen of the prostatic ducts that do not express the OTR. (Negative controls without primary antibodies showed no autofluorescence or non-specific fluorescence.)

Rat prostate

Rat prostatic ducts were distinguished from glands following the description that the rat prostatic ducts possess multiple layers of smooth muscle cells proximal to the urethra (Nemeth and Lee 1996), whereas the prostatic glands possess only a single layer of smooth muscle cells, as clearly visible in the following images.

Using immunohistochemistry, it was found that the OTR was expressed in the rat prostate (n=3).

In the chromogenic immunohistochemistry images, the OTR was found to be expressed throughout the rat prostate (likewise around glands (g) as well as ducts (d)) and in a similar manner to the expression of SMA-positive cells. There was no staining of OTR in the epithelium of the rat prostate (Fig. 38).

Figure 38: Detection of the distribution of SMA- or OTR-positive cells surrounding ducts and glands of the rat prostate using chromogenic immunohistochemistry

Ducts (d) and glands (g) from rat prostatic tissue samples were identified and displayed using AZAN staining. Detection of the distribution of SMA- or OTR-positive cells surrounding ducts and glands of the rat prostate was shown using chromogenic immunohistochemistry (black scale bar: 100 µm, epithelium (*)). The distribution of SMA and OTR staining seems very similar, suggesting an expression of OTR in the smooth muscle cells of the rat prostate. No staining of OTR in the epithelium (*) was observed. (Negative controls without primary antibodies showed no staining.)

In the rat prostate, double staining for SMA and OTR using immunofluorescence (n=3) showed that all OTR were localized in SMA-positive cells likewise surrounding ducts (d) or glands (g). There was no detectable staining of OTR in the epithelium (*). There were no cells expressing only SMA or OTR (Fig. 39).

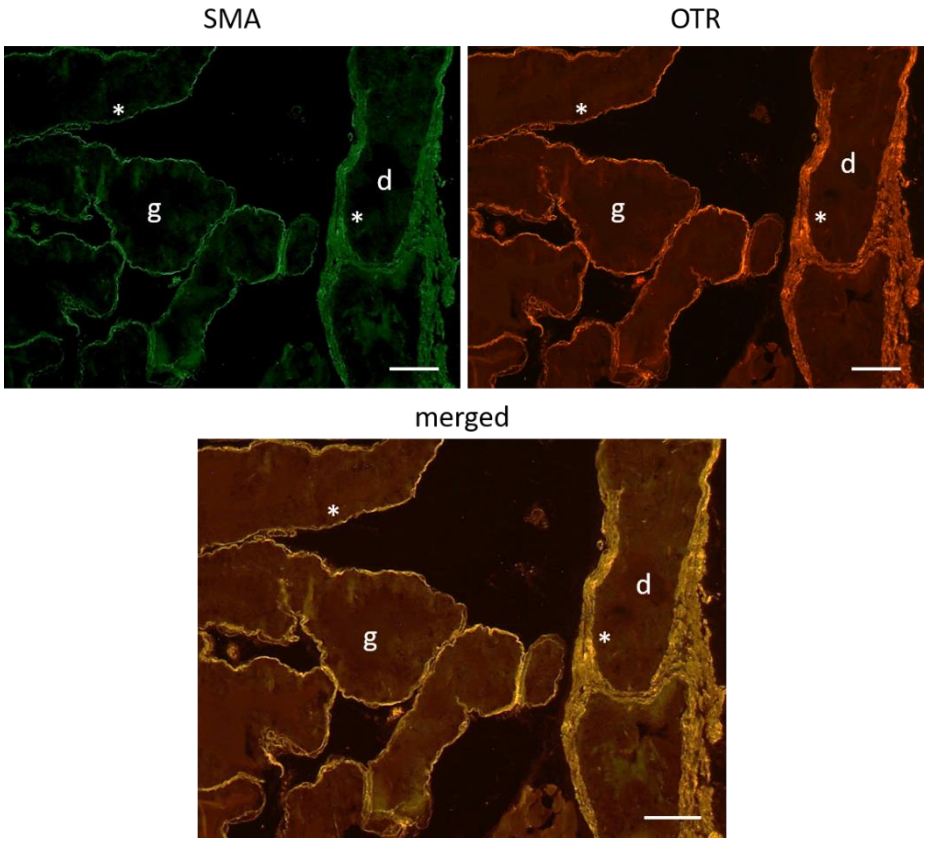

Figure 39: Detection of the distribution of SMA- and/or OTR-positive cells surrounding ducts and glands of the rat prostate using immunofluorescence

The distribution of SMA- and/or OTR-positive cells surrounding the prostatic ducts (d) and glands (g) of the rat prostate using immunofluorescence showed that all OTR seem to be expressed in the smooth muscle cells (white scale bar: 100 µm). No staining of OTR was found in the epithelium (*). There seem to be no cells expressing only the OTR or SMA. (Negative controls without primary antibodies showed no autofluorescence or non-specific fluorescence.)

Rat epididymis

In the adult rat epididymis, double staining for SMA and OTR using immunofluorescence (n=3) showed that all OTR were localized in SMA-positive cells. There was no detectable staining of OTR in the epithelium (*). There were no cells expressing only SMA or OTR (Fig. 40). Since there are more smooth muscle cell layers surrounding the epididymal duct distally, there is also more OTR expression detected. However, there was no apparent increase in OTR expression in S19 other than due to a thicker smooth muscle cell layer.

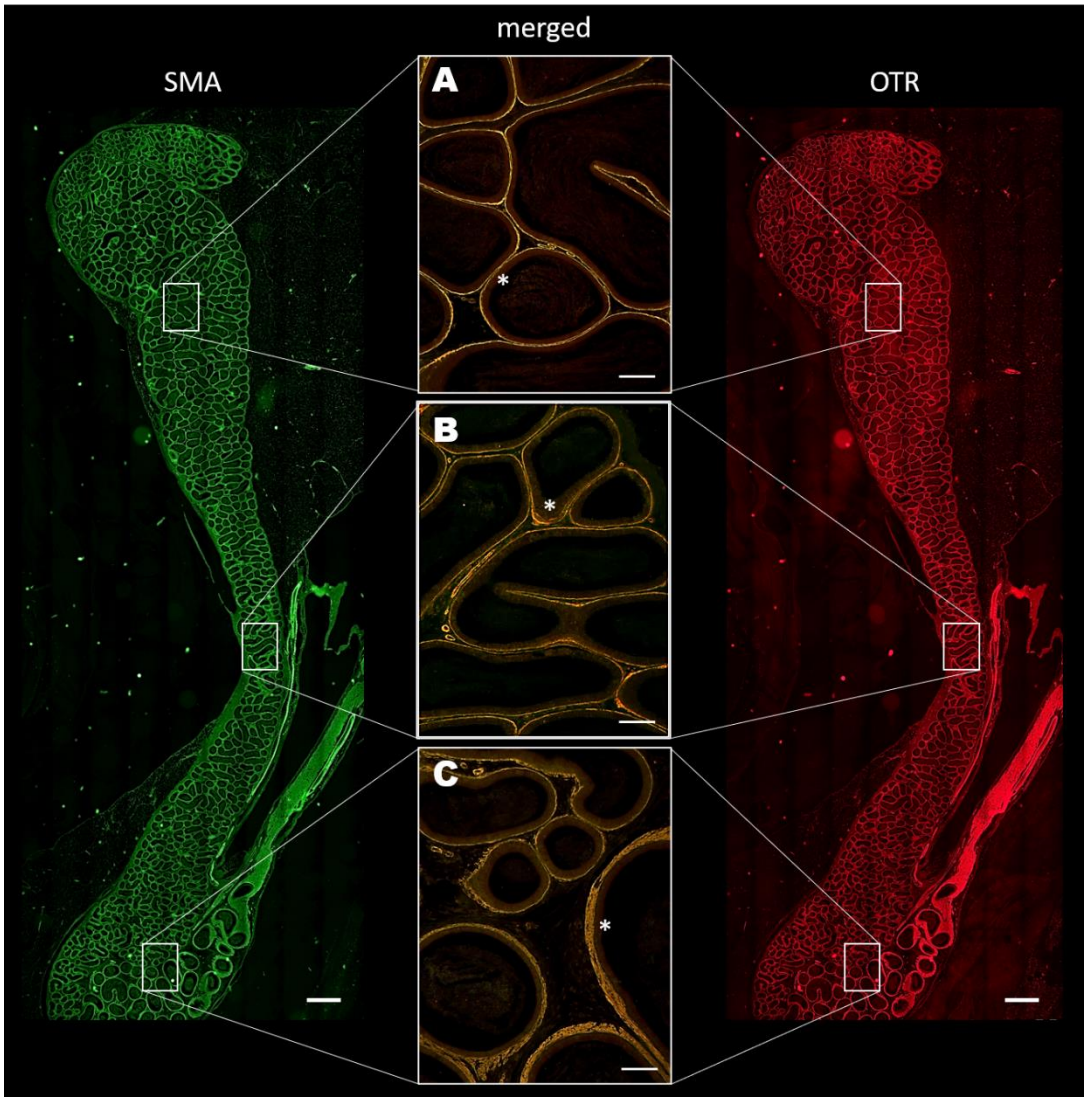

Figure 40: Detection of the distribution of SMA- and/or OTR-positive cells in the adult rat epididymis using immunofluorescence

The distribution and possible colocalization of SMA- and OTR-positive cells around the adult epididymal duct of the rat using immunofluorescence showed that all OTR are expressed in the smooth muscle cells (white scale bar in overview: 1 mm). There seem to be no cells expressing only the OTR or SMA (exemplary magnifications of caput (A), corpus (B) and cauda (C) (scale bar in magnifications: 100 µm). No staining of OTR was found in the epithelium (*). (Negative controls without primary antibodies showed no autofluorescence or non-specific fluorescence.)

In the neonatal rat epididymis, double staining for SMA and OTR using immunofluorescence (n=3) showed that all OTR were localized in SMA-positive cells. There was no detectable staining of OTR in the epithelium (*). There were no cells expressing only SMA or OTR (Fig. 41). There was no apparent increase in OTR expression at any distinct location of the neonatal rat epididymis.

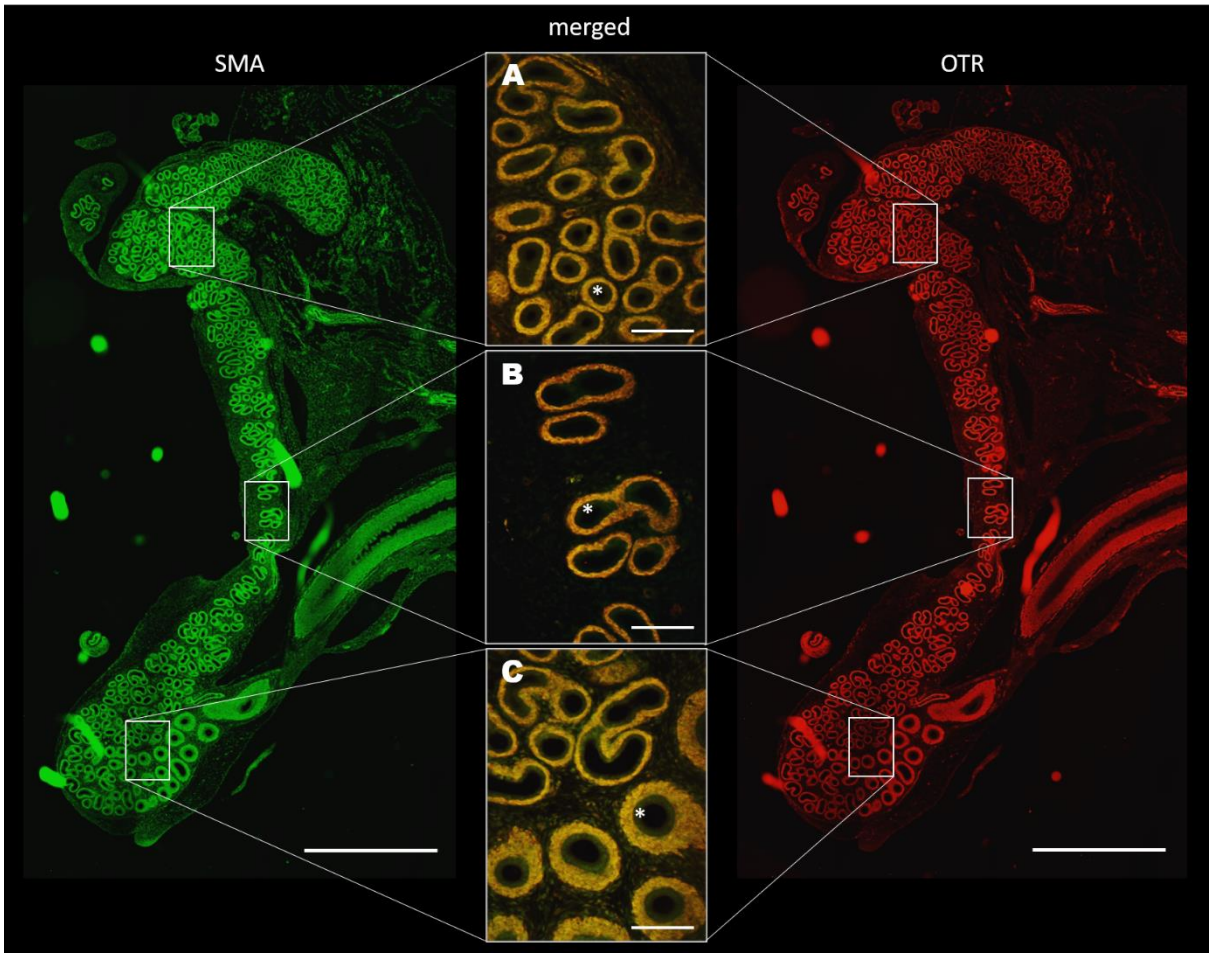

Figure 41: Detection of the distribution of SMA- and/or OTR-positive cells in the neonatal rat epididymis using immunofluorescence

The distribution and possible colocalization of SMA- and OTR-positive cells around the neonatal epididymal duct of the rat using immunofluorescence showed that all OTR are expressed in the smooth muscle cells (white scale bar in overview: 1 mm). There seem to be no cells expressing only the OTR or SMA (exemplary magnifications of caput (A), corpus (B) and cauda (C) (scale bar in magnifications: 100 µm). No staining of OTR was found in the epithelium (*). (Negative controls without primary antibodies showed no autofluorescence or non-specific fluorescence.)

Fine structure of the human prostatic ductal system

Technovit® injection

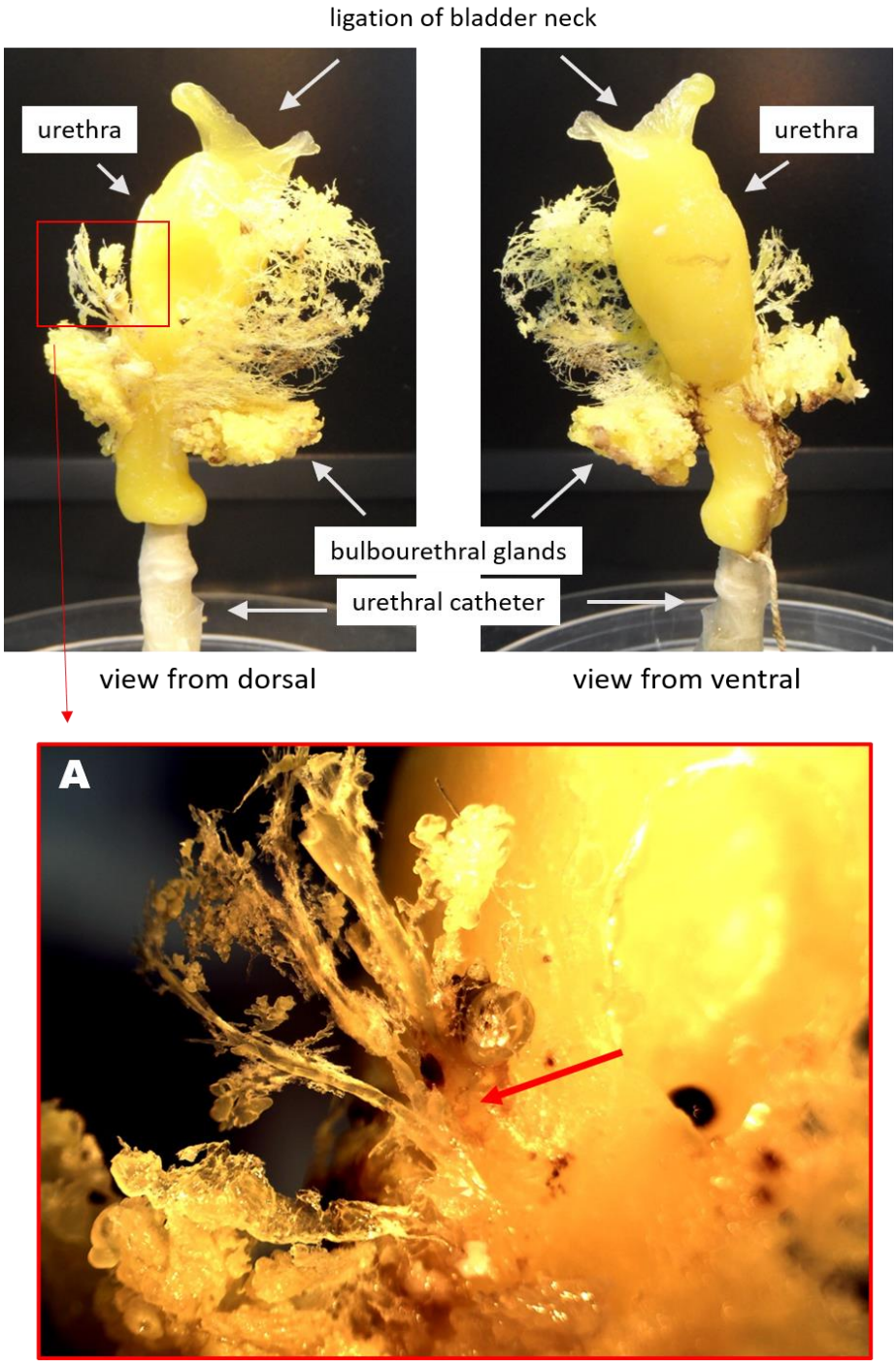

Figure 42: Corrosion cast model of the human prostate from injection with Technovit

A *Magnified image of the region of interest (red rectangle) showing prostatic ducts draining into the urethra (red arrow).*

The corrosion cast model of a human prostate (n=1) using Technovit® (Fig. 42) gave a first impression of the organization of the prostatic duct system. Seemingly all ducts feed into the urethra only on the dorsal side of the human prostate. There seems to be a complex tree-like branching of the ducts, fanning around to the ventral side separately for each side.

MICROFIL® injection and reconstruction

The injection of the radiopaque MICROFIL® (n=1) allowed for 3D reconstruction of single structures using ANALYZE® software after micro-CT imaging. A single duct (green) connected to the urethra (red) was then segmented backwards following up to the terminal tubulo-alveolar glands (green distally) of the human prostate. As such a single duct of the human prostate connecting to the glands was visualized in 3D (Fig. 43).

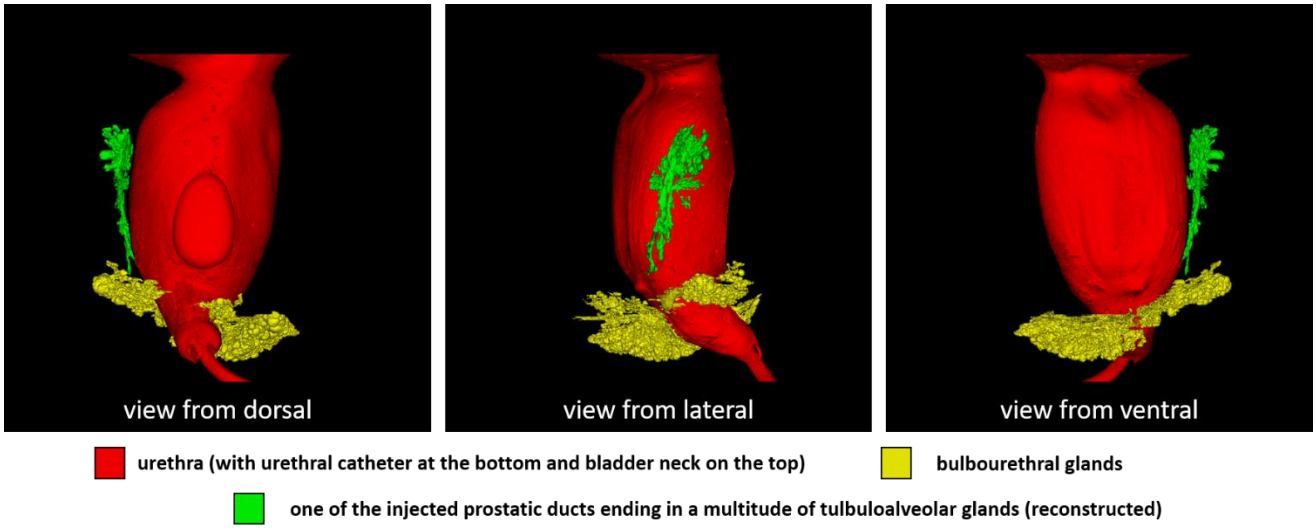

Figure 43: 3D reconstruction of the human prostate injected with MICROFIL®

Segmentation and 3D reconstruction of a single prostatic duct (green) following backwards from the urethra to the terminal tubulo-alveolar glands in a human prostate injected with the radiopaque MICROFIL® and imaged using micro-CT.

Micro-CT imaging of human prostate

Using human prostate (n=1) from formaldehyde-fixed body donors that had been incubated in the contrast agent PTA (5 %), a micro-CT scan of the prostate was performed displaying the fine structure of the human prostatic duct system in its entirety. By scrolling through the tissue using Data Viewer software (as presented in the movie in a transversal view), more details about the prostatic duct system became apparent (Fig. 44).

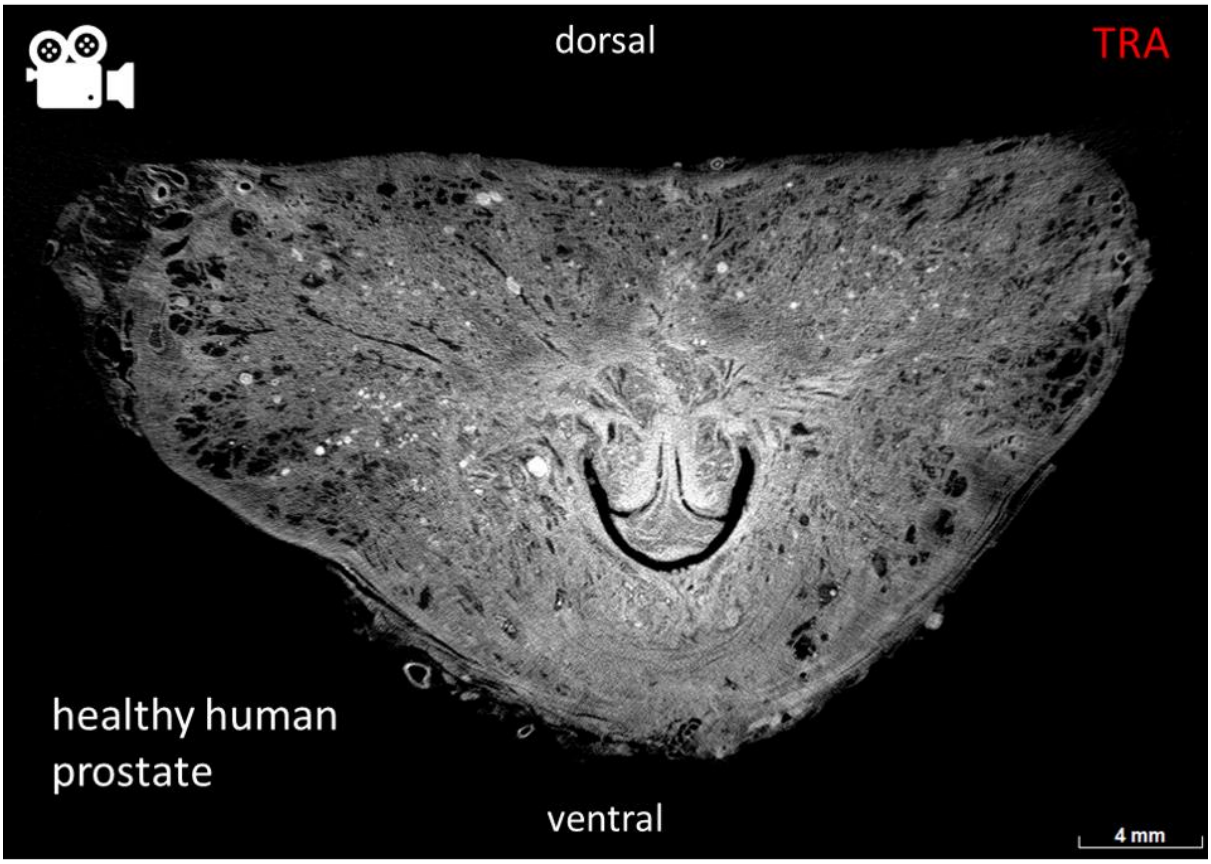

Figure 44: Micro-CT image of human prostate incubated in 5 % PTA

One representative slice of a transversal view of a prostate that had been incubated in 5 % PTA and scanned in the micro CT (movie of a representative stack included) (white scale bar: 4 mm).
There are long branch-like structures (prostatic ducts) leading towards the colliculus seminalis (and into the urethra) and glandular structures on the rim of the dorsal and lateral parts of the prostate. The two very prominent ducts draining into the urethra at a 90° angle on the colliculus seminalis are the ejaculatory ducts.

The impression of the prostatic ducts predominantly draining into the urethra on the dorsal side was observed here as well, as previously suggested through the Technovit® Model (Fig. 42). Additionally, most of the ducts seem to be leading onto the colliculus seminalis where the ejaculatory ducts could

also be observed to drain into the urethra. The anterior prostatic gland-free zone after McNeal could also be clearly distinguished in the micro-CT images. Additionally, it could be observed that some prostatic ducts seemed to have a more radiopaque tissue surrounding them (visible as brighter tissue).

Micro-CT imaging of human prostate and corresponding histology

The brighter tissue surrounding the ducts was also noticed in another sample (n=1) that was afterwards successfully processed for histology. The advantage of a combination of first micro-CT imaging and then histological work-up of that same tissue, allowed to accurately pinpoint prostatic ducts (Fig. 45).

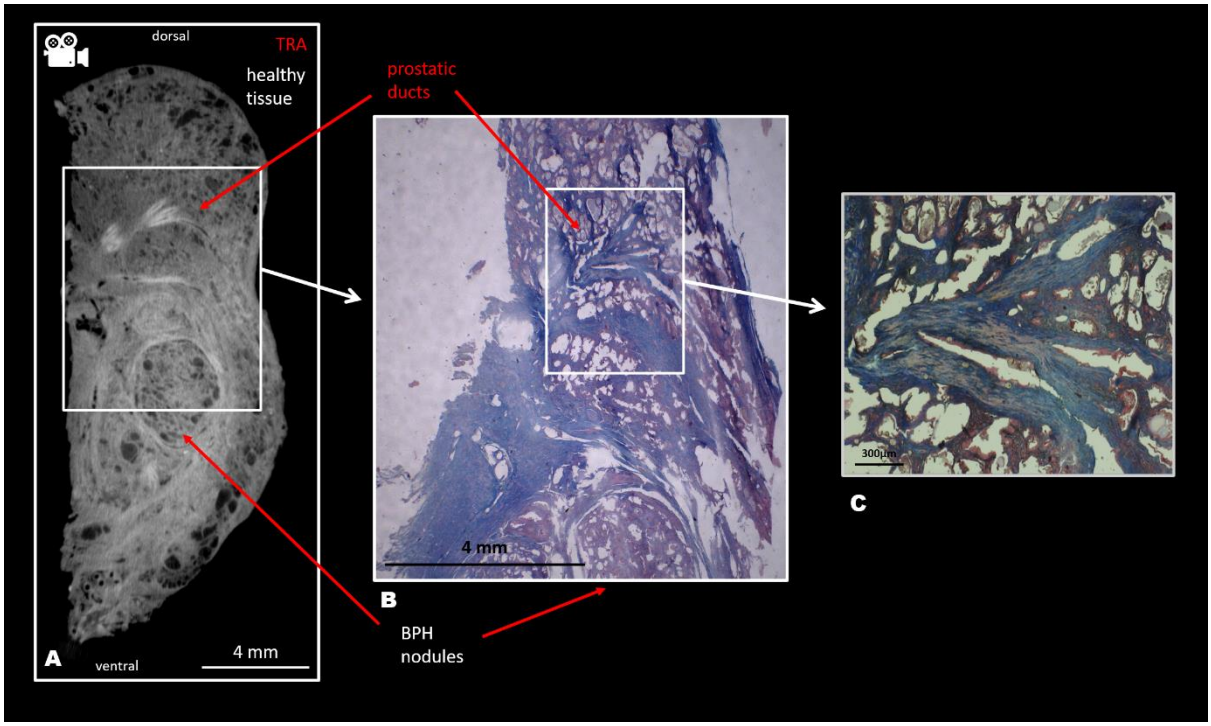

Figure 45: Micro-CT image of human prostate, same tissue then in two AZAN-stained magnifications

***A** The slice with the region of interest as found in the micro-CT scan (white scale bar: 4 mm).*
***B** The same region after cutting and AZAN staining (black scale bar: 4 mm).*
***C** Magnification of the identified prostatic ducts suggesting a special organization of tissue surrounding the human prostatic ducts (black scale bar: 100 µm).*

Regions of interest containing prostatic ducts could be localized using the advantage of reorientating and working through the different slices and views of the micro-CT images. Then, using the integrated scale the location of the ducts for histological investigation were approximated in the original tissue sample. The tissue could then be cut to best represent the chosen orientation and region of interest as seen in the micro-CT images. After embedding and staining the tissue, that same location could be retraced and the region of interest evaluated histologically. These as such defined ducts of the human prostate seem to have a special organization of the surrounding tissue, as already indicated by the brighter surrounding tissue in the micro-CT scans and furthered by the structures found here in the AZAN staining and should be further investigated.

Further investigation into the prostatic duct system of these two samples and in additional samples (including 3D reconstruction of the ducts and further histological characterization) will be continued by a PhD colleague of mine, due to time constraints.

SMA orientation human prostatic gland vs duct

The possible special organization of tissue surrounding the prostatic ducts was further investigated by evaluating the organization of smooth muscle cells in the human prostate using chromogenic immunohistochemistry (Fig. 46). The SMA-positive cells surrounding the glands (g) are seemingly distributed in multiple directions, whereas the layers of SMA-positive cells surrounding the ducts (d) seem more uniform. There was no staining of SMA in the epithelium (*) of either glands or ducts.

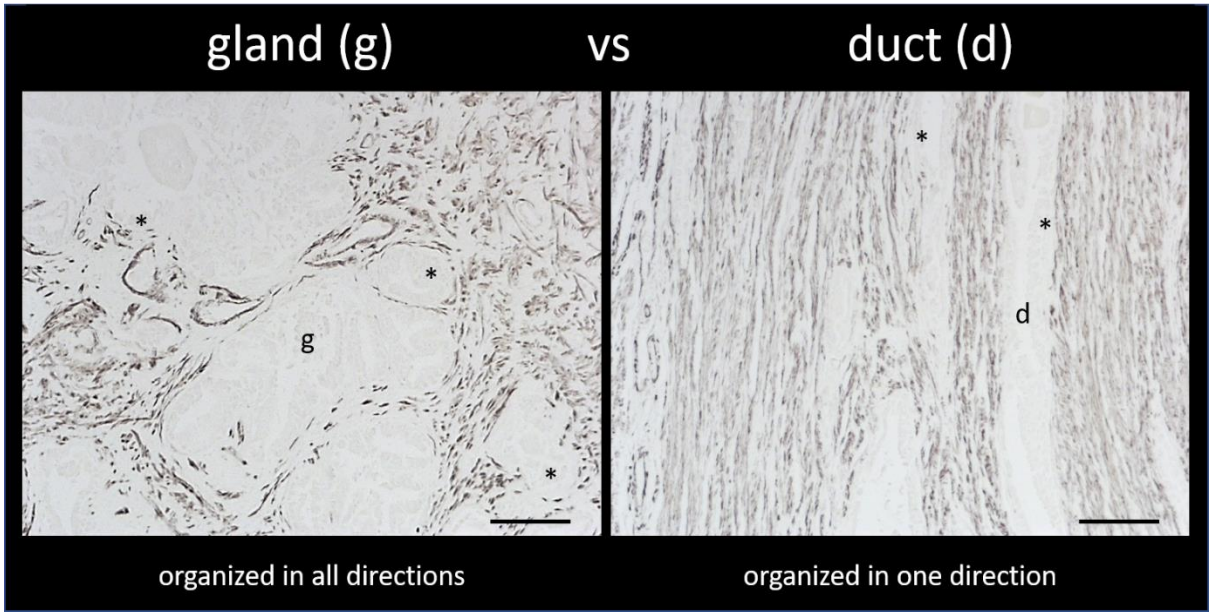

Figure 46: Detection of SMA distribution in the human prostate using chromogenic immunohistochemistry and comparing gland vs duct

The SMA-positive cells surrounding the human prostate gland (g) seem to be organized in multiple directions, whereas the ones surrounding the duct (d) seem to be more uniform (black scale bar: 100 µm, epithelium (*)). (Negative controls without primary antibodies showed no staining.)

Discussion

A new analyzing method for live imaging data

Reslicing the data from live imaging and thereby counting the frequency of the contractions was shown to work effectively with regular single contractions as seen in most of the epididymis (Mietens et al. 2014). However, when it comes to multiple regions of interest distributed over the entire tissue (as in the prostate) or a multidirectional or complex contraction (as in the last part of the epididymis), this function reaches its limits as it is only visualizing movement along a single line as region of interest which must be manually chosen. Therefore, we investigated another method to quantify the change of movement while considering the tissue in its entirety and thus eliminating user bias in choosing a specific region of interest. The previously developed Wiggle Index (Denecke et al. 2015; Preston et al. 2015; Preston et al. 2016) only summed up the movement in the field of view and how that changed. The enhanced version developed specifically for this thesis subdivided the defined and complex region of interest (the tissue without the translucent background of the dish) into data points for each of which a movement score was calculated as well as a relative fold change in relation to every other part of the experiment. As such it allowed us not only to evaluate how the sum of movement changed throughout the experiment but how each data point by itself evolved. In addition, calculating the relative fold-change of movement from one section of the experiment to another (e.g. "no treatment" to "+ oxytocin") allowed us to accurately compare one experimental setup to others, since all experiments incorporated their own "baseline" (the "no treatment" period). This was substantiated by the fact that in three different experimental setups that were carried out more than a year apart but theoretically should yield the same relative change ("no treatment" to "+ oxytocin" vs "no treatment + DMSO" to "+ oxytocin" vs "no treatment + tamsulosin +NE" to "+ oxytocin") ended up being statistically not significant to each other. The other major advantage can also be challenging depending on the technique of the experimenter, since this new analysis method detects very small movements (as seen with 1 nM oxytocin). But since the method cannot distinguish between movement of the tissue and movement of the fluid in the dish, particles floating over the tissue or changes in light, some additional care should be used when filming the tissue from above (as done at JLU). These things are still important to consider when filming from beneath (as done at Monash), but they are less pronounced. However, if the experiments are conducted in a careful manner these "issues" do not impede the analysis but make the experimental setup more sensitive. The open-source code available freely on https://doi.org/10.26180/13653614 works together with the freeware Fiji (Schindelin et al. 2012) and automatically saves the data as excel sheets with the raw data points, the relative change and a quick overview to get a sense of how the movement score changes throughout the experiment. Additionally, it saves movies and summarizes images (heat maps) displaying the movement and change of movement respectively in a colour coded manner, with red and

grey representing the higher scores and blue indicating the lower scores. Since movement in live imaging data is hard to convey in still images, these heat maps are an easy-to-understand representation of the data at one glance, without losing the dynamic of the movie completely.

The effect of oxytocin in the prostate

The only previous functional oxytocin study with human prostatic tissue samples found an increase in prostatic tone as well as contractions after OT application using organ bath (Bodanszky et al. 1992). However, because of the scarce availability of human prostatic tissue samples, they only used tissue obtained from patients undergoing resection for benign prostatic hypertrophy. Since the expression of OTR has been shown to be increased in BPH-tissue (Sendemir et al. 2008; Xu et al. 2017b; Li et al. 2018b), it is plausible that this tissue could react with greater force than "normal" prostatic tissue. Another factor to consider is that the smooth muscle cells in the prostate are not orientated in a specific way visible during preparation as it is in e.g. the bladder. Thus, since the organ bath method only registers the sum of contractions in line with the force transducers, there is the possibility of contractions cancelling each other out or being not recorded at all.

Therefore, we used live imaging in our experiments and found that OT had an increasing effect on the contractions of the tissue originating from either prostatectomy or TUR-P. However, the tissue originating from prostatectomy was already contracting more during the "no treatment" period and the response to OT was greater compared to the tissue originating from TUR-P. We would attribute this fact mostly to the method of how prostatic tissue has been removed rather than expression of OTR. In the samples originating from prostatectomies, the cancerous tissue was identified by a pathologist and a "healthy" prostate sample was extracted with a scalpel for our live imaging experiments. (Although BPH can coincide with prostate cancer especially in the older men (Kumar 2007a), the tissue obtained for our live imaging experiments was deemed BPH-free by histological screening). During the TUR-P procedure however, the tissue was stripped away by an electrode that simultaneously cauterized the tissue to prevent blood loss for the patient. As such (described in the method section of this thesis) the edges of the tissue originating from TUR-P are burned. It seems plausible that therefore this tissue might also be less viable than the tissue originating from prostatectomy. In the previous paper by Bodanzky et. al (Bodanszky et al. 1992) the method used for extracting the BPH-tissue has not been described, however it seems likely that they used the well-established method of TUR-P. All the samples from our prostatectomy patients originated from older men. Since the OTR expression was also described to increase with age (Herbert et al. 2007; Sendemir et al. 2008), this might account for some of the increased responses to OT observed in our experiments.

There were only three other studies investigating the effect of OT on the contractility of the prostate in other mammals. Two studies using organ bath found an increasing effect of OT in the rat, dog and guinea pig prostate (Bodanszky et al. 1992; Sharaf et al. 1992), while another study also using organ bath found there to be no effect in the rat and rabbit prostate (Gupta et al. 2008). These contradictory reports on the effect of OT in the rat prostate might be explained by how delicate the rat prostatic tissue

is and how small the contractions were that we did observe. In addition the smooth muscle cells in the rat prostate are orientated in a circular manner around the glands and ducts (Kügler et al. 2018) which would make it less efficient to monitor them in a longitudinal set-up (as it would have been in the organ bath).

In our experiments we used live imaging, but still found OT to have no significant effect on the rat prostate. However, there was a difference in reaction observed from one video to another. In most of the videos there were pre-existing small spontaneous movements that only occurred on the walls of the recorded prostatic glands, which were not influenced by OT. In some videos however, also showing the small pre-existing spontaneous wall movements, OT did induce bigger contractions compressing the lumen of the glands in a circular manner. Since these bigger contractions only occurred in a few videos, in summation the effect of OT was statistically not significant. In further studies it would be interesting to separate these two groups and search for histological differences.

The expression of the OTR in the prostate of the human, rat and other animals has been widely described in previous studies (Table 1). Our data is in accordance with what was found previously. It is still unclear whether the OTR is expressed in the stromal or epithelial cells or both.

In this context we found using chromogenic immunohistochemistry some evidence that the OTR might be expressed in the epithelial cells of the human prostate (not the rat though), but when the same antibody and tissue was investigated using immunofluorescence, we found the OTR to only be present in the stroma.

Since the OTR was expressed in both species, it is even more perplexing that OT did not alter contractions in the rat prostate significantly.

One explanation for the lack of a big response to OT in the rat compared to the human prostate could be that the rat normally does not develop BPH. It was proposed that in the rat prostate (but not in the human) OT seems to be involved in a negative feedback mechanism with androgens, that counteracts the stimulus for overgrowth (Popović et al. 1990; Nicholson 1996; Jenkin and Nicholson 1999; Assinder et al. 2004). This mechanism, although mostly related to proliferation not contraction, could still have a counteracting measure on the contractile response as well.

Another, perhaps more plausible explanation could be that all the rats were 6-8 weeks old when sacrificed for the experiments and as such just barely reached full reproductive age (6 weeks) (Sengupta 2013). Also, there are variations of maturity depending on size, weight etc. that can be strikingly different, even in the same litter. In addition, a variance to the human, the rat prostate matures only after birth and is still growing until fully differentiated, at around week 8 after birth (Hayashi et al. 1991a). In comparison, all the human tissue was collected from patients of older age (at least 55 years, usually

around 65 years). Therefore, it is quite possible that age is an important factor in the rat as well, which is being investigated by a junior PhD student, extending the research I commenced.

Since it is not possible to obtain viable healthy human prostate samples from younger men and the rat model does not seem a good substitute so far, we would recommend to mostly rely on data collected through prostatectomy in the future (while testing the contractility of prostatic tissue from older rats).

The effect of oxytocin in the epididymis

The direct effect of OT on the epididymis has been of great interest but was mostly investigated using organ bath, electrical activity or intraluminal catheter as listed in the Introduction and Table 2. However, only one study monitored the contractions using live imaging (Studdard et al. 2002). Also, all previous studies only differentiated the epididymis by the three main regions: caput, corpus and cauda, with the exception of Mewe et. al who defined additional regions using cow epididymis and organ baths (Mewe et al. 2007). By doing so they reported regional differences of the effect of OT, even reporting a diminishing effect of OT on the contractions in corpus and proximal cauda of the cow epididymis. In addition, they compared the effect of OT to NE which seemed comparable in the distal cauda epididymidis. We wanted to extend this investigation even further using rat and human tissue by dividing the epididymis into the segments formed by the connective tissue septa (19 in the rat (Turner et al. 2003; Jelinsky et al. 2007) and 9 in the human (Holstein 1969)). These segments were found to express different genes and proteins while creating a changing microenvironment that could be essential for proper sperm maturation (Domeniconi et al. 2016). Therefore, it seemed likely that they would also have separate contractile patterns. Especially in case of the cauda epididymidis which is where sperm cells are stored until ejaculation and then propelled forward during the ejaculatory process, a unique contractile pattern seemed plausible. To the best of my knowledge, there has been no functional research published using human epididymis to date.

Two previous studies using rat tissue found there to be no effect of OT on the epididymis (Jaakkola and Talo 1981; Gupta et al. 2008), while two other studies both using caput epididymis found OT to have an increasing effect (Hib 1977; Studdard et al. 2002).

Using live imaging, we found that the effect of OT did in fact vary depending on the segment of the epididymis investigated and that the distal cauda epididymidis, especially the very last segment behaves uniquely and much more forcefully than the rest of the epididymis.

Using epididymis of the adult rat, we found that OT slightly but significantly increased the pre-existing contractions in the adult S5 (caput) and S15 (proximal cauda) but not in S12 (corpus). This was similar in the neonatal rat epididymis, in which OT only slightly but significantly increased contractions in the caput, but not in the corpus and proximal cauda region. In the experiments with the human tissue a similar trend could be observed using caput epididymidis.

The last two segments of the epididymis behaved differently. For one they did not display the spontaneous regular contractions that were present in all the other segments investigated, but were very quiet (in both the rat and the human tissue). The most interesting part was their difference in response to stimuli (to OT as well as NE). In the adult rat epididymis S18 responded with strong singular

contractions, while S19 reacted with a forceful series of contractions that compressed the epididymal duct, thereby forcing the content (sperm) to be expelled. In the experiments with the human tissue (S8 and S9) a similar trend could be observed.

This forceful reaction of the very last segment of the adult epididymis was interestingly absent in the neonatal epididymis (of the rat), where only strong singular contractions were induced by either stimulus (OT or NE). This suggests that the epididymis undergoes change until reaching sexual maturity, when these forceful contractions will be needed for a proper ejaculatory process. Furthermore, it indicates that only the very last segment of the epididymis is driving sperm from the epididymis during the emission phase of the ejaculatory process. Since the intensity of the movement induced by OT in S19 of the adult rat epididymis was equal to the one induced by NE during the first 30 seconds after addition and this reaction was localized to the part of the epididymis that stores sperm until ejaculation, it seems plausible that OT is directly involved in the physiology of the ejaculatory process. This is substantiated by the fact that in a knockout mouse model where all three α1 adrenoreceptor subtypes were deleted, the extracted vas deferens did not respond to NE (thought of as being the main transmitter for ejaculation) and 10 % of the mice were still able to sire offspring (Sanbe et al. 2007) implicating other regulating factors of ejaculation.

It is surprising how much the response to stimuli is different in the very last segment (S19 or S9 respectively) compared to the segment just proximal from it (S18 or S8) and how S18 (or S8) is quiet without stimuli but then coordinates into distinctly singular contractions once activated. We investigated using immunofluorescence if an increase in OTR expression unique to S19 could be an explanation, but found no evidence. We found that OTRs are expressed equally in all smooth muscle cells of the adult as well as the neonatal epididymis. As such, the supposed slight increase in signal from caput to cauda in the adult rat epididymis is only attributed to the increase in smooth muscle cell layers circumferentiating the epididymal duct. We propose that rather than an increased prevalence of the OTR (or the adrenergic receptor), the smooth muscle cells themselves could be the explanation for the difference in contractile pattern. One hypothesis proposed that the smooth muscle cells are reorientated into a more longitudinal manner rather than a circumferentiating manner in the distal cauda epididymis (Holstein 1969), which could account for the more disorganized contractions distally that be observed. Another, more likely explanation could be that the smooth muscle cells in S19 might not be communicating as they do in the rest of the epididymis, but resemble the vas deferens. In the rest of the epididymis reslicing the data showed spontaneous regular contractions. This is indicative of a single-unit smooth muscle type where the single smooth muscle cells are linked through gap junctions, transferring the signal induced by pacemaker cells from cell to cell thus coordinating distinctly singular contractions (Pape et al. 2018). The multi-unit smooth muscle type (as seen in the vas deferens) usually shows no spontaneous activity. Here only a few muscle cells are linked through gap junctions, contracting as a unit, but since the link to other groups is missing the contractions look more uncoordinated (Pape et al. 2018). When there are no pacemaker cells and no continuous communication

is possible because of the lack of gap junctions, each group must be individually innervated by vegetative nerves. This sum of small contractions (possibly uncoordinated) is what we saw in S19 of the adult rat epididymis. It still does not explain though how S18 can be both, showing no spontaneous contractions but still single coordinated contractions when activated. Maybe the smooth muscle cells of S18 are indeed linked with gap junctions (accounting for the coordinated contractions after stimulus) but without pacemaker cells and therefore no spontaneous contractions. Parts of all segments have been isolated for the experimental setup of our experiment. To investigate if the spontaneous regular contractions as seen in the more proximal parts of the epididymis (S1-17) would normally be transduced to S18 and S19 when the tissue is connected, experiments using longer parts of the ducts including S17 and S18 could be conducted as well as experiments with only the tunica incised or even *in vivo* imaging. It does seem likely though that the signal coming from S17 is stopped by the CTS border from S17 to S18, keeping S18 and S19 quiet, so as to not disturb the proper storage of sperm in the distal cauda epididymidis.

The last segment of the human epididymis did react markedly weaker to the same concentration of OT than seen in our rat experiments. In a similar manner OT has failed to show an effect on sperm count, semen volume or time until ejaculation in previous human studies (Powers et al. 1982; Goverde et al. 1998; Walch et al. 2001; Byrne et al. 2003), whereas it has been effective in numerous animal models (see "The effect of oxytocin on semen parameters" in the Introduction). However, since the strong reaction to NE was present in the same human experiments and the response to OT in the human tissue resembled closely the response of the rat tissue to a lower concentration of OT (10 nM), we would speculate that with a higher concentration of OT in the human experiments the same big response could be achieved. Perhaps the ineffectiveness of OT in the previously conducted studies with humans could be partially attributed to the need for a higher concentration of OT than anticipated. In addition, the awareness of the human test subjects of the rather intime experimental setup itself could have an influence on the results as well, since part of the emission phase of ejaculation can be actively controlled by the human mind.

From our data, we do believe the rat epididymis especially S19 to be an optimal substitute for human tissue and propose S19 to be an advantageous model altogether for testing bioactivity of agonists and antagonists.

The lack of OT effect in the rat epididymis observed by two of the previous papers might be explained by the region they chose. One paper did not clarify which portion of the rat epididymis they chose exactly (Gupta et al. 2008) and the other used a 5 cm part of the epididymal duct that was 20 cm away from the end of the epididymis (Jaakkola and Talo 1981). This leads us to believe that since, in all other regions of the epididymis except for the last two segments the effect of OT was only small or non-existent, it is likely that this is the reason why OT was deemed as ineffective in contracting the rat

epididymis in those two studies. One of the previous papers that found OT to have no effect on the epididymis using organ bath additionally declared that the OT-induced contractions in the ejaculatory tissues are mediated through the arginine vasopressin 1A receptor and not the OTR. They demonstrated this by using the highly selective arginine vasopressin 1A receptor antagonist SR49059. Since OT is very similar to arginine vasopressin in its peptide structure and their receptors are very similar as well (Song and Albers 2017), it is important to determine which receptor to target and to develop highly selective drugs to exclude off-target effects as much as possible.

To clarify whether the reaction we saw in our experiments was mainly mediated through the OTR or the arginine vasopressin 1A receptor, we performed a series of experiments with antagonists. We chose the most commonly used OT antagonist atosiban (which actually seems to have higher affinity to the arginine vasopressin receptor than to the OTR (Phaneuf et al. 1994)), the highly selective OTR antagonist cligosiban (Wayman et al. 2018) and the highly selective arginine vasopressin 1A receptor antagonist SR49059 (Serradeil-Le Gal et al. 1993).

From our results we conclude that the effect of OT in S19 of the rat epididymis is mainly mediated through the OTR, since cligosiban was able to block a reaction to OT whereas SR49059 failed to completely block the response to OT. The ability of SR49059 to elicit some degree of blockage observed in this experimental set-up might be explained by a cross-reactivity with the OTR (especially because of the high concentration used).

Lastly, one paper already demonstrated that OT could contract the cauda epididymidis of sheep that had been blocked with an α-adrenergic antagonist (and were unresponsive to NE) (Knight 1974). To determine if the two pathways were in fact independent in the rat as well as in the human epididymis, we conducted the experiments using the α1 adrenoreceptor antagonist tamsulosin.

Our data showed that the rat tissue that had been unresponsive to NE was still excitable by OT. The response to OT in the tissue that had been pretreated with tamsulosin was not significantly different when compared to the tissue without tamsulosin pretreatment, showing that the OT effect is completely unimpaired by adrenergic inhibition. In a similar manner in our OTR antagonist experiments, we added NE as a last step to check for tissue viability which also showed that inhibiting the OT pathway does not impair the adrenergic pathway. The experiments with human tissue showed the same tendencies as in the rat experiments. However, the same concentration of tamsulosin was not able to completely abolish the reaction to NE in human tissue (as seen before in the rat tissue). We would also attribute this to a need for a higher drug concentration in the human compared to the rat. The response to OT was still greater than the one to NE in these tamsulosin treated human tissue samples, allowing us to draw similarities to the rat data.

Oxytocin as a therapeutic

OT-based medications have a long-standing history of being used for either agonizing (Attilakos et al. 2010) or antagonizing contractions in the uterus (Pierzynski et al. 2004) and inducing milk ejection (Nishimori et al. 1996) in women (targeting the contractile abilities of OT). In the male however, despite the great interest of studies in the 70s in the effect of OT on the male reproductive system, no OT-based medications have yet been prescribed for furthering or inhibiting contractions in the male reproductive system. Here I would like to discuss OT-based medication as a therapeutic for BPH and/or ejaculatory disorders.

As first line of medical BPH treatment, α1 adrenoreceptor blockers are prescribed to relax the smooth muscle cells of the prostate and relieve lower urinary tract symptoms (Silva et al. 2014b). Since α1 adrenoreceptors are present throughout the male reproductive tract, often side effects such as ejaculatory disorders are noted after oral application of α1 blockers as in medical treatment of BPH (especially with tamsulosin treatment) (Narayan and Lepor 2001; Carbone and Hodges 2003) but also in the treatment of high blood pressure (Pandit 1996). For the treatment of ejaculatory disorders there is no gold standard because of their entirely different etiologies (e.g. physiological, anatomical or psychological origin) (Rowland et al. 2010). There are also few agents used to target the contractile pathologies of ejaculation. The adrenergic and purinergic pathways seem to be the most targeted. Targeting the mostly ubiquitous adrenergic receptor is often difficult and a variety of potentially dangerous side effects (especially on the heart (Lepor et al. 2008)) have to be considered. Thus, an alternative to targeting the adrenergic pathway for the treatment of BPH as well as ejaculatory disorders is elemental.

Given the significant effect OT had in both our experiments with the prostate and distal epididymis, we endorse the OT pathway as a viable alternative to existing treatment options for BPH as well as ejaculatory disorders. Comparing the contractile effect of OT between the epididymis and the prostate, the epididymal effect was much stronger. This could be indicative for OT antagonists having a similar negative impact on ejaculation as seen with the α1 blockers when used for BPH treatment. In addition, a long-term treatment as such required for the treatment of BPH might be more difficult to achieve with OT-based medications, since they mostly present with short half-lifes. Nevertheless, further studies with OT antagonists in the prostate are necessary to evaluate the effect on spontaneous tension and contractility and to assess their usability for BPH treatment (as being conducted by PhD colleagues of mine). The more intriguing aspect of targeting the OT pathway for the treatment of BPH might be that OT has been discussed to have a contractile as well as proliferative influence in this organ. As such it might be of special interest to develop more targeted OT analogues only activating Gq, Gs or Gi individually, or even simultaneously inhibiting contractions as well as proliferation with the same drug.

From our results we do believe OT-based medications could show great potential for the treatment of delayed ejaculation or even anejaculation, especially in cases where this pathology results from adrenergic impairment (such as from spinal cord injury). Our experiments comparing the effect of OT to NE in S19 of the adult rat epididymis showed that the response induced by OT was in fact equal to NE and the content was visibly expelled from the duct in the videos. The human tissue did react markedly weaker than the rat epididymis. Therefore, further experiments using live imaging and human S9 should be conducted to clarify if this indeed can be attributed to the need of a higher drug concentration as suggested by us or not. As a next step applying OT in experiments with the triple α1 adrenoreceptor knock-out model (Sanbe et al. 2007) it would be ideal to observe if OT by itself could restore normal sexual function to some degree in these mice. If so, OT could not only be helpful in restoring some ejaculatory function in BPH patients, but be a great hope for patients with spinal cord injuries often affecting younger men still wanting to father children.

Concerning OT-based medications for the treatment of premature ejaculation or even as a male contraceptive, previous studies in the rat seemed promising for the inhibition of apomorphine-induced ejaculation using cligosiban (Wayman et al. 2018). From our rat experiments we deduced that although cligosiban potently inhibited a response to OT, the adrenergic pathway (being the main inducer of contractions during the ejaculatory process (Pacini et al. 2018)) was unimpaired and therefore a monotherapy targeting the OTR to prevent or delay ejaculation seems unlikely. In the human, one study found cligosiban to be effective in prolonging intravaginal ejaculation latency time compared to placebo (McMahon et al. 2019) while another found it to be not effective (Althof et al. 2019). We suggest that a combined treatment targeting the OT as well as the adrenergic pathway to prevent or delay ejaculation could yield much better results.

S19 as a model

Testing smooth muscle responses to different stimuli is an essential tool in drug development. Often the structural changes made to cater for more desirable attributes such as heat stability or longer half-lives result in a diminished or even abolished bioactivity. From experience a drug is difficult to assess in a tissue that contracts spontaneously since there will be changes of frequency, amplitude and tension already from one tissue to another in the "no treatment" period.

S19 of the rat epididymis uniquely qualifies for a testing model since it is rather rare to have a tissue that is this quiescent without stimulus and then reacts in such a strong manner to OT or NE. Our data shows that S19 in combination with live imaging and our analysis method could accurately detect different concentrations of OT, clearly grouping together statistically as well as from visual inspection of their contractile patterns in the videos. Our antagonist experiments showed how straightforward it was to evaluate the blocking effect of different OT antagonists, an arginine-vasopressin antagonist and an α1 adrenoreceptor antagonist, especially in determining a maximum response by testing out different concentrations.

The S19 of the rat epididymis is abundantly available and using live imaging allows for a large number of experiments per animal, since it only uses very little tissue. Other models using human myometrium have been proposed (Arrowsmith et al. 2018), but human tissue is always harder to acquire and human uterine strips (like most smooth muscle models) do contract spontaneously, making evaluating agonistic and antagonistic effects challenging.

Therefore, we strongly recommend to take advantage of S19 of the rat epididymis as a testing model for at least any drugs targeting the OT or the α1 adrenergic pathway. We especially propose this model for a first screening process if the drug shows any bioactivity, even if subsequent tissue targets are different (e.g. gastro-intestinal tract or uterus).

The human prostatic duct system

The prostatic duct system of the rat with its different lobulation has been previously studied (Lee et al. 1990b; Hayashi et al. 1991a; Nemeth et al. 1997), while there is no such information about the human prostatic duct system. More recently, a single study has reconstructed one structure of what they found histologically to be a prostatic duct of the human prostate (Sherstyuk et al. 2015). In textbooks the only remark given is that there are around 15-30 prostatic ducts draining into the urethra (Kummer and Welsch 2018). Especially compared to other organs in which the draining duct system is histologically characterized, including the description of the surrounding tissue, it is striking how little is known of the prostatic duct system. In the rat, especially the duct segments closest to the urethra have thicker smooth muscle cell layers (Nemeth and Lee 1996) and functionally behave differently from the prostatic glands (Lee et al. 1990b; Kügler et al. 2018). Therefore, a more in-depth knowledge of the human prostatic duct system is essential.

We started out to search for prostatic ducts histologically by slicing through two entire human prostates. However, the accurate detection of prostatic ducts was rather difficult. We were uncertain if the longitudinal structures we identified were prostatic ducts, the tubular part of a tubulo-alveolar gland or an artefact through BPH, since most prostate samples we received from human body donors were from older men and therefore showed different stages of BPH. Also, it did not clarify how the entirety of the prostatic duct system would be orientated. Therefore, in a next step the idea was to demonstrate the prostatic duct system in a corrosion cast model similar to well-known models showing the vasculature of different organs on display in numerous institutes, including the human and veterinary anatomy buildings in Giessen. The procedure however has not been commonly used for decades and therefore compromises had to be made when creating the model presented in this thesis (e.g. no vacuum chamber). In addition, the tissue we could use for injection was extracted from fresh frozen human body donors that were thawed for harvesting of the prostate. For this reason and due to it being the first experimental experience, the tissue was leaking the plastic fluid when injected during the experiment, also signifying that not enough pressure could be maintained when injecting the plastic throughout the prostate. Additionally, since the surrounding tissue is dissolved away every part that is not directly and strongly attached to the urethra will break away as well. Still, the resulting corrosion cast model gave a first impression of the branching-like structure of the prostatic ducts all pointing towards one side and roughly one point to drain into the urethra. In the next experiment a radiopaque fluid was used in combination with micro-CT imaging, allowing for the tissue to remain around the hardened plastic and therefore displaying every accumulation of the MICROFIL® material. During the injection process with MICROFIL® it was apparent that this time no leak was found, and more pressure could be built up using the three-way valve. However, it already was visible that the tissue expanded markedly and

when evaluated in the micro-CT scan it became obvious that the urethra expanded because of the pressure. Thus, not enough pressure might have been left to inject the prostatic ducts presenting with a smaller luminal diameter and therefore with a bigger resistance to fill compared to the urethra. Still, one single duct was clearly distinguished, enabling a 3D reconstruction from the scans. Previous studies used PTA as a contrast agent in combination with CT scans to visualize the 3D structure of tissue and slice through it in different orientations (Dullin et al. 2017). We thought this might be on the one hand a good way to find and define prostatic ducts while being able to 3D reconstruct them. On the other hand, we hoped that we could then use the same sample from the micro-CT image to work up histologically. Luckily, we had one intact prostate sample from a human body donor that showed no signs of BPH and when scrolling through the slides in the different orientations and angles the prostatic duct system was clearly visible. We saw that the ducts all seemed to only drain into the urethra on the dorsal side of the prostate and the ducts seemed to be pointing towards the colliculus seminalis on which the ejaculatory ducts visibly drained into the urethra. In addition, in multiple samples it looked like the signal surrounding the prostatic ducts (especially closer to the urethra) was higher in intensity, indicating a special organization of surrounding tissue. After the micro-CT scans, we embedded the samples in paraffin. Using the measurements gained through the scans we could predict where and in which angle the ducts we found on the scans would run in the tissue, which was then achieved by cutting the tissue in that angle on the microtome. Therefore, we could accurately define prostatic ducts via histology and investigate the surrounding tissue closer. However, it appeared that the PTA remaining in the tissue hardened it, which made some of the samples break and becoming unusable to cut for a histological work-up. From the single sample that I obtained; it did seem that there is a special organization of the surrounding tissue. This could also be observed in separate human prostate tissue samples that were not scanned in the micro-CT, but the knowledge of the visual aspect of prostatic ducts gained through the micro-CT experiments applied to identify the prostatic ducts in the other prostate samples. These very interesting pilot studies are being further pursued by a PhD colleague of mine with more samples, including new approaches to a histological work-up.

Summary

The adrenergic pathway is said to transmit the main contractile effects in the male reproductive tract. However, the underlying mechanisms and the interplay of the different components involved is unclear. The first line of medical treatment options today for patients with benign prostatic hyperplasia (BPH) targets the α1-adrenoreceptor. Since the α1-adrenoreceptor is expressed throughout the male reproductive tract and is heavily involved in mediating the ejaculatory process, BPH patients often complain about off-target effects such as ejaculatory disorders, especially when using tamsulosin. Other than from complications with adrenergic blockers, ejaculatory disorders are quite common as well. Finding other agents that are involved in transmitting contractile effects in the male reproductive tract, such as oxytocin, would further our basic understanding of male reproduction and open up new strategies in the treatment of ejaculatory disorders and BPH.

To clarify if oxytocin-based medications could be an alternative to existing treatment options for BPH as well as ejaculatory disorders, we used live imaging to investigate the effect of oxytocin as a contractile agent in the prostate and the epididymis in both rat and human tissue. At the same time, we wanted to provide further insight into the differences of prostatic ducts compared to glands. This had originally been observed in the rat and we sought to clarify the structure of the prostatic duct system in the human prostate, where it has not been fully described to date.

We demonstrated that oxytocin had an increasing effect on the contractility of the human prostate but not on the rat prostate. Furthermore, we showed that the effect of oxytocin on the contractility of the epididymis varied depending on the segment investigated. We found that only the very last segment of the adult epididymis (S19 in the rat and S9 in the human) showed a uniquely strong response, indicative of its function as the driving force in expelling the sperm from epididymal storage during the ejaculatory process. This strong response in S19 of the adult rat epididymis was equally induced by either oxytocin or norepinephrine and absent in neonatal tissue. Furthermore, the response to oxytocin was concentration dependent and mainly mediated through the oxytocin receptor. Our results also showed that the oxytocin pathway signalling was completely independent from the adrenergic pathway, and vice versa, in the last segment of the epididymis.

Taken together this leads us to conclude that using oxytocin-based medication could be an effective and new approach in treating BPH and ejaculatory disorders, especially by supporting ejaculation. In addition, we propose that S19 is an advantageous model to test newly developed molecules targeting either the oxytocin or the adrenergic pathway. To reach this conclusion we also created a new method to analyze contractions in live imaging data.

We also gained first insights into the human prostatic duct system structure indicating a branching system predominantly draining into the urethra on the dorsal aspect, probably on the colliculus seminalis. We suggest that the combination of micro-CT imaging and then embedding these scanned samples for a histological work-up to be a valuable tool in localizing and investigating previously unknown structures (such as the prostatic ducts) accurately. We also obtained preliminary evidence in our prostate micro-CT scans for a specific organization of the tissue surrounding the prostatic ducts in the human prostate, which could also implicate a specific function and possibly a differing contractile pattern.

Zusammenfassung

Der adrenerge Signalweg scheint hauptverantwortlich für die Vermittlung von kontraktilen Effekten im männlichen Reproduktionstrakt zu sein, wobei die genauen regulatorischen Abläufe und Zusammenhänge noch Klärung bedürfen. Die medikamentöse Therapie für Patienten mit einer gutartigen Vergrößerung der Prostata (BPH) ist zurzeit häufig in erster Linie die Einnahme von α1 adrenergen Rezeptorblockern. Da die α1-Adrenorezeptoren aber nicht nur in der Prostata, sondern auch im Rest des männlichen Reproduktionstraktes vorkommen, berichten BPH-Patienten häufig über unerwünschte Nebeneffekte wie z.B. Ejakulationsstörungen, vor allem nach der Einnahme von Tamsulosin. Nicht nur in Verbindung mit BPH, sondern auch generell sind Ejakulationsstörungen recht häufig. Weitere Substanzen zu finden, wie z.B. Oxytocin, die an der Vermittlung von kontraktilen Prozessen im männlichen Reproduktionstrakt beteiligt sein könnten, würde unser Verständnis der physiologischen Abläufe verbessern und neue Therapieansätze für Ejakulationsstörungen und BPH eröffnen.

Mit Hilfe von Videomikroskopie wollten wir den Effekt von Oxytocin als kontraktionsförderndes Mittel in Prostata und Nebenhoden von Ratte und Mensch untersuchen, um zu evaluieren, ob etwaige Effekte zur Therapie von BPH und/oder Ejakulationsstörungen nutzbar wären. Im Zusammenhang mit ihrer Bedeutung für die Funktionsweise der Prostata wollten wir auch die bisher im Menschen im Vergleich zu der Ratte schlecht erforschte Feinstruktur der Prostatagänge vorantreiben.

Wir konnten beobachten, dass Oxytocin einen stimulierenden Effekt auf die Kontraktilität der humanen Prostata hatte, aber nicht auf die der Ratte. Außerdem zeigten wir, dass der Effekt von Oxytocin auf die Kontraktilität des Nebenhodens je nach Segment variierte. Interessanterweise reagierte nur das allerletzte Segment des adulten Nebenhodens (S19 bei der Ratte und S9 beim Menschen) mit einer starken Reaktion, die darauf hindeutet, die treibende Kraft des Austreibens der Spermien vom Nebenhodenreservoir während der Ejakulation zu sein. Diese starke Reaktion von S19 des adulten Nebenhodens der Ratte war gleichwertig induzierbar sowohl durch Oxytocin als auch durch Noradrenalin. Diese starke Reaktion war nicht vorhanden im neonatalen Nebenhoden der Ratte. Des Weiteren war die Oxytocin-Reaktion des adulten S19 konzentrationsabhängig und hauptsächlich durch den Oxytocin-Rezeptor vermittelt. Unsere Ergebnisse zeigten ebenfalls, dass der Oxytocin-Signalweg vollkommen unabhängig vom adrenergen Signalweg wirkte und vice versa.

All dies führt zu der Annahme, dass Medikamente aus der Oxytocin-Familie einen guten neuen Ansatz bieten könnten für die Behandlung von BPH wie auch von Ejakulationsstörungen, insbesondere, um die Ejakulation zu unterstützen. Des Weiteren legen wir nahe, dass Segment 19 ein vorteilhaftes Modell für die Testung neuentwickelter Moleküle sein könnte, die am Oxytocin-Signalweg oder am adrenergen

Signalweg ansetzen sollen. Zusätzlich haben wir eine neue Methode zur Auswertung von Kontraktionen in Videomikroskopie-Aufnahmen entwickelt.

Des Weiteren konnten wir erste Eindrücke über die Feinstruktur des humanen Prostatagangsystems gewinnen, die darauf hindeuten, dass das verzweigte System hauptsächlich auf der dorsalen Seite, Region des Samenhügels, in die Harnröhre mündet. Wir sind der Meinung, dass die Kombination aus Mikro-CT-Scans und anschließender Einbettung dieser gescannten Proben für eine histologische Aufarbeitung ein vorteilhaftes Herangehen sein kann, um zunächst unbekannte Strukturen, wie hier die Prostatagänge, eindeutig identifizieren und lokalisieren zu können. Wir konnten auch schon Hinweise auf den Prostata Mikro-CT-Scans feststellen, die auf eine besondere Organisation des umgebenden Gewebes der Prostatagänge hindeuten und damit auch auf eine mögliche funktionelle Sonderstellung der Prostatagänge.

References

Ahn TG, Han SJ, Cho YS, An TH, Pak SC, Flouret G (2004) In vivo activity of the potent oxytocin antagonist on uterine activity in the rat. In Vivo 18: 763–766

Akerlund M, Bossmar T, Brouard R, Kostrzewska A, Laudanski T, Lemancewicz A, Serradeil-Le Gal C, Steinwall M (1999) Receptor binding of oxytocin and vasopressin antagonists and inhibitory effects on isolated myometrium from preterm and term pregnant women. Br J Obstet Gynaecol 106: 1047–1053

Althof S, Osterloh IH, Muirhead GJ, George K, Girard N (2019) The Oxytocin Antagonist Cligosiban Fails to Prolong Intravaginal Ejaculatory Latency in Men with Lifelong Premature Ejaculation: Results of a Randomized, Double-Blind, Placebo-Controlled Phase IIb trial (PEDRIX). J Sex Med 16: 1188–1198. doi: 10.1016/j.jsxm.2019.05.015

Alves EF, Freitas Ribeiro BLM de, Costa WS, Gallo CBM, Sampaio FJB (2018) Histological and quantitative analyzes of the stromal and acinar components of normal human prostate zones. Prostate 78: 289–293

Alwaal A, Breyer BN, Lue TF (2015) Normal male sexual function: emphasis on orgasm and ejaculation. Fertil Steril 104: 1051–1060. doi: 10.1016/j.fertnstert.2015.08.033

Andersson KE (1995) Alpha1 adrenergic receptor blockade in the male lower urinary tract and other body systems. Scand J Urol Nephrol Suppl 168: 13–19

Anjum S, Anuradha A, Krishna A (2018) A possible direct action of oxytocin on spermatogenesis and steroidogenesis in pre-pubertal mouse. Andrologia. doi: 10.1111/and.12958

Arenas MI, Pérez-Márquez J (2002) Cloning, expression, and regulation by androgens of a putative member of the oxytocinase family of proteins in the rat prostate. Prostate 53: 218–224. doi: 10.1002/pros.10150

Arrotéia KF, Garcia PV, Barbieri MF, Justino ML, Pereira VLA (2012) The Epididymis: Embryology, Structure, Function and Its Role in Fertilization and Infertility. In: Violin Pereira L (ed) Embryology - Updates and Highlights on Classic Topics. InTech

Arrowsmith S, Keov P, Muttenthaler M, Gruber CW (2018) Contractility Measurements of Human Uterine Smooth Muscle to Aid Drug Development. J Vis Exp. doi: 10.3791/56639

Assinder SJ (2008) Oxytocin increases 5alpha-reductase activity of human prostate epithelial cells, but not stromal cells. Prostate 68: 115–121

Assinder SJ, Carey M, Parkinson T, Nicholson HD (2000) Oxytocin and vasopressin expression in the ovine testis and epididymis: changes with the onset of spermatogenesis. Biol Reprod 63: 448–456

Assinder SJ, Johnson C, King K, Nicholson HD (2004) Regulation of 5alpha-reductase isoforms by oxytocin in the rat ventral prostate. Endocrinology 145: 5767–5773

Assinder SJ, Rezvani A, Nicholson HD (2002) Oxytocin promotes spermiation and sperm transfer in the mouse. Int J Androl 25: 19–27

Attilakos G, Psaroudakis D, Ash J, Buchanan R, Winter C, Donald F, Hunt LP, Draycott T (2010) Carbetocin versus oxytocin for the prevention of postpartum haemorrhage following caesarean

section: the results of a double-blind randomised trial. BJOG 117: 929–936. doi: 10.1111/j.1471-0528.2010.02585.x

Baker JG (2010) The selectivity of beta-adrenoceptor agonists at human beta1-, beta2- and beta3-adrenoceptors. Br J Pharmacol 160: 1048–1061. doi: 10.1111/j.1476-5381.2010.00754.x

Barberis C, Mouillac B, Durroux T (1998) Structural bases of vasopressin/oxytocin receptor function. J Endocrinol 156: 223–229

Barua HR, Barua RR, Barua S, Barua AK, Begum K (2017) Carbetocin and oxytocin in the active management of third stage of labor after vaginal birth of baby. Bangladesh Med J 46: 7–10. doi: 10.3329/bmj.v46i1.34631

Beard R, Stucki A, Schmitt M, Py G, Grundschober C, Gee AD, Tate EW (2018) Building bridges for highly selective, potent and stable oxytocin and vasopressin analogs. Bioorg Med Chem 26: 3039–3045. doi: 10.1016/j.bmc.2018.03.019

Beneit JV, Hidalgo A, Tamargo JL (1980) Effects of oxytocin on the isolated vas deferens of the rat. Br J Pharmacol 69: 379–382

Bisset GW, Clark BJ, Haldar J, Harris MC, Lewis GP, Rocha e Silva R (1967) The assay of milk-ejecting activity in the lactating rat. British Journal of Pharmacology and Chemotherapy 31: 537–549. doi: 10.1111/j.1476-5381.1967.tb00418.x

Bodanszky M, Sharaf H, Roy JB, Said SI (1992) Contractile activity of vasotocin, oxytocin, and vasopressin on mammalian prostate. European Journal of Pharmacology 216: 311–313

Borthwick AD (2010) Oral oxytocin antagonists. J Med Chem 53: 6525–6538. doi: 10.1021/jm901812z

Breton C, Chellil H, Kabbaj-Benmansour M, Carnazzi E, Seyer R, Phalipou S, Morin D, Durroux T, Zingg H, Barberis C, Mouillac B (2001) Direct identification of human oxytocin receptor-binding domains using a photoactivatable cyclic peptide antagonist: comparison with the human V1a vasopressin receptor. J Biol Chem 276: 26931–26941. doi: 10.1074/jbc.M102073200

Brinsko SP (1997) Reproductive Physiology of the Male. In: Cunningham JG (ed) Textbook of veterinary physiology. The Cell Steven R. Heidemann Neurophysiology James G. Cunningham. 2nd edn. Saunders. Philadelphia, USA

Busnelli M, Kleinau G, Muttenthaler M, Stoev S, Manning M, Bibic L, Howell LA, McCormick PJ, Di Lascio S, Braida D, Sala M, Rovati GE, Bellini T, Chini B (2016) Design and characterization of superpotent bivalent ligands targeting oxytocin receptor dimers via a channel-like structure. J Med Chem 59: 7152–7166. doi: 10.1021/acs.jmedchem.6b00564

Busnelli M, Rimoldi V, Viganò P, Persani L, Am Di B, Chini B (2010) Oxytocin-induced cell growth proliferation in human myometrial cells and leiomyomas. Fertil Steril 94. doi: 10.1016/j.fertnstert.2009.10.064

Byrne MM, Rolf C, Depenbusch M, Cooper TG, Nieschlag E (2003) Lack of effect of a single i.v. dose of oxytocin on sperm output in severely oligozoospermic men. Hum Reprod 18: 2098–2102

Caine M, Raz S, Zeigler M (1975) Adrenergic and cholinergic receptors in the human prostate, prostatic capsule and bladder neck. Br J Urol 47: 193–202

Caligioni CS, Oliver C, Jamur MC, Franci CR (2007) Presence of oxytocin receptors in the gonadotrophin-releasing hormone (GnRH) neurones in female rats: a possible direct action of oxytocin on GnRH neurones. J Neuroendocrinol 19: 439–448. doi: 10.1111/j.1365-2826.2007.01550.x

Carbone DJ, Hodges S (2003) Medical therapy for benign prostatic hyperplasia: sexual dysfunction and impact on quality of life. Int J Impot Res 15: 299–306. doi: 10.1038/sj.ijir.3901017

Carlson BM (2014) Human embryology and developmental biology. Study smart with student consult, 5th edn. Elsevier. Philadelphia, PA

Cassoni P, Sapino A, Negro F, Bussolati G (1994) Oxytocin inhibits proliferation of human breast cancer cell lines. Virchows Archiv : an international journal of pathology 425. doi: 10.1007/BF00197549

Cassoni P, Sapino A, Papotti M, Bussolati G (1996) Oxytocin and oxytocin-analogue F314 inhibit cell proliferation and tumor growth of rat and mouse mammary carcinomas. Int J Cancer 66: 817–820. doi: 10.1002/(SICI)1097-0215(19960611)66:6<817::AID-IJC18>3.0.CO;2-#

Chan WY, Rockway TW, Hruby VJ (1987) Long-acting oxytocin antagonists: effects of 2-D-stereoisomer substitution on antagonistic potency and duration of action. Proc Soc Exp Biol Med 185: 187–192. doi: 10.3181/00379727-185-42533

Chatterjee O, Patil K, Sahu A, Gopalakrishnan L, Mol P, Advani J, Mukherjee S, Christopher R, Prasad TSK (2016) An overview of the oxytocin-oxytocin receptor signaling network. J Cell Commun Signal 10: 355–360. doi: 10.1007/s12079-016-0353-7

Chini B, Fanelli F (2000) Molecular basis of ligand binding and receptor activation in the oxytocin and vasopressin receptor family. Exp Physiol 85 Spec No: 59S-66S

Christ GJ, Andersson K-E (2007) Rho-kinase and effects of Rho-kinase inhibition on the lower urinary tract. Neurourol Urodyn 26: 948–954. doi: 10.1002/nau.20475

Clément P, Bernabé J, Compagnie S, Alexandre L, McCallum S, Giuliano F (2013) Inhibition of ejaculation by the non-peptide oxytocin receptor antagonist GSK557296: a multi-level site of action. Br J Pharmacol 169: 1477–1485. doi: 10.1111/bph.12198

Conti F, Sertic S, Reversi A, Chini B (2009) Intracellular trafficking of the human oxytocin receptor: evidence of receptor recycling via a Rab4/Rab5 "short cycle". Am J Physiol Endocrinol Metab 296: E532-42. doi: 10.1152/ajpendo.90590.2008

Cross BA (1955) The posterior pituitary gland in relation to reproduction and lactation. Br Med Bull 11: 151–155

Cunha GR, Vezina CM, Isaacson D, Ricke WA, Timms BG, Cao M, Franco O, Baskin LS (2018) Development of the human prostate. Differentiation. doi: 10.1016/j.diff.2018.08.005

Cunningham JG (ed) (1997) Textbook of veterinary physiology. The Cell Steven R. Heidemann Neurophysiology James G. Cunningham, 2nd edn. Saunders. Philadelphia, USA

Denecke S, Nowell CJ, Fournier-Level A, Perry T, Batterham P (2015) The Wiggle Index: An Open Source Bioassay to Assess Sub-Lethal Insecticide Response in Drosophila melanogaster. PLoS ONE 10: e0145051. doi: 10.1371/journal.pone.0145051

Devost D, Zingg HH (2004) Homo- and hetero-dimeric complex formations of the human oxytocin receptor. J Neuroendocrinol 16: 372–377. doi: 10.1111/j.0953-8194.2004.01188.x

Domeniconi RF, Souza ACF, Xu B, Washington AM, Hinton BT (2016) Is the Epididymis a Series of Organs Placed Side By Side? Biol Reprod 95: 10. doi: 10.1095/biolreprod.116.138768

du Vigneaud V, Ressler C, Trippett S (1953) The sequence of amino acids in oxytocin, with a proposal for the structure of oxytocin. J Biol Chem 205: 949–957

Dullin C, Ufartes R, Larsson E, Martin S, Lazzarini M, Tromba G, Missbach-Guentner J, Pinkert-Leetsch D, Katschinski DM, Alves F (2017) µCT of ex-vivo stained mouse hearts and embryos enables a precise match between 3D virtual histology, classical histology and immunochemistry. PLoS ONE 12: e0170597. doi: 10.1371/journal.pone.0170597

Einspanier A, Ivell R (1997) Oxytocin and oxytocin receptor expression in reproductive tissues of the male marmoset monkey. Biol Reprod 56: 416–422

Engstrøm T, Barth T, Melin P, Vilhardt H (1998) Oxytocin receptor binding and uterotonic activity of carbetocin and its metabolites following enzymatic degradation. European Journal of Pharmacology 355: 203–210. doi: 10.1016/S0014-2999(98)00513-5

Fibbi B, Filippi S, Morelli A, Vignozzi L, Silvestrini E, Chavalmane A, Vita G de, Marini M, Gacci M, Manieri C, Vannelli GB, Maggi M (2009) Estrogens regulate humans and rabbit epididymal contractility through the RhoA/Rho-kinase pathway. J Sex Med 6: 2173–2186. doi: 10.1111/j.1743-6109.2009.01282.x

Filippi S, Luconi M, Granchi S, Vignozzi L, Bettuzzi S, Tozzi P, Ledda F, Forti G, Maggi M (2002a) Estrogens, but not androgens, regulate expression and functional activity of oxytocin receptor in rabbit epididymis. Endocrinology 143: 4271–4280. doi: 10.1210/en.2002-220384

Filippi S, Morelli A, Vignozzi L, Vannelli GB, Marini M, Ferruzzi P, Mancina R, Crescioli C, Mondaini N, Forti G, Ledda F, Maggi M (2005) Oxytocin mediates the estrogen-dependent contractile activity of endothelin-1 in human and rabbit epididymis. Endocrinology 146: 3506–3517. doi: 10.1210/en.2004-1628

Filippi S, Vannelli GB, Granchi S, Luconi M, Crescioli C, Mancina R, Natali A, Brocchi S, Vignozzi L, Bencini E, Noci I, Ledda F, Forti G, Maggi M (2002b) Identification, localization and functional activity of oxytocin receptors in epididymis. Mol Cell Endocrinol 193: 89–100

Filippi S, Vignozzi L, Vannelli GB, Ledda F, Forti G, Maggi M (2003) Role of oxytocin in the ejaculatory process. J Endocrinol Invest 26: 82–86

Flenady V, Reinebrant HE, Liley HG, Tambimuttu EG, Papatsonis DNM (2014) Oxytocin receptor antagonists for inhibiting preterm labour. Cochrane Database Syst Rev: CD004452. doi: 10.1002/14651858.CD004452.pub3

Foo NC, Carter D, Murphy D, Ivell R (1991) Vasopressin and oxytocin gene expression in rat testis. Endocrinology 128: 2118–2128. doi: 10.1210/endo-128-4-2118

Foster RA, Ladds PW (eds) (2007) Male genital system. Pathology of domestic animals. Maxie, M. Grant, 5th edn. Saunders. Philadelphia, USA

Frayne J, Nicholson HD (1998) Localization of oxytocin receptors in the human and macaque monkey male reproductive tracts: evidence for a physiological role of oxytocin in the male. Mol Hum Reprod 4: 527–532

Gemmell RT, Sernia C (1989) The localization of oxytocin and mesotocin in the reproductive tract of the male marsupial bandicoot Isoodon macrourus. Gen Comp Endocrinol 75: 103–109

Gimpl G, Fahrenholz F (2001) The oxytocin receptor system: structure, function, and regulation. Physiol Rev 81: 629–683. doi: 10.1152/physrev.2001.81.2.629

Ginja M, Pires MJ, Gonzalo-Orden JM, Seixas F, Correia-Cardoso M, Ferreira R, Fardilha M, Oliveira PA, Faustino-Rocha AI (2019) Anatomy and Imaging of Rat Prostate: Practical Monitoring in Experimental Cancer-Induced Protocols. Diagnostics (Basel) 9. doi: 10.3390/diagnostics9030068

Giuliano F, Clément P (2005) Physiology of ejaculation: emphasis on serotonergic control. Eur Urol 48: 408–417. doi: 10.1016/j.eururo.2005.05.017

Gould ML, Nicholson HD (2019) Changes in receptor location affect the ability of oxytocin to stimulate proliferative growth in prostate epithelial cells. Reprod Fertil Dev. doi: 10.1071/RD18362

Goverde HJ, Bisseling JG, Wetzels AM, Braat DD, Pesman GJ, Sweep FC, Meuleman EJ (1998) A neuropeptide in human semen: oxytocin. Arch Androl 41: 17–22. doi: 10.3109/01485019808988540

Guldenaar SE, Pickering BT (1985) Immunocytochemical evidence for the presence of oxytocin in rat testis. Cell Tissue Res 240: 485–487. doi: 10.1007/bf00222364

Gupta J, Russell R, Wayman C, Hurley D, Jackson V (2008) Oxytocin-induced contractions within rat and rabbit ejaculatory tissues are mediated by vasopressin V1A receptors and not oxytocin receptors. Br J Pharmacol 155: 118–126

Guzzi F, Zanchetta D, Cassoni P, Guzzi V, Francolini M, Parenti M, Chini B (2002) Localization of the human oxytocin receptor in caveolin-1 enriched domains turns the receptor-mediated inhibition of cell growth into a proliferative response. Oncogene 21: 1658–1667. doi: 10.1038/sj.onc.1205219

Harris GC, Frayne J, Nicholson HD (1996) Epididymal oxytocin in the rat: its origin and regulation. Int J Androl 19: 278–286

Harris GC, Nicholson HD (1998) Stage-related differences in rat seminiferous tubule contractility in vitro and their response to oxytocin. J Endocrinol 157: 251–257

Hayashi N, Sugimura Y, Kawamura J, Donjacour AA, Cunha GR (1991a) Morphological and functional heterogeneity in the rat prostatic gland. Biol Reprod 45: 308–321

Hayashi N, Sugimura Y, Kawamura J, Donjacour AA, Cunha GR (1991b) Morphological and functional heterogeneity in the rat prostatic gland. Biol Reprod 45: 308–321

Herbert Z, Bötticher G, Aschoff A, Sendemir E, Zermann D-H, Arnold R, Mall G, Jirikowski GF (2007) Changing caveolin-1 and oxytocin receptor distribution in the ageing human prostate. Anat Histol Embryol 36: 361–365. doi: 10.1111/j.1439-0264.2007.00775.x

Herbert Z, Weigel S, Sendemir E, Marshall A, Caldwell JD, Petrusz P, Peuckert C, Jirikowski GF (2005) Androgen-binding protein is co-expressed with oxytocin in the male reproductive tract. Anat Histol Embryol 34: 286–293. doi: 10.1111/j.1439-0264.2005.00605.x

Hib J (1974a) The contractility of the cauda epididymidis of the mouse, its spontaneous activity in vitro and the effects of oxytocin. J Reprod Fertil 36: 191–193

Hib J (1974b) The in vitro effects of oxytocin and vasopressin on spontaneous contractility of the mouse cauda epididymidis. Biol Reprod 11: 436–439

Hib J (1977) The 'in vivo' effects of oxytocin and vasopressin on spontaneous contractility of the rat epididymis. Int J Fertil 22: 63–64

Hib J, Ponzio R, Vilar O (1983) In vivo recording of contractile activity of pelvic urethra and seminal vesicle in rats. Effects of electrical stimulations and neurohypophysial hormones. Andrologia 15: 480–485

Hicks C, Ramos L, Reekie T, Misagh GH, Narlawar R, Kassiou M, McGregor IS (2014) Body temperature and cardiac changes induced by peripherally administered oxytocin, vasopressin and the non-peptide oxytocin receptor agonist WAY 267,464: a biotelemetry study in rats. Br J Pharmacol 171: 2868–2887. doi: 10.1111/bph.12613

Hinton BT, Galdamez MM, Sutherland A, Bomgardner D, Xu B, Abdel-Fattah R, Yang L (2011) How do you get six meters of epididymis inside a human scrotum? J Androl 32: 558–564. doi: 10.2164/jandrol.111.013029

Holstein AF (1969) Morphologische Studien am Nebenhoden des Menschen. Thieme

Hruby VJ, Chow MS, Smith DD (1990) Conformational and structural considerations in oxytocin-receptor binding and biological activity. Annu Rev Pharmacol Toxicol 30: 501–534. doi: 10.1146/annurev.pa.30.040190.002441

Hunter DJ, Schulz P, Wassenaar W (1992) Effect of carbetocin, a long-acting oxytocin analog on the postpartum uterus. Clin Pharmacol Ther 52: 60–67. doi: 10.1038/clpt.1992.103

Ibrahim E, Lynne CM, Brackett NL (2016) Male fertility following spinal cord injury: an update. Andrology 4: 13–26. doi: 10.1111/andr.12119

Inaba T, Nakayama Y, Tani H, Tamada H, Kawate N, Sawada T (1999) Oxytocin gene expression and action in goat testis. Theriogenology 52: 425–434. doi: 10.1016/S0093-691X(99)00140-5

Ittmann M (2017) Anatomy and Histology of the Human and Murine Prostate. Cold Spring Harb Perspect Med: 8(5). doi: 10.1101/cshperspect.a030346

Ivell R, Bathgate R, Kimura T, Parry L (1997) Molecular biology of the oxytocin receptor: a comparative approach. Biochem Soc Trans 25: 1058–1066

Ivell R, Furuya K, Brackmann B, Dawood Y, Khan-Dawood F (1990) Expression of the oxytocin and vasopressin genes in human and baboon gonadal tissues. Endocrinology 127: 2990–2996. doi: 10.1210/endo-127-6-2990

Ivell R, Walther N (1999) The role of sex steroids in the oxytocin hormone system. Mol Cell Endocrinol 151: 95–101. doi: 10.1016/S0303-7207(99)00025-8

Jaakkola UM, Talo A (1981) Effects of oxytocin and vasopressin on electrical and mechanical activity of the rat epididymis in vitro. J Reprod Fertil 63: 47–51. doi: 10.1530/jrf.0.0630047

Janthur M (2016) Akzessorische Geschlechtsdrüsen 687–698. In: Günzel-Apel A-R, Bostedt H (eds) Reproduktionsmedizin und Neonatologie von Hund und Katze. Schattauer. Stuttgart

Jelinsky SA, Turner TT, Bang HJ, Finger JN, Solarz MK, Wilson E, Brown EL, Kopf GS, Johnston DS (2007) The rat epididymal transcriptome: comparison of segmental gene expression in the rat and mouse epididymides. Biol Reprod 76: 561–570. doi: 10.1095/biolreprod.106.057323

Jenkin L, Nicholson HD (1999) Evidence for the regulation of prostatic oxytocin by gonadal steroids in the rat. J Androl 20: 80–87

Jesik CJ, Holland JM, Lee C (1982) An anatomic and histologic study of the rat prostate. Prostate 3: 81–97. doi: 10.1002/pros.2990030111

Jones RC (1999) To store or mature spermatozoa? The primary role of the epididymis. Int J Androl 22: 57–67. doi: 10.1046/j.1365-2605.1999.00151.x

Kimura T, Saji F, Nishimori K, Ogita K, Nakamura H, Koyama M, Murata Y (2003) Molecular regulation of the oxytocin receptor in peripheral organs. J Mol Endocrinol 30: 109–115

Knickerbocker JJ, Sawyer HR, Amann RP, Tekpetey FR, Niswender GD (1988) Evidence for the presence of oxytocin in the ovine epididymis. Biol Reprod 39: 391–397

Knight TW (1974) A qualitative study of factors affecting the contractions of the epididymis and ductus deferens of the ram. J Reprod Fertil 40: 19–29

Koohi MK, Ivell R, Walther N (2005) Transcriptional activation of the oxytocin promoter by oestrogens uses a novel non-classical mechanism of oestrogen receptor action. J Neuroendocrinol 17: 197–207. doi: 10.1111/j.1365-2826.2005.01298.x

Kraft T, Brenner B (2018) Muskulatur. Glatte Muskulatur. In: Pape H-C, Kurtz A, Silbernagl S (eds) Physiologie. 8th edn. Thieme. Stuttgart [u.a.]

Kügler R, Mietens A, Seidensticker M, Tasch S, Wagenlehner FM, Kaschtanow A, Tjahjono Y, Tomczyk CU, Beyer D, Risbridger GP, Exintaris B, Ellem SJ, Middendorff R (2018) Novel imaging of the prostate reveals spontaneous gland contraction and excretory duct quiescence together with different drug effects. FASEB J 32: 1130–1138. doi: 10.1096/fj.201700430R

Kumar V (2007a) Robbins basic pathology, 8th edn. Saunders. Philadelphia, USA

Kumar V (2007b) Robbins basic pathology, 8th edn. Saunders. Philadelphia, USA

Kummer W, Welsch U (2018) Männliche Geschlechtsorgane. In: Welsch U, Kummer W (eds) Histologie - Das Lehrbuch. Zytologie, Histologie und mikroskopische Anatomie. 5th edn. Urban & Fischer Verlag/Elsevier GmbH. München

La Vignera S, Condorelli RA, Russo GI, Morgia G, Calogero AE (2016) Endocrine control of benign prostatic hyperplasia. Andrology 4: 404–411. doi: 10.1111/andr.12186

Lee C, Sensibar JA, Dudek SM, Hiipakka RA, Liao ST (1990a) Prostatic ductal system in rats: regional variation in morphological and functional activities. Biol Reprod 43: 1079–1086

Lee C, Sensibar JA, Dudek SM, Hiipakka RA, Liao ST (1990b) Prostatic ductal system in rats: regional variation in morphological and functional activities. Biol Reprod 43: 1079–1086

Lee C-L, Kuo H-C (2017) Pathophysiology of benign prostate enlargement and lower urinary tract symptoms. Current concepts. Ci Ji Yi Xue Za Zhi 29: 79–83

Lee SN, Chakrabarty B, Wittmer B, Papargiris M, Ryan A, Frydenberg M, Lawrentschuk N, Middendorff R, Risbridger GP, Ellem SJ, Exintaris B (2017) Age Related Differences in Responsiveness to Sildenafil and Tamsulosin are due to Myogenic Smooth Muscle Tone in the Human Prostate. Sci Rep 7: 10150

Lepor H (2006) The evolution of alpha-blockers for the treatment of benign prostatic hyperplasia. Rev Urol 8 Suppl 4: S3-9

Lepor H, Lepor NE, Hill LA, Trohman RG (2008) The QT Interval and Selection of Alpha-Blockers for Benign Prostatic Hyperplasia. Rev Urol 10: 85–91

Lerman B, Harricharran T, Ogunwobi OO (2018) Oxytocin and cancer: An emerging link. World J Clin Oncol 9: 74–82. doi: 10.5306/wjco.v9.i5.74

Lesciotto KM, Motch Perrine SM, Kawasaki M, Stecko T, Ryan TM, Kawasaki K, Richtsmeier JT (2020) Phosphotungstic acid-enhanced microCT: Optimized protocols for embryonic and early postnatal mice. Dev Dyn 249: 573–585. doi: 10.1002/dvdy.136

Li J, Tian Y, Guo S, Gu H, Yuan Q, Xie X (2018a) Testosterone-induced benign prostatic hyperplasia rat and dog as facile models to assess drugs targeting lower urinary tract symptoms. PLoS ONE 13: e0191469

Li Z, Xiao H, Wang K, Zheng Y, Chen P, Wang X, DiSanto ME, Zhang X (2018b) Upregulation of oxytocin receptor in the hyperplastic prostate. Front Endocrinol (Lausanne) 9: 403. doi: 10.3389/fendo.2018.00403

Lippert H (2000) Lehrbuch Anatomie, 5th edn. Urban & Fischer. München, Germany

Lippert H (2017) Lehrbuch Anatomie, 8th edn. Elsevier. München

Madersbacher S (1999) The chimpanzee as a model of human benign prostatic hyperplasia. J Urol: 1245

McCafferty GP, Pullen MA, Wu C, Edwards RM, Allen MJ, Woollard PM, Borthwick AD, Liddle J, Hickey DMB, Brooks DP, Westfall TD (2007) Use of a novel and highly selective oxytocin receptor antagonist to characterize uterine contractions in the rat. Am J Physiol Regul Integr Comp Physiol 293: R299-305. doi: 10.1152/ajpregu.00057.2007

McMahon C, Althof S, Rosen R, Giuliano F, Miner M, Osterloh IH, Muirhead GJ, Harty B (2019) The Oxytocin Antagonist Cligosiban Prolongs Intravaginal Ejaculatory Latency and Improves Patient-Reported Outcomes in Men with Lifelong Premature Ejaculation: Results of a Randomized, Double-Blind, Placebo-Controlled Proof-of-Concept Trial (PEPIX). J Sex Med 16: 1178–1187. doi: 10.1016/j.jsxm.2019.05.016

McMahon CG, Abdo C, Incrocci L, Perelman M, Rowland D, Waldinger M, Xin ZC (2004) Disorders of orgasm and ejaculation in men. J Sex Med 1: 58–65. doi: 10.1111/j.1743-6109.2004.10109.x

McNeal JE (1988) Normal histology of the prostate. Am J Surg Pathol 12: 619–633

Melin P (1970) Effects in vivo of neurohypophysial hormones on the contractile activity of accessory sex organs in male rabbits. J Reprod Fertil 22: 283–292

Melin P (1971) Spermatogenesis and sperm output in rabbits after long-term treatment with oxytocin. Acta Endocrinol 66: 515–528. doi: 10.1530/acta.0.0660515

Mewe M, Wulfsen I, Middendorff R, Bauer CK (2007) Differential modulation of bovine epididymal activity by oxytocin and noradrenaline. Reproduction 134: 493–501

Michel MC (2007) Alpha1-adrenoceptors and ejaculatory function. Br J Pharmacol 152: 289–290. doi: 10.1038/sj.bjp.0707369

Mietens A, Tasch S, Stammler A, Konrad L, Feuerstacke C, Middendorff R (2014) Time-lapse imaging as a tool to investigate contractility of the epididymal duct--effects of cGMP signaling. PLoS ONE 9: e92603

Moore KL, Persaud TVN, Torchia MG (eds) (2013) Embryologie. Entwicklungsstadien - Frühentwicklung - Organogenese - Klinik, 6th edn. Urban & Fischer in Elsevier. München

Murphy D, Funkhouser J, Ang HL, Foo NC, Carter D (1993) Extrahypothalamic expression of the vasopressin and oxytocin genes. Annals of the New York Academy of Sciences 689: 91–106

Narayan P, Lepor H (2001) Long-term, open-label, phase III multicenter study of tamsulosin in benign prostatic hyperplasia. Urology 57: 466–470. doi: 10.1016/s0090-4295(00)01042-6

Nemeth JA, Lee C (1996) Prostatic ductal system in rats: regional variation in stromal organization. Prostate 28: 124–128. doi: 10.1002/(SICI)1097-0045(199602)28:2<124::AID-PROS8>3.0.CO;2-G

Nemeth JA, Sensibar JA, White RR, Zelner DJ, Kim IY, Lee C (1997) Prostatic ductal system in rats: tissue-specific expression and regional variation in stromal distribution of transforming growth factor-beta 1. Prostate 33: 64–71

Nicholson HD (1996) Oxytocin: a paracrine regulator of prostatic function. Rev Reprod 1: 69–72

Nicholson HD, Hardy MP (1992) Luteinizing hormone differentially regulates the secretion of testicular oxytocin and testosterone by purified adult rat Leydig cells in vitro. Endocrinology 130: 671–677. doi: 10.1210/endo.130.2.1733715

Nicholson HD, Swann RW, Burford GD, Wathes DC, Porter DG, Pickering BT (1984) Identification of oxytocin and vasopressin in the testis and in adrenal tissue. Regul Pept 8: 141–146

Nicholson HD, Worley RT, Charlton HM, Pickering BT (1986) LH and testosterone cause the development of seminiferous tubule contractile activity and the appearance of testicular oxytocin in hypogonadal mice. J Endocrinol 110: 159–167

Nicholson HD, Worley RT, Guldenaar SE, Pickering BT (1987) Ethan-1,2-dimethanesulphonate reduces testicular oxytocin content and seminiferous tubule movements in the rat. J Endocrinol 112: 311–316

Nilsson L, Reinheimer T, Steinwall M, Akerlund M (2003) FE 200 440: a selective oxytocin antagonist on the term-pregnant human uterus. BJOG 110: 1025–1028

Nishimori K, Young LJ, Guo Q, Wang Z, Insel TR, Matzuk MM (1996) Oxytocin is required for nursing but is not essential for parturition or reproductive behavior. Proc Natl Acad Sci U S A 93: 11699–11704

Oakley RH, Laporte SA, Holt JA, Barak LS, Caron MG (2001) Molecular determinants underlying the formation of stable intracellular G protein-coupled receptor-beta-arrestin complexes after receptor endocytosis*. J Biol Chem 276: 19452–19460. doi: 10.1074/jbc.M101450200

O'Donnell J, Zeppenfeld D, McConnell E, Pena S, Nedergaard M (2012) Norepinephrine: a neuromodulator that boosts the function of multiple cell types to optimize CNS performance. Neurochem Res 37: 2496–2512. doi: 10.1007/s11064-012-0818-x

Pacini ESA, Castilho ACS, Hebeler-Barbosa F, Pupo AS, Kiguti LRA (2018) Contraction of rat cauda epididymis smooth muscle to α1-adrenoceptor activation is mediated by α1A-adrenoceptors. J Pharmacol Exp Ther 366: 21–28. doi: 10.1124/jpet.117.246710

Pandit RB (1996) Hypertension and CHD risk: whither alpha-1 blockers? Indian Heart J 48: 265–271

Pape H-C, Kurtz A, Silbernagl S (eds) (2018) Physiologie, 8th edn. Thieme. Stuttgart [u.a.]

Parry LJ, Bathgate RA (1998) Mesotocin receptor gene and protein expression in the prostate gland, but not testis, of the tammar wallaby, Macropus eugenii. Biol Reprod 59: 1101–1107. doi: 10.1095/biolreprod59.5.1101

Pejčić T, Tosti T, Tešić Ž, Milković B, Dragičević D, Kozomara M, Čekerevac M, Džamić Z (2017) Testosterone and dihydrotestosterone levels in the transition zone correlate with prostate volume. Prostate 77: 1082–1092

Peters NCJ, Duvekot JJ (2009) Carbetocin for the prevention of postpartum hemorrhage: a systematic review. Obstet Gynecol Surv 64: 129–135. doi: 10.1097/OGX.0b013e3181932e5b

Phaneuf S, Asbóth G, MacKenzie IZ, Melin P, López Bernal A (1994) Effect of oxytocin antagonists on the activation of human myometrium in vitro: Atosiban prevents oxytocin-induced desensitization. Am J Obstet Gynecol 171: 1627–1634. doi: 10.1016/0002-9378(94)90414-6

Pickering BT, Ayad VJ, Birkett SD, Gilbert CL, Guldenaar SE, Nicholson HD, Worley RT, Wathes DC (1990) Neurohypophysial peptides in the gonads: are they real and do they have a function? Reprod Fertil Dev 2: 245–262. doi: 10.1071/rd9900245

Pierzynski P, Gajda B, Smorag Z, Rasmussen AD, Kuczynski W (2007) Effect of atosiban on rabbit embryo development and human sperm motility. Fertil Steril 87: 1147–1152. doi: 10.1016/j.fertnstert.2006.08.089

Pierzynski P, Lemancewicz A, Reinheimer T, Akerlund M, Laudanski T (2004) Inhibitory effect of barusiban and atosiban on oxytocin-induced contractions of myometrium from preterm and term pregnant women. J Soc Gynecol Investig 11: 384–387. doi: 10.1016/j.jsgi.2004.02.008

Plećas B, Popović A, Jovović D, Hristić M (1992) Mitotic activity and cell deletion in ventral prostate epithelium of intact and castrated oxytocin-treated rats. J Endocrinol Invest 15: 249–253

Plested CP, Bernal AL (2001) Desensitisation of the oxytocin receptor and other G-protein coupled receptors in the human myometrium. Exp Physiol 86: 303–312

Pohl O, Perks D, Rhodes J, Comotto L, Baldrick P, Chollet A (2016) Effects of the oral oxytocin receptor antagonist tocolytic OBE001 on reproduction in rats. Reprod Sci 23: 439–447. doi: 10.1177/1933719115607979

Popović A, Plećas B, Milićević Z, Hristić M, Jovović D (1990) Stereologic analysis of ventral prostate of oxytocin-treated rats. Arch Androl 24: 247–253

Portis AJ, Mador DR (1997) Treatment options for benign prostatic hyperplasia. Can Fam Physician 43: 1395–1404

Powers RE, Derrick FC, Jonsson HT (1982) Lack of oxytocin effect on sperm output in oligospermic males. Urology 19: 523–524

Preston S, Jabbar A, Nowell C, Joachim A, Ruttkowski B, Baell J, Cardno T, Korhonen PK, Piedrafita D, Ansell BRE, Jex AR, Hofmann A, Gasser RB (2015) Low cost whole-organism screening of compounds for anthelmintic activity. Int J Parasitol 45: 333–343. doi: 10.1016/j.ijpara.2015.01.007

Preston S, Jabbar A, Nowell C, Joachim A, Ruttkowski B, Cardno T, Hofmann A, Gasser RB (2016) Practical and low cost whole-organism motility assay: A step-by-step protocol. Mol Cell Probes 30: 13–17. doi: 10.1016/j.mcp.2015.08.005

Rath W (2009) Prevention of postpartum haemorrhage with the oxytocin analogue carbetocin. Eur J Obstet Gynecol Reprod Biol 147: 15–20. doi: 10.1016/j.ejogrb.2009.06.018

Reid JL (1986) Alpha-adrenergic receptors and blood pressure control. The American Journal of Cardiology 57: E6-E12. doi: 10.1016/0002-9149(86)90716-2

Reinheimer TM, Bee WH, Resendez JC, Meyer JK, Haluska GJ, Chellman GJ (2005) Barusiban, a new highly potent and long-acting oxytocin antagonist: pharmacokinetic and pharmacodynamic comparison with atosiban in a cynomolgus monkey model of preterm labor. J Clin Endocrinol Metab 90: 2275–2281. doi: 10.1210/jc.2004-2120

Reversi A, Rimoldi V, Marrocco T, Cassoni P, Bussolati G, Parenti M, Chini B (2005) The oxytocin receptor antagonist atosiban inhibits cell growth via a "biased agonist" mechanism. J Biol Chem 280: 16311–16318. doi: 10.1074/jbc.M409945200

Richard S, Zingg HH (1990) The human oxytocin gene promoter is regulated by estrogens. J Biol Chem 265: 6098–6103

Rimoldi V, Reversi A, Taverna E, Rosa P, Francolini M, Cassoni P, Parenti M, Chini B (2003) Oxytocin receptor elicits different EGFR/MAPK activation patterns depending on its localization in caveolin-1 enriched domains. Oncogene 22: 6054–6060. doi: 10.1038/sj.onc.1206612

Ring RH, Schechter LE, Leonard SK, Dwyer JM, Platt BJ, Graf R, Grauer S, Pulicicchio C, Resnick L, Rahman Z, Sukoff Rizzo SJ, Luo B, Beyer CE, Logue SF, Marquis KL, Hughes ZA, Rosenzweig-Lipson S (2010) Receptor and behavioral pharmacology of WAY-267464, a non-peptide oxytocin receptor agonist. Neuropharmacology 58: 69–77. doi: 10.1016/j.neuropharm.2009.07.016

Roehrborn CG (2008) Pathology of benign prostatic hyperplasia. Int J Impot Res 20 Suppl 3: 11-18

Romero R, Sibai BM, Sanchez-Ramos L, Valenzuela GJ, Veille JC, Tabor B, Perry KG, Varner M, Goodwin TM, Lane R, Smith J, Shangold G, Creasy GW (2000) An oxytocin receptor antagonist (atosiban) in the treatment of preterm labor: a randomized, double-blind, placebo-controlled trial with tocolytic rescue. Am J Obstet Gynecol 182: 1173–1183. doi: 10.1067/mob.2000.95834

Rowland D, McMahon CG, Abdo C, Chen J, Jannini E, Waldinger MD, Ahn TY (2010) Disorders of orgasm and ejaculation in men. J Sex Med 7: 1668–1686. doi: 10.1111/j.1743-6109.2010.01782.x

Sanbe A, Tanaka Y, Fujiwara Y, Tsumura H, Yamauchi J, Cotecchia S, Koike K, Tsujimoto G, Tanoue A (2007) Alpha1-adrenoceptors are required for normal male sexual function. Br J Pharmacol 152: 332–340. doi: 10.1038/sj.bjp.0707366

Saníger MA, Ramírez-Expósito MJ, La Chica S de, Carrera-González MP, Mayas MD, Manuel Martínez-Martos J (2011) Alpha-1-adrenergic receptor blockade modifies insulin-regulated aminopeptidase (IRAP) activity in rat prostate and modulates oxytocin functions. Drug Metab Lett 5: 192–196

Schindelin J, Arganda-Carreras I, Frise E, Kaynig V, Longair M, Pietzsch T, Preibisch S, Rueden C, Saalfeld S, Schmid B, Tinevez J-Y, White DJ, Hartenstein V, Eliceiri K, Tomancak P, Cardona A (2012) Fiji: an open-source platform for biological-image analysis. Nat Methods 9: 676–682. doi: 10.1038/nmeth.2019

Schulte E (2017) Männliches Genitale. In: Aumüller G, Aust G, Engele J, Kirsch J, Maio G, Mayerhofer A, Mense S, Reißig D (eds) Anatomie. 4th edn. Georg Thieme Verlag. Stuttgart

Selman SH (2011) The McNeal prostate. A review. Urology 78: 1224–1228

Sendemir E, Herbert Z, Sivukhina E, Zermann D-H, Arnold R, Jirikowski GF (2008) Colocalization of androgen binding protein, oxytocin receptor, caveolin 1 and proliferation marker p21 in benign prostate hyperplasia. Anat Histol Embryol 37: 325–331. doi: 10.1111/j.1439-0264.2008.00848.x

Sengupta P (2013) The Laboratory Rat: Relating Its Age With Human's. Int J Prev Med 4: 624–630

Serradeil-Le Gal C, Valette G, Foulon L, Germain G, Advenier C, Naline E, Bardou M, Martinolle J-P, Pouzet B, Raufaste D, Garcia C, Double-Cazanave E, Pauly M, Pascal M, Barbier A, Scatton B, Maffrand J-P, Le Fur G (2004) SSR126768A (4-chloro-3-(3R)-(+)-5-chloro-1-(2,4-dimethoxybenzyl)-3-methyl-2-oxo-2,3-dihydro-1H-indol-3-yl-N-ethyl-N-(3-pyridylmethyl)-benzamide, hydrochloride): a new selective and orally active oxytocin receptor antagonist for the prevention of preterm labor. J Pharmacol Exp Ther 309: 414–424

Serradeil-Le Gal C, Wagnon J, Garcia C, Lacour C, Guiraudou P, Christophe B, Villanova G, Nisato D, Maffrand JP, Le Fur G (1993) Biochemical and pharmacological properties of SR 49059, a new, potent, nonpeptide antagonist of rat and human vasopressin V1a receptors. J Clin Invest 92: 224–231. doi: 10.1172/JCI116554

Sharaf H, Foda HD, Said SI, Bodanszky M (1992) Oxytocin and related peptides elicit contractions of prostate and seminal vesicle. Annals of the New York Academy of Sciences 652: 474–477

Sherstyuk OA, Ustenko RL, Pilyugin AV, Svintsitskaya NL (2015) Stereomorphological pecularities of the structure of human prostate and complications of its nomenclature. Galician Medical Journal 22(3): 104–107

Shinghal R, Barnes A, Mahar KM, Stier B, Giancaterino L, Condreay LD, Black L, McCallum SW (2013) Safety and efficacy of epelsiban in the treatment of men with premature ejaculation: a randomized, double-blind, placebo-controlled, fixed-dose study. J Sex Med 10: 2506–2517. doi: 10.1111/jsm.12272

Silva J, Silva CM, Cruz F (2014a) Current medical treatment of lower urinary tract symptoms/BPH. Do we have a standard? Curr Opin Urol 24: 21–28

Silva J, Silva CM, Cruz F (2014b) Current medical treatment of lower urinary tract symptoms/BPH: do we have a standard? Curr Opin Urol 24: 21–28. doi: 10.1097/MOU.0000000000000007

Smith JS, Lefkowitz RJ, Rajagopal S (2018) Biased Signalling: From Simple Switches to Allosteric Microprocessors. Nat Rev Drug Discov 17: 243–260. doi: 10.1038/nrd.2017.229

Smith MP, Ayad VJ, Mundell SJ, McArdle CA, Kelly E, López Bernal A (2006) Internalization and desensitization of the oxytocin receptor is inhibited by Dynamin and clathrin mutants in human embryonic kidney 293 cells. Mol Endocrinol 20: 379–388. doi: 10.1210/me.2005-0031

Song Z, Albers HE (2017) Cross-talk among oxytocin and arginine-vasopressin receptors: Relevance for basic and clinical studies of the brain and periphery. Front Neuroendocrinol

Stadler B, Nowell CJ, Whittaker MR, Arnhold S, Pilatz A, Wagenlehner FM, Exintaris B, Middendorff R (2021) Physiological and pharmacological impact of oxytocin on epididymal propulsion during the ejaculatory process in rodents and men. FASEB J 35: e21639. doi: 10.1096/fj.202100435R

Stadler B, Whittaker MR, Exintaris B, Middendorff R (2020) Oxytocin in the Male Reproductive Tract; The Therapeutic Potential of Oxytocin-Agonists and-Antagonists. Front Endocrinol (Lausanne) 11. doi: 10.3389/fendo.2020.565731

Steinwall M, Bossmar T, Brouard R, Laudanski T, Olofsson P, Urban R, Wolff K, Le-Fur G, Akerlund M (2005) The effect of relcovaptan (SR 49059), an orally active vasopressin V1a receptor antagonist, on uterine contractions in preterm labor. Gynecol Endocrinol 20: 104–109. doi: 10.1080/09513590400021144

Strosberg AD (1993) Structure, function, and regulation of adrenergic receptors. Protein Sci. 2: 1198–1209. doi: 10.1002/pro.5560020802

Studdard PW, Stein JL, Cosentino MJ (2002) The effects of oxytocin and arginine vasopressin in vitro on epididymal contractility in the rat. Int J Androl 25: 65–71

Sun F, Báez-Díaz C, Sánchez-Margallo FM (2017a) Canine prostate models in preclinical studies of minimally invasive interventions. Part II, benign prostatic hyperplasia models. Transl Androl Urol 6: 547–555

Sun F, Báez-Díaz C, Sánchez-Margallo FM (2017b) Canine prostate models in preclinical studies of minimally invasive interventions:. Part I, canine prostate anatomy and prostate cancer models. Transl Androl Urol 6: 538–546

Terrillon S, Durroux T, Mouillac B, Breit A, Ayoub MA, Taulan M, Jockers R, Barberis C, Bouvier M (2003) Oxytocin and vasopressin V1a and V2 receptors form constitutive homo- and heterodimers during biosynthesis. Mol Endocrinol 17: 677–691. doi: 10.1210/me.2002-0222

Thackare H, Nicholson HD, Whittington K (2006) Oxytocin--its role in male reproduction and new potential therapeutic uses. Hum Reprod Update 12: 437–448

Thornton S, Goodwin TM, Greisen G, Hedegaard M, Arce J-C (2009) The effect of barusiban, a selective oxytocin antagonist, in threatened preterm labor at late gestational age: a randomized, double-blind, placebo-controlled trial. Am J Obstet Gynecol 200: 627.e1-10. doi: 10.1016/j.ajog.2009.01.015

Thornton S, Miller H, Valenzuela G, Snidow J, Stier B, Fossler MJ, Montague TH, Powell M, Beach KJ (2015) Treatment of spontaneous preterm labour with retosiban: a phase 2 proof-of-concept study. Br J Clin Pharmacol 80: 740–749. doi: 10.1111/bcp.12646

Tom N, Assinder SJ (2010a) Oxytocin in health and disease. Int J Biochem Cell Biol 42: 202–205. doi: 10.1016/j.biocel.2009.10.008

Tom NC, Assinder SJ (2010b) Oxytocin: recent developments. Biomol Concepts 1: 367–380. doi: 10.1515/bmc.2010.036

Tsatsaris V, Carbonne B, Cabrol D (2004) Atosiban for preterm labour. Drugs 64: 375–382. doi: 10.2165/00003495-200464040-00003

Tsujimoto M, Mizutani S, Adachi H, Kimura M, Nakazato H, Tomoda Y (1992) Identification of human placental leucine aminopeptidase as oxytocinase. Arch Biochem Biophys 292: 388–392

Turner TT, Bomgardner D, Jacobs JP, Nguyen QAT (2003) Association of segmentation of the epididymal interstitium with segmented tubule function in rats and mice. Reproduction 125: 871–878

Turner TT, Gleavy JL, Harris JM (1990) Fluid movement in the lumen of the rat epididymis: effect of vasectomy and subsequent vasovasostomy. J Androl 11: 422–428

Ungefroren H, Davidoff M, Ivell R (1994) Post-transcriptional block in oxytocin gene expression within the seminiferous tubules of the bovine testis. J Endocrinol 140: 63–72. doi: 10.1677/joe.0.1400063

Vignozzi L, Filippi S, Morelli A, Luconi M, Jannini E, Forti G, Maggi M (2008) Regulation of epididymal contractility during semen emission, the first part of the ejaculatory process: a role for estrogen. J Sex Med 5: 2010-6; quiz 2017. doi: 10.1111/j.1743-6109.2008.00914.x

Voglmayr JK (1975) Output of spermatozoa and fluid by the testis of the ram and its response to oxytocin. J Reprod Fertil 43: 119–122

Walch K, Eder R, Schindler A, Feichtinger W (2001) The effect of single-dose oxytocin application on time to ejaculation and seminal parameters in men. J Assist Reprod Genet 18: 655–659

Wang W, Qiao Y, Li Z (2018) New Insights into Modes of GPCR Activation. Trends in pharmacological sciences 39. doi: 10.1016/j.tips.2018.01.001

Watson ED, Nikolakopoulos E, Gilbert C, Goode J (1999) Oxytocin in the semen and gonads of the stallion. Theriogenology 51: 855–865

Wayman C, Russell R, Tang K, Weibly L, Gaboardi S, Fisher L, Allers K, Jackson M, Hawcock T, Robinson N, Wilson L, Gupta J, Casey J, Gibson KR (2018) Cligosiban, a novel brain-penetrant, selective oxytocin receptor antagonist, inhibits ejaculatory physiology in rodents. J Sex Med 15: 1698–1706. doi: 10.1016/j.jsxm.2018.10.008

Webb CR (2003) Smooth muscle contraction and relaxation. Adv Physiol Educ 27: 171–182

Weiser D, Mietens A, Stadler B, Ježek D, Schuler G, Middendorff R (2020) Contractions transport exfoliated epithelial cells through the neonatal epididymis. Reproduction 160: 109–116. doi: 10.1530/REP-19-0617

Westergaard JG, Lange AP, Pedersen GT, Secher NJ (1983) Use of oral oxytocics for stimulation of labor in cases of premature rupture of the membranes at term. A randomized comparative study of prostaglandin E2 tablets and demoxytocin resoriblets. Acta Obstet Gynecol Scand 62: 111–116. doi: 10.3109/00016348309155773

Whittington K, Assinder S, Gould M, Nicholson H (2004) Oxytocin, oxytocin-associated neurophysin and the oxytocin receptor in the human prostate. Cell Tissue Res 318: 375–382

Whittington K, Assinder SJ, Parkinson T, Lapwood KR, Nicholson HD (2001) Function and localization of oxytocin receptors in the reproductive tissue of rams. Reproduction 122: 317–325

Whittington K, Connors B, King K, Assinder S, Hogarth K, Nicholson H (2007) The effect of oxytocin on cell proliferation in the human prostate is modulated by gonadal steroids: implications for benign prostatic hyperplasia and carcinoma of the prostate. Prostate 67: 1132–1142. doi: 10.1002/pros.20612

Widmer M, Piaggio G, Nguyen TMH, Osoti A, Owa OO, Misra S, Coomarasamy A, Abdel-Aleem H, Mallapur AA, Qureshi Z, Lumbiganon P, Patel AB, Carroli G, Fawole B, Goudar SS, Pujar YV, Neilson J, Hofmeyr GJ, Su LL, Ferreira de Carvalho J, Pandey U, Mugerwa K, Shiragur SS, Byamugisha J, Giordano D, Gülmezoglu AM (2018) Heat-stable carbetocin versus oxytocin to prevent hemorrhage after vaginal birth. N Engl J Med 379: 743–752. doi: 10.1056/NEJMoa1805489

Wing DA, Goharkhay N, Felix JC, Rostamkhani M, Naidu YM, Kovacs BW (2006) Expression of the oxytocin and V1a vasopressin receptors in human myometrium in differing physiologic states and following misoprostol administration. Gynecol Obstet Invest 62: 181–185. doi: 10.1159/000093588

Xu H, Fu S, Chen Q, Gu M, Zhou J, Liu C, Chen Y, Wang Z (2017a) The function of oxytocin: a potential biomarker for prostate cancer diagnosis and promoter of prostate cancer. Oncotarget 8: 31215–31226. doi: 10.18632/oncotarget.16107

Xu H, Fu S, Chen Y, Chen Q, Gu M, Liu C, Qiao Z, Zhou J, Wang Z (2017b) Oxytocin: its role in benign prostatic hyperplasia via the ERK pathway. Clin Sci 131: 595–607. doi: 10.1042/CS20170030

Yeung WS, Guldenaar SE, Worley RT, Humphrys J, Pickering BT (1988) Oxytocin in Leydig cells: an immunocytochemical study of Percoll-purified cells from rat testes. Cell Tissue Res 253: 463–468. doi: 10.1007/bf00222304

Publications, talks, posters and prizes/grants

Publications in peer-reviewed journals

Weiser D, Mietens A, Stadler B, Ježek D, Schuler G, Middendorff R. Contractions transport exfoliated epithelial cells through the neonatal epididymis. Reproduction. 2020 Jul;160(1):109-116. doi: 10.1530/REP-19-0617

Stadler B, Whittaker MR, Exintaris B and Middendorff R (2020) Oxytocin in the Male Reproductive Tract; The Therapeutic Potential of Oxytocin-Agonists and-Antagonists. *Front. Endocrinol.* 11:565731. doi: 10.3389/fendo.2020.565731

Stadler B, Nowell CJ, Whittaker MR, Arnhold S, Pilatz A, Wagenlehner FM, Exintaris B, Middendorff R (2021) Physiological and pharmacological impact of oxytocin on epididymal propulsion during the ejaculatory process in rodents and men. The FASEB Journal 2021;00:e21639. https://doi.org/10.1096/fj.202100435R

Talks

"The difference in contractility between prostatic ducts and glands, and how oxytocin is involved" B Stadler; D Beyer; M Kampschulte; F Wagenlehner; B Exintaris; R Middendorff (52th Annual Meeting of "Physiologie & Pathologie der Fortpflanzung" and 44th Meeting of the "Veterinär-Humanmedizinische Gemeinschaftstagung" 2019)

"Oxytocin as a new treatment option for ejaculatory disorders" Beatrix Stadler, Michael R. Whittaker, Cameron J. Nowell, Betty Exintaris, Ralf Middendorff (Virtual Symposium on Advances in Gastrointestinal & Urogenital Research 2020)

Posters

"Prostatic ducts vs glands and what oxytocin has to say about it" Stadler B., Beyer D., Wagenlehner F., Exintaris B., Middendorff R. (113th Annual Meeting of "Anatomische Gesellschaft" 2018)

"The difference in contractility between prostatic ducts and glands, and how oxytocin is involved" Stadler B., Beyer D., Wagenlehner F., Kampschulte M., Exintaris B., Middendorff R. (11th Annual GGL Conference 2018)

"Die Kontraktilität von Prostatadrüsen in Unterscheidung zu Prostatagängen und Oxytocins Einfluss hierauf" Stadler B., Beyer D., Wagenlehner F., Kampschulte M., Exintaris B., Middendorff R. (30th Annual Meeting of „Deutsche Gesellschaft für Andrologie" 2018)

"Die Kontraktilität von Prostatadrüsen in Unterscheidung zu Prostatagängen und Oxytocins Einfluss hierauf" Stadler B., Beyer D., Wagenlehner F., Kampschulte M., Exintaris B., Middendorff R. (Annual "Posterparty" of the Institute for Anatomy and Cell Biology Giessen, 2018)

„The difference in contractility between prostatic ducts and glands, and how oxytocin is involved" B Stadler; D Beyer; M Kampschulte; F Wagenlehner; B Exintaris; R Middendorff (ESA-SRB-AOTA 2019)

"Impact of the oxytocin antagonist atosiban on BPH by using time-lapse-imaging" Gronau AC., Stadler B., Wagenlehner F., Middendorff R. (Molecular Andrology Workshop 2019)

"Impact of the oxytocin antagonist atosiban on BPH by using time-lapse-imaging" Gronau AC., Stadler B., Wagenlehner F., Middendorff R. (12th Annual Meeting of the "Network for Young Researchers in Andrology" 2019)

"Oxytocin as a new target in treating ejaculatory disorders?" Stadler B., Exintaris B., Middendorff R. (SfE BES 2019)

"Oxytocin as a new target in treating ejaculatory disorders? - Welchen Nutzen können Oxytocin-Agonisten im Zusammenhang mit Ejakulationsstörungen haben?" Stadler B., Exintaris B., Whittaker M., Tasch S., Middendorff R. (8th DVR-Congress 2019)

"Oxytocin as a new target in treating ejaculatory disorders? - Welchen Nutzen können Oxytocin-Agonisten im Zusammenhang mit Ejakulationsstörungen haben?" Stadler B., Exintaris B., Whittaker M., Tasch S., Middendorff R. (Annual "Posterparty" of the Institute for Anatomy and Cell Biology Giessen, 2019)

"Oxytocin as a new treatment option for ejaculatory disorders - S19 of the rat epididymis as a testing model" Stadler B, Whittaker MR, Nowell CJ, Wagenlehner F, Exintaris B, Middendorff R (12th International, 11th European and 32nd German (digital) Congress of Andrology 2020)

"Oxytocin as a new treatment option for ejaculatory disorders - S19 of the rat epididymis as a testing model" Stadler B, Whittaker MR, Nowell CJ, Wagenlehner F, Exintaris B, Middendorff R (Annual "Posterparty" of the Institute for Anatomy and Cell Biology Giessen, 2020)

"The involvement of oxytocin in propulsing sperm during ejaculation – physiological and clinical implications" Stadler, Beatrix; Whittaker, Michael; Nowell, Cameron; Wagenlehner, Florian; Exintaris, Betty; Middendorff, Ralf (21st ETW, Virtual Edition, 2021)

"Character and relevance of superficial wall movements in seminiferous tubules" Mietens, Andrea; Rager, Christine; Tasch, Sabine; Stadler, Beatrix; Nowell, Cameron; Middendorff, Ralf (21st ETW, Virtual Edition, 2021)

Prizes/grants

Poster:

"The difference in contractility between prostatic ducts and glands, and how oxytocin is involved" Stadler B., Beyer D., Wagenlehner F., Kampschulte M., Exintaris B., Middendorff R. (11th Annual GGL Conference 2018)

"Die Kontraktilität von Prostatadrüsen in Unterscheidung zu Prostatagängen und Oxytocins Einfluss hierauf" Stadler B., Beyer D., Wagenlehner F., Kampschulte M., Exintaris B., Middendorff R. (30th Annual Meeting of „Deutsche Gesellschaft für Andrologie" 2018)

"Oxytocin as a new target in treating ejaculatory disorders? - Welchen Nutzen können Oxytocin-Agonisten im Zusammenhang mit Ejakulationsstörungen haben?" Stadler B., Exintaris B., Whittaker M., Tasch S., Middendorff R. (8th DVR-Congress 2019)

"Oxytocin as a new treatment option for ejaculatory disorders - S19 of the rat epididymis as a testing model" Stadler B, Whittaker MR, Nowell CJ, Wagenlehner F, Exintaris B, Middendorff R (Annual "Posterparty" of the Institute for Anatomy and Cell Biology Giessen, 2020)

Talk:

"Oxytocin as a new treatment option for ejaculatory disorders" Beatrix Stadler, Michael R. Whittaker, Cameron J. Nowell, Betty Exintaris, Ralf Middendorff (Virtual Symposium on Advances in Gastrointestinal & Urogenital Research 2020)

Travel grant:

For the SfE BES 2019 conference.

Adendum

Following the reviewer comments the following amendments were made:

1. *A sentence about the neural control was added: "Like other organs of the male reproductive tract, the prostate is heavily innervated by the autonomic nervous system (McMahon et al. 2004; Lippert 2017).".*
2. *The list of oxytocin receptor-targeted agents with their clinical application was added (see page 46-48).*
3. *In Figure 1 only the accessory sex glands important in the human (prostate and seminal vesicles) are highlighted with colour (page 17). The respective colours were included in the text for clarification.*
4. *To better comply with the flow from general to specific information the concept of segments in Figure 6 was replaced with a more general regional description.*
5. *We have moved the adrenergic pathway section together with smooth muscle contraction further to the beginning of the "Introduction". In addition, we added one sentence about the alpha1A subtype (see page 16): "For example, targeting specifically the α1A-receptor has been the focus in the development of pharmaceuticals intended for the treatment of benign prostatic hyperplasia (Andersson 1995; Lepor 2006)."*
6. *For clarification this sentence was added on page 33: Mesotocin is an oxytocin-like peptide present in non-mammalian vertebrates and most marsupials.*
7. *The "Aim of this study" was extended to include more detail/objectives as suggested (see page 49).*
8. *We added the n numbers in the tissue table (page 50/51).*
9. *We adjusted the rat collagen portion to past tense.*
10. *We added the n number in each respective paragraph of the manuscript for a better understanding (pages 96-101).*
11. *As detailed in the "Introduction" crosstalk always needs to be considered with the OTR and AVP receptor especially since all concentrations of the antagonists used are rather high. This sentence was added for clarification in the "Discussion": "The ability of SR49059 to elicit some degree of blockage observed in this experimental set-up might be explained by a cross-reactivity with the OTR (especially because of the high concentration used)."*
12. *A short abstract was included at the beginning of the thesis (see page 11).*
13. *A statement was included at the beginning of the thesis to clarify that there are multiple cited paragraphs in this thesis (see page 12).*
14. The respective catalogue numbers were added in the antibody table (page 56).
15. Negative controls were performed but not shown in this thesis. Following your suggestion, we included a sentence for each IHC image stating: "Negative controls without primary antibodies showed no staining." and a sentence for each IF image stating: "Negative controls without primary antibodies showed no autofluorescence or non-specific fluorescence."
16. *We agree the description of the statistical analysis was incomplete and amended in the manuscript (page 73): "All data generated with the adaptation of the Wiggle Index (S19 and S9 of the epididymis and all data from prostate experiments) were analyzed as followed: First*

the frequency distribution was determined, followed by running a non-linear regression (curve fit) using exponential one phase association testing if one curve adequately fits all data sets."

17. *These paragraphs were added for better clarification of the statistics and significances for the two types of figures in the "Statistical Analysis" (page 73/74) and indicated under each respective graph in the figure legend:*
    For the cumulative frequency data figures the two data sets displayed in the graph were determined to be significantly different if by running a non-linear regression (curve fit) using exponential one phase association testing, one curve did not adequately fit both data sets.

    In the relative cumulative frequency data figures: Each relative data set displayed in the graph (depicting one set of experiments) was first determined to be significantly different to baseline if by running a non-linear regression (curve fit) using exponential one phase association testing, one curve did not adequately fit both data sets. Second, using the relative fold changes of each of those experiments depicted in the graph, it was determined (also using curve fit) if the outcome of the experiments (e.g. the effect of oxytocin, or the blocking ability of an antagonist) was significantly different from one experimental set-up to another.